Online ISSN: 2249-4596
Print ISSN: 0975-5861
DOI: 10.17406/GJRE

Global Journal

of Researches in Engineering: J

General Engineering

Relativistic Effect of Rotation

Infrastructure Projects Failures

Highlights

Automation of Gas Leak Detection

Magnetic Resonance Therapy (MRT)

Discovering Thoughts, Inventing Future

VOLUME 25 ISSUE 1 VERSION 1.0

Global Journal of Researches in Engineering: J
General Engineering

Global Journal of Researches in Engineering: J
General Engineering

Volume 25 Issue 1 (Ver. 1.0)

Open Association of Research Society

Incorporation No.: 0423089
License No.: 42125/022010/1186
Registration No.: 430374
Import-Export Code: 1109007027
Employer Identification Number (EIN):
USA Tax ID: 98-0673427

Global Journals Inc.

*(A Delaware USA Incorporation with "Good Standing"; **Reg. Number: 0423089**)*

Sponsors: *Open Association of Research Society*
Open Scientific Standards

Publisher's Headquarters office

Global Journals® Headquarters
945th Concord Streets,
Framingham Massachusetts Pin: 01701,
United States of America
USA Toll Free: +001-888-839-7392
USA Toll Free Fax: +001-888-839-7392

Offset Typesetting

Global Journals Incorporated
2nd, Lansdowne, Lansdowne Rd., Croydon-Surrey,
Pin: CR9 2ER, United Kingdom

Packaging & Continental Dispatching

Global Journals Pvt Ltd
E-3130 Sudama Nagar, Near Gopur Square,
Indore, M.P., Pin:452009, India

Find a correspondence nodal officer near you

To find nodal officer of your country, please email us at *local@globaljournals.org*

eContacts

Press Inquiries: *press@globaljournals.org*
Investor Inquiries: *investors@globaljournals.org*
Technical Support: *technology@globaljournals.org*
Media & Releases: *media@globaljournals.org*

Pricing (Excluding Air Parcel Charges):

Yearly Subscription (Personal & Institutional)
250 USD (B/W) & 350 USD (Color)

Contents of the Issue

Global Journal of Researches in Engineering: J
General Engineering
Volume 25 Issue 1 Version 1.0 Year 2025
Type: Double Blind Peer Reviewed International Research Journal
Publisher: Global Journals
Online ISSN: 2249-4596 & Print ISSN: 0975-5861

Magnetic Resonance Therapy (MRT) and Relativistic Effect of Rotation

By Yin Rui, Yin Ming & Wang Yang
Bei Hang University

Abstract- Epoxide within molecular structures is recognized as hallmarks of potent carcinogenic cells. This paper proposes a novel approach: Magnetic Resonance Therapy (MRT), which selectively eliminates epoxide in cancerous tissues while preserving oxygen in healthy tissues, offering a potentially side-effect-free method for cancer treatment and prevention. The study presents a series of in vitro, in vivo, and clinical experiments to support this innovative therapeutic strategy. The underlying mechanism of MRT is grounded in the principles of relativity for rotational frames, and an experimental validation of this theoretical framework is provided. Furthermore, this research unveils previously undescribed relativistic phenomena, including space-time exchange, critical cylinder effects, strong and sub-strong and weak interactions as well as the source of quantum property and the source of mass as well as dark mas. Due to space constraints, the detailed mechanism of epoxide elimination will be elucidated in a subsequent publication.

Keywords: cancer, epoxide, magnetic resonance therapy, relativity for rotational frames.

GJRE-J Classification: LCC: QC173.96

MAGNETICRESONANCETHERAPYMRTANDRELATIVISTICEFFECTOFROTATION

Strictly as per the compliance and regulations of:

Magnetic Resonance Therapy (MRT) and Relativistic Effect of Rotation

Yin Rui α, Yin Ming σ & Wang Yang ρ

Abstract- Epoxide within molecular structures is recognized as hallmarks of potent carcinogenic cells. This paper proposes a novel approach: Magnetic Resonance Therapy (MRT), which selectively eliminates epoxide in cancerous tissues while preserving oxygen in healthy tissues, offering a potentially side-effect-free method for cancer treatment and prevention. The study presents a series of in vitro, in vivo, and clinical experiments to support this innovative therapeutic strategy. The underlying mechanism of MRT is grounded in the principles of relativity for rotational frames, and an experimental validation of this theoretical framework is provided. Furthermore, this research unveils previously undescribed relativistic phenomena, including space-time exchange, critical cylinder effects, strong and sub-strong and weak interactions as well as the source of quantum property and the source of mass as well as dark mas. Due to space constraints, the detailed mechanism of epoxide elimination will be elucidated in a subsequent publication.

Keywords: *cancer, epoxide, magnetic resonance therapy, relativity for rotational frames.*

Global Journal of Research in Engineering (J) XXV Issue I Version I Year 2025 1

Part 1. The Practice of MRT Treating Cancer

I. Introduction

It is well known that lots of diseases is caused by oxidation of cell molecules. As pointed by James D. Watson in his book "Molecular Biology of the Gene" (1): *"the procarcinogens become into powerful carcinogens, as the epoxide appears in their molecules."* An efficient and non-hazardous way to clean epoxide is proposed in this paper. We call it Magnetic Resonance Therapy (MRT). No medicine, no radioactivity, no scalpel, the MRT uses very weak magnetic field (less than 10 Gs) to clean epoxide. Its equipment is consisted of a signal generator (the gray box in Fig. 1) and a group of coils with air core (the white cylinder in Fig. 1). The signal generator produces currents, those flow through the coils to generate both main and RF magnetic fields acting on the lesion. The coils are positioned 20 cm away from the body surface, since the resonance happens beyond that place until 60 cm. The treatment starts when the signal generator is turned on. The standard dosage is three times one-hour per day. The device is very light (the total weight is 2 Kgs only), easy-managed, so that it can be used not only in hospital but also at home. And since it is no-hazard but benefit for body, it can be used to prevent cancer. Every year take MRT a month, even in sleep time, can keep the cancer away all life.

Fig. 1: Equipment and usage

a) Cell and Animal Experiments

i. *The Killed Process of Cancer Cells by MRT–Cell Experiment in Vitro*

Giving cultured squamous cancer cells MRT and observing the killed process of cells, we find that as MRT has been given for 5 minutes, lots of expanding bubbles bulge on the membrane of cells; as MRT has been given for 10 minutes, all bubbles expand to break, perforations appear at the place covered by bubbles before. The cell is dead currently. Continue MRT, perforations become bigger and bigger, the cell is broken.

Author α σ ρ: Bei Hang University. e-mail: yr195@buaa.edu.cn

ii. *Cell Experiment in Vivo*

Five days later after inoculating the Ehrlich (liver ascites cancer) line into the abdomen of 20 mice (BALB/c), every mouse grew up ascites including lots of Ehrlich cancer cells. Take 10 of them as experimental group and give them 8 days MRT (90minutes/day). The microscope photo-pictures are shown as Figure 2, where upper left is the cancer cells in control mice, every cell is complete. Upper right are the cells in experimental mice, perforations, overflowing cytoplasm, pieces of broken cells and dissolving into ascites can be observed. Lower left are the blood cells in control mice, lower right are the blood cells in experiment mice. They are no difference, means MRT does not damage blood cells.

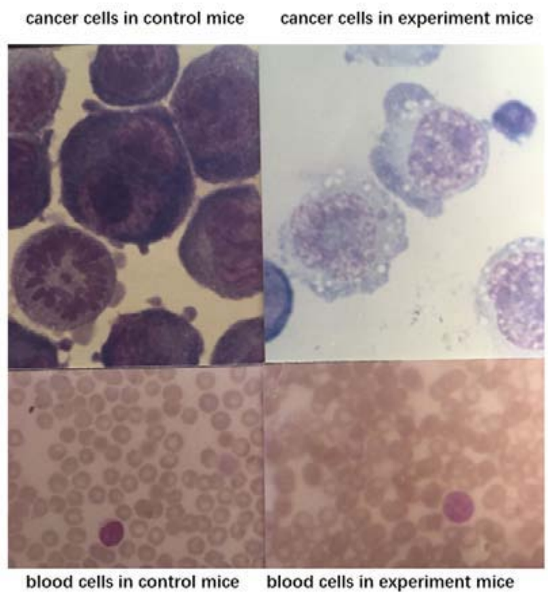

Fig. 2: MRT kill cancer cells but no effect to blood cells

iii. *The Efficiency of MRT on Ascitic Hepatoma (Ehrlich) in Mice*

Mice were inoculated with Ehrlich line, and significant ascitic growth was observed five days post-inoculation. On the tenth day, efficacy experiments were conducted. Before MRT, a small volume of ascitic fluid was extracted and examined under a microscope for cell count, yielding a concentration of 3.13×10^{8}/ml. Magnified images of the cells are shown in Figure 3 (left panel).

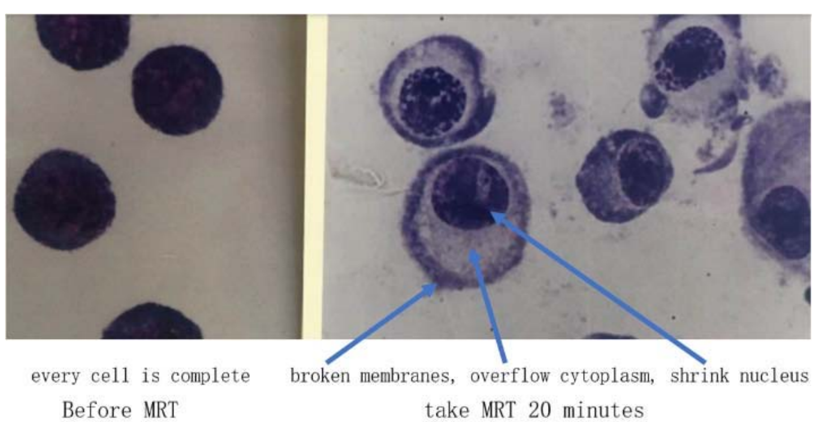

Fig. 3: MRT can kill Ehrlich cancer cell in 20 minutes

After 20 minutes of MRT, another small sample of ascitic fluid was collected for observation. The resulting image is displayed in Figure 3 (the right panel)). It was observed that, prior MRT, the cancer cells appeared intact. However, following 20 minutes of MRT, the cell nuclei exhibited pyknosis, ruptured, and released bubbles, causing perforation (visible as white spots in the images). The cell membranes fragmented, and cytoplasm leakage occurred, displacing membrane debris into a hollow area approximately twice the size of the nucleus. At this stage, the cells were confirmed to be dead, although complete dissolution into the surrounding fluid required less than an hour

At 1.5 hours MRT, a subsequent ascitic fluid sample was analyzed for cell count, yielding a concentration of 0.117×10^8/ml. Compared to pre-treatment levels, this indicated a cell kill rate of 96%.

At 5.5 hours post-treatment, another ascitic fluid sample was examined, showing a cell count of 0.094×10^8/ml. This further confirmed a cell kill rate of 97% relative to pre-treatment levels.

iv. *MRT Treated Lewis Lung Cancer in Black Mice With 100% Cure Rate*

Four days after inoculating Lewis's lung cancer line, eleven mice of C57BL/6J all grew cancer blocks with the size of about 3mm. Three of them were taken as the control group, four of them were taken as the experimental group with small dose (10 minutes/day), and the other four mice were taken as big dose group (70 minutes/ day). One week later we ended MRT, the cancer blocks in control mice all grew to the size of about 2cm, but the cancer blocks in six experimental mice (four of big dose group and two of small dose group) disappeared. However, there was a tuber in the size of about 1cm for two mice of small dose group. We dissected four mice. The cancer block in control mouse is shown as Figure 4 (the upper middle one), the upper right one is the tuber in the mouse taken small dose. The picture of dissected mouse without cancer block is shown in Figure 4 lower middle, The lower right is the tuber under Electron-Microscope. It is shown that there isn't any cancer embolus in it.

Two weeks later the other two mice of control group dead. However, one month later the tuber in the left mouse of the small dose group naturally disappeared. Nine months later the left five mice were all alive with very good health, and we ended this experiment. Such cure rate (100%) was scarce for animal experiment of cancer.

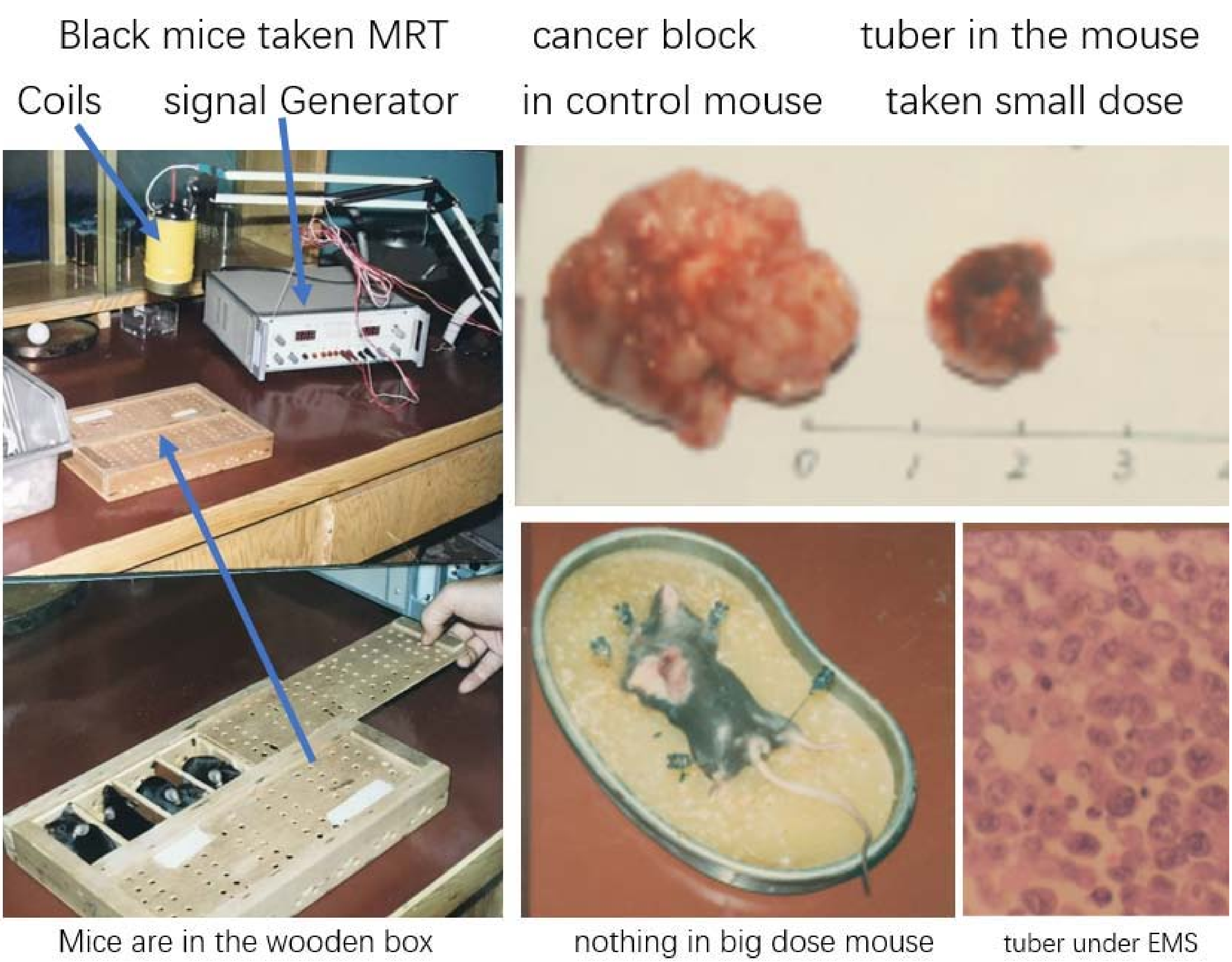

Fig. 4: MRT treated Lewis Lung Cancer in Black Mice

Global Journal of Research in Engineering (J) XXV Issue I Version I Year 2025

b) Clinical Experiments

More than 50 volunteers have taken MRT, Follows are some cases.

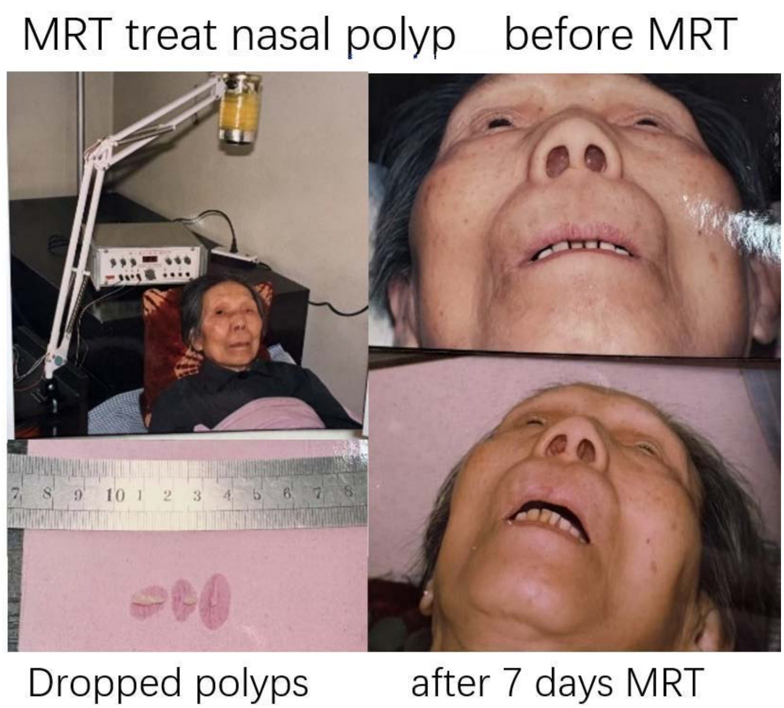

Fig. 5: MRT treat nasal polyp

Case 1: A 93-year-old woman suffered from nasal polyp. The polyps filled both nostrils as shown in Fig.5 (upper right). She toke one week MRT (2 hours/day) at her bedroom as shown in Fig.5 (upper left). During the second day's MRT, some polyps with the size about 2mm×8mm were come down on their own, as shown in Fig.5(lower left). After a week MRT the polyps were disappeared completely, as shown in Fig. 5 (lower right).

Case 2: A fifteen years old boy suffered from finger tumor as shown in Fig.6 (a). Two months later after taking MRT three days (3×1hour/day), a piece of hard crust shell was taken off the tumor as shown in Fig.6 (b). After taking another three days MRT, the tumor constricted month by month as shown in Fig.6 (c) (d) (e). Another picture taken at 30 years later is shown on Fig.6.(f).

(a)3 days MRT (b) 2 months later (c) 3 days MRT (d)4 months later (e)6 months later (f) 30 years later

Fig. 6: MRT Treated Finger Tumor

Case 3: The bile duct of an old man was obstructed. Jaundice appeared on his face, hands and body as shown in Fig. 7 (a). He had no appetite and dregs-like stool. He toke MRT at home. As the MRT had been given for three hours, a boundary line of jaundice appeared on his forehead, above this line the jaundice disappeared. As the MRT was continuing, the boundary line was going down and down. As the MRT had been given for six hours, the jaundice on his face and hands disappeared. As the MRT had been given for nine hours, the old man said: 'I am so hungry'. We ended that day's MRT and give him a bowl of gruel. Gobbling up the gruel, he said: 'I am hungry too'. His daughter smiled and asked: 'can he eat so much?' We said: 'doesn't matter, give him a diner please'. On the second day his stool became normal. Nevertheless, we gave him another two days MRT again, the picture taken on the third MRT day is shown in Fig. 7 (b).

Fig. 7: MRT Treated Bile Duct Blockage

Case 4: MRT Treat Lung Cancer

A 64-year-old man suffered from lung squamous cancer. The x-ray photo taken on 14.3.1994 is shown as Figure 8(a), where the white elliptic part in upper left lung is the original cancer block. Two weeks later the metastasized cancer blocked the bronchus, air couldn't get into left lung, the left lung atelectasis (so-called white lung) as shown in Figure 8(b). Before MRT, the patient could neither sit nor lay, four or five times of shock happened every day. We gave him a one-week MRT. On the second MRT day he could sit, after the third MRT day he could walk in the garden of the hospital. The x-ray photo taken on the last MRT day is shown as Figure 8(c). His left lung could expanse again. 40 days later another x-ray photo was taken and is shown in Fig.8 (d). The situation was much better (Figure 5).

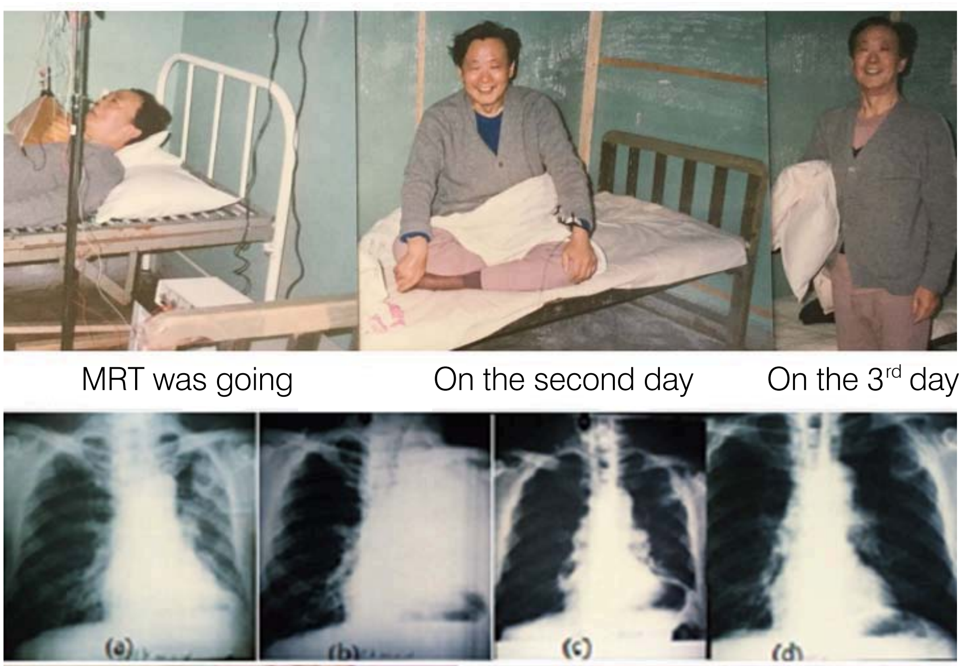

Fig. 8: MRT Treated Lung Cancer

Case 5: MRT Treat Gastric Cancer

Before treatment, the patient's pylorus was completely obstructed by cancer, rendering oral intake impossible, as shown in Figure 9 (upper left). A narrow channel was created using laser treatment, allowing the patient to sustain life by consuming milk and fruit juice. By the fifth day of MRT (3×1hour/day), the patient expelled a significant amount of scabs, part of them displayed in Figure 9 (lower right). Following this, the patient was able to consume stewed beef.

The next day, a gastroscopy was performed. Figure 9 (upper right) presents a video screenshot of the pyloric region, showing that the obstructing cancer around the pylorus had disappeared. Other areas of the gastric wall still exhibited scabs tissue that had not yet shed, as indicated in the gastroscopic video screenshot in Figure 9 (lower right). The image reveals that all areas infiltrated by the tumor had formed scabs, while the uninvolved gastric wall remained its original white color. This indicates that MRT not only avoids damage to normal tissue but also ensures comprehensive targeting of pathological tissue.

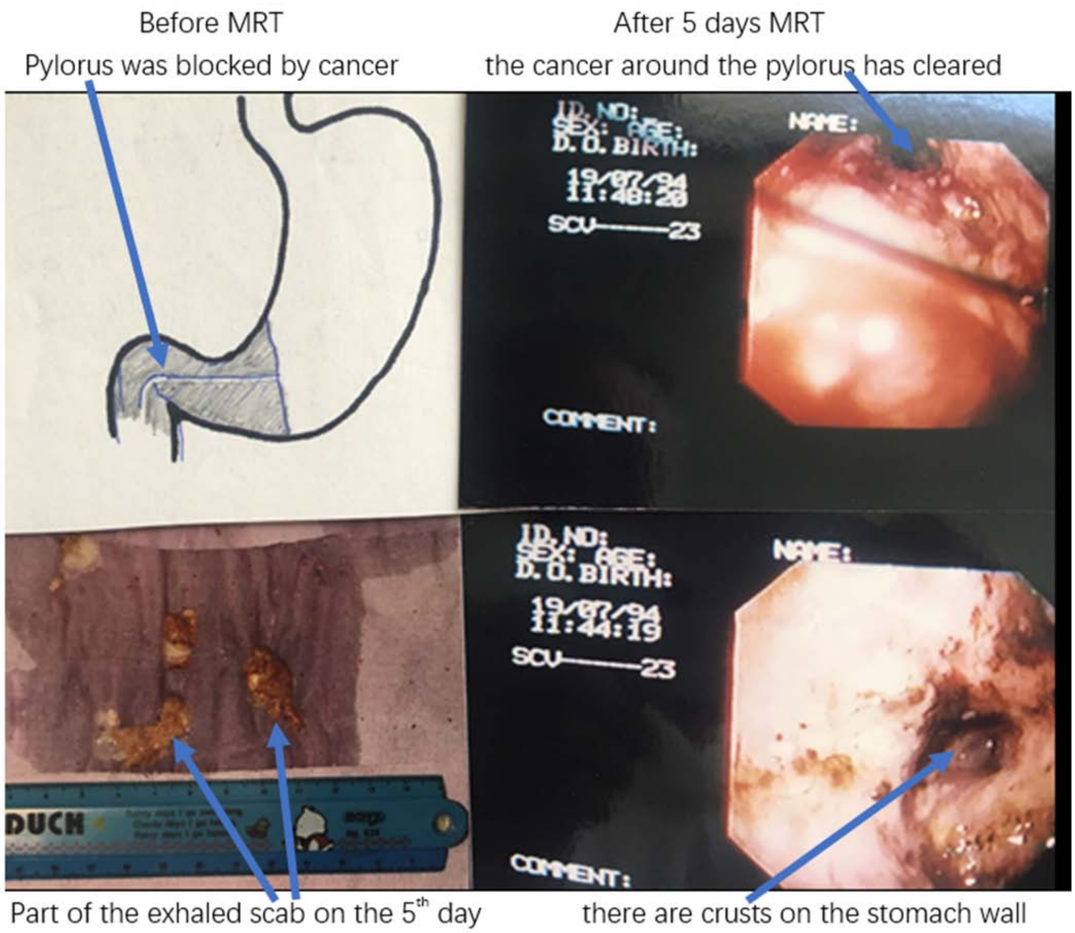

Fig. 9: 5 Days MRT (3hours/day) Cure the Pylorus Cancer

It should be noted that some gastric cancer patients, instead of vomiting necrotic tissue after 4–5 days of treatment, expelled it through defecation, like patients with colorectal cancer.

Above cases show that one or two weeks MRT can cure the cancer with small size. But the big size cancer should take MRT for long time. In this case, MRT can be taken at home and self-service by patients without the help of doctor. Follows are some cases.

Case 6: MRT Treat Lower Jawbone Cancer

A 78 years old woman suffered from lower jawbone cancer, and metastasized. She couldn't eat and sleep. She toke MRT at home. The dose was 4×40 minutes/day. Since taking MRT, she could go to sleep every night, because the pain relaxed. Fig. 10 (a) and (b) are the pictures taken before MRT, (c) and (d) are those taken after one month MRT. Comparing them, we see that the cheek swollen disappeared, large area of cancer-ulcer with liquid oozed on chin healed up.

Fig. 10: MRT Treated Lower Jawbone Cancer

Case 7: MRT Treat Breast Small Cell Cancer

At the beginning the size of cancer block was 14cm×12cm as shown in Fig.11. After one-month MRT (3×1hour/day), the mass in the upper left region disappeared, while the middle portion was charred and necrotic with a cavity being formed as shown in Fig.11. After one year MRT, the cancer tissue carbonized and necrotized into cavities as shown in Fig.11. But the skin around the cancer was without any change, although it suffered one-year MRT as well. This means the MRT can only kill cancer and no affect to normal tissue.

Fig. 11: MRT Treated Breast Small Cell Cancer

Case 8: MRT Treat Prostate Cancer

A 86-year-old man has suffered from prostate cancer for several years. His PSA was 100 ↑ (below 4 normal) on 25.5.2020. The PET-CT photo taken on 2020.6.5 is shown as Fig. 12, where every black point in bone was the cancer metastasis. Since 2020.7.19 he had taken MRT at home (3×1hour/day). After 5 months MRT the PSA was decreased to 2.1, then stop MRT. However, the PSA was still decreased, two months later decreased to 1.1, then increased, five months later increased to 1.89. Then started MRT again, one month later PSA decreased to 0.431. The PET-CT photo taken in September of 2021 is shown in Fig.12. In terms of this photo, we know lots of bone metastasis disappeared.

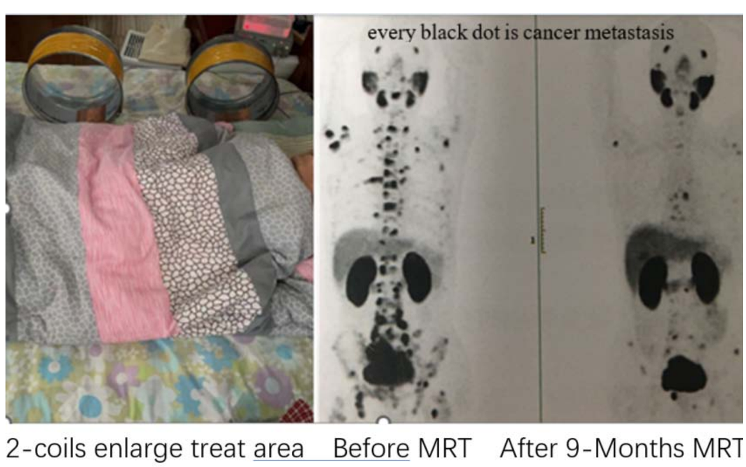

Fig. 12: MRT Treated Prostate Cancer

c) Prevention and Early-Treatment of Cancer

MRT can be used not only to treat cancer but also to prevent cancer. Following is an example.

Case 9: A 43-year-old female teacher was tested squamous cancer cells in white deposits on her tongue in 1994. The doctor suggested her to cut part of tongue. She was a teacher; without a complete tongue how could she give lecture? She asked us for help. We gave her one-week MRT (90 minutes/day) at the very beginning, then 3 months MRT (60 minutes per week). Now, 30 years is over, she fulfilled work and retired with wonderful health.

Tumor markers in the blood have exceeded the standard before cancer forms solid tumors. This is the best time for early treatment. MRT can be used as “pre-cancer” treatment, since its device is tiny, its operation is simple, it has no side effect, and it can be used at any place (home, office, class, etc.). Generally, 2 or 3 months later after 3 weeks MRT(3×40 minutes/day) the positive tumor marker can become negative. Following is an example:

Case 10: A 79-year-old academician in physical examination on 2014.12.29 was found that his Squamous Cell Carcinoma (SCC) cell antigen was 12.9 (below 1.5 normal). The doctor in no way helped him, only allowed him to take another test after 3 months. He asked us for help and toke 20 days MRT at home from 2015.1.10 to 2015.1.30 After that 3 examinations were performed on 2015.1.30. 2015.3.13. and 2015.4.10. The results were: 8.1;4.1 and 0.8. Then in 2016,17,18,19 every year he tokes one-month MRT. Till now, ten years have been over, his SCC has always been in the normal region.

The essence of MRT is deoxidation, It not only no hazard but benefit to body. Put the device on the bed and turn on it before going to sleep and turn it off after waking up. Doing it like this one month per year can keep cancer away all life.

d) MRT treat cardio- and brain-vascular diseases

MRT can be used to treat cardio- and brain-vascular diseases because they are caused by oxidation of cell molecules. Now let us give some cases.

Case 11: 67 years old women suffered from cerebral hemorrhage, after emergency operation, she kept life but left wet brain as shown in Figure 13 (left), so that she couldn’t walk, eat and speak. We gave her three months MRT (3×40 minutes/day). After one-month MRT, she could eat meal with chopsticks, go to bathroom freely, and talk fluently. However, there was blood in her brain as shown in Figure 13 (middle). After three months MRT the blood in her brain disappeared. The place where the blood occupied before became empty as shown in Figure 13 (right).

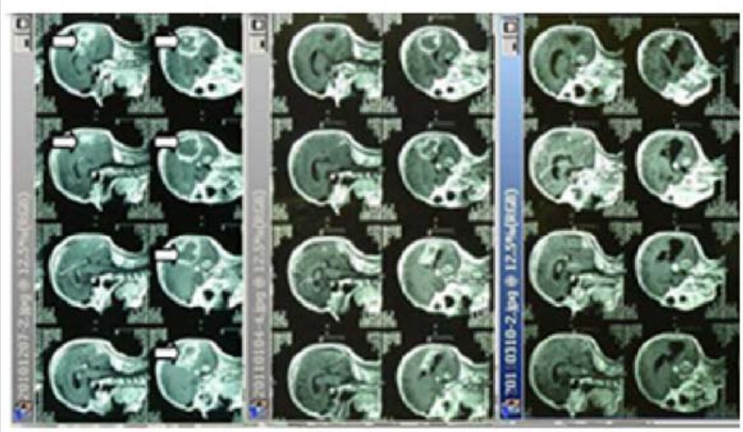

Fig.14 arteria peroneal blocked

Fig. 13: MRT treated cerebral hemorrhage

Case 12: The arteria peroneal of a 76-year-old man was blocked as shown in Fig. 14. Doctor suggested him to take an operation after the other two vascular being blocked. He asked us to help. We gave him 40 minutes MRT in the afternoon. At that night, as he was sleeping, he felt terrible itch on shank and foot. And he thought why there were so many mosquitoes this night. Suddenly, he understood that not mosquito but the blood was flowing though the shank and foot. Nevertheless, we gave him two days MRT again (40 minutes/day) and suggested him to take another test. He said: “no need, I can feel it is very well”. Now he is 90 years old and can walk 500m by push a wheelchair.

Case 13: Prevention of cerebral infarction: One of A 63-year-old man had a precursor to cerebral infarction: dropping chopsticks as eating and speaking incoherently. After 3 days of MRT, the precursor symptoms disappeared. Seven years have passed, and during these years, he has taken MRT regularly, and the condition has been good.

Case 14: Treatment of atrial fibrillation: One of a retired professor had two atrial fibrillations in 2014 and 15, and each time he had two days and three nights of continuous infusion in hospital before returning to normal. In 2016, when he had another attack, he happened to have an MRT device at home, and after one hour of treatment, he returned to normal.

No need for more cases, the efficiency of MRT has been exhibited. Now let us turn to the mechanism of MRT, that is based on Relativistic Effect of Rotation (RER), which was proposed by us in references [2-4]. Since lots of natural laws revealed by RER are unknown for modern physics, we have to give an experiment to prove it first [5].

Part 2. The Relativistic Effect of Rotation

a) Experimental observation of relativistic effect of rotation

It is well known that the tangential velocity v, angular velocity ω, and the radial distance r have the relation of $v=r\omega$. Therefore, any rotation has a corresponding radial distance $r_{c,}$ where v reaches the speed of light c: $r_c=c/\omega$. We call r_c critical radius. All points with their radial distance being r_c form a cylindrical surface called critical cylinder. Almost everyone believes that the tangential velocity Outside Critical Cylinder (OCC) will surpass the speed of light, and superluminal is impossible, so they give-up researching it. However, our experiments demonstrate that there is observable physical phenomena in OCC, which are opposite to those Inside Critical Cylinder (I CC). Now let us show the experiments

The experiment setup and result

A helical electrode is connected to the negative output terminal of a DC high voltage generator (HVG). When the HVG is turned on, an abundance of free electrons will accumulate on the electrode. The electrode is affixed to a resin plate, which is secured in a plastic dish. The two ends of two U-type ferrite cores clamp the electrode, resin plate and the plastic dish together, while the other two ends are inserted into the exciting coils, as shown in Fig. 1. A square wave current generator (SWCG) feeds the coils, producing a magnetic field that is transferred to the electrode via two ferrite cores, causing the free electrons on the electrode to precession. The angular velocity of precession is given by Larmor equation: $\omega=\gamma B$. for electron, its gyromagnetic ratio $\gamma=2.6667\times10^{10}$ (Hz/Tesla), as B= 0.12 Tesla, the precession angular velocity is $\omega=2.01\times10^{10}$ (r/s), the corresponding critical radius rc is 1.492 cm, approximately 1.5 cm. A 20% carbon ink containing a high concentration of anionic surfactants (negatively charged ions) was utilized as the test charge. To begin, warm water is added to the plastic dish, and a small quantity of ink is injected 1 to 1.3 cm to the right of the electrode.

a) Electrode is connected with HVG

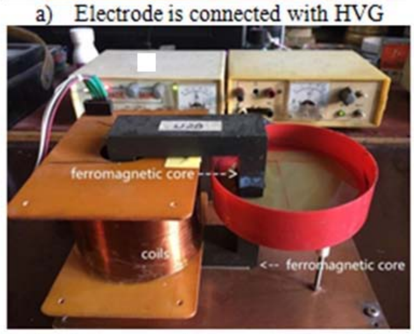

b) Two ferromagnetic cores clamp electrode

Fig. 1: The experimental device

The HVG is then turned on to recharge electrons on the electrode. The ink is repelled by the electrons, showing a distinct rightward shift as illustrated in the 4 sequential screenshots from the video presented in Figure 2(b).

Once the ink's right edge is repelled to the black mark indicating the resin board's center, the SWCG is activated to induce precession of the electrons. Subsequently, the ink in left side of 1.5cm continues being repelled rightward, whereas the ink in right side of 1.5cm begins being attracted leftward by the precession electrons. Figure 2(c) sequentially presents 6 screenshots from the experimental video depicting this stage of the precession.

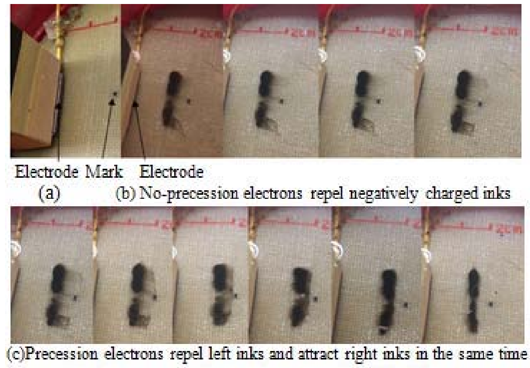

Fig. 2: Ten screenshots of an experimental video

Following is the experiment video: https://youtu.be/c6YwqfB1KvM

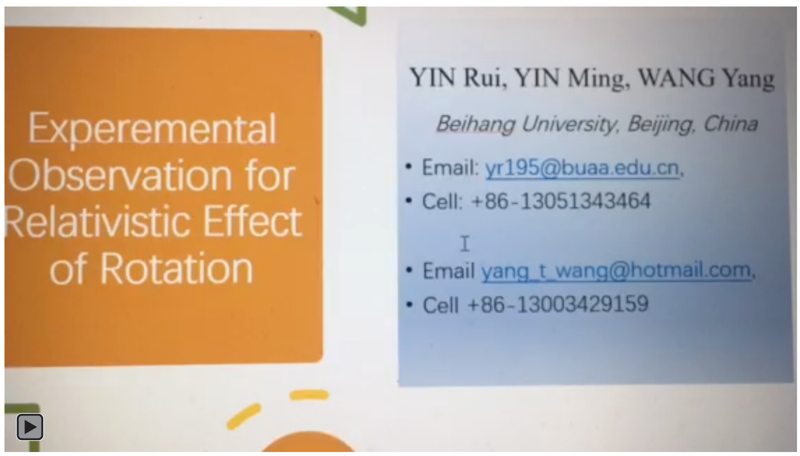

This experimental result demonstrates following conclusions

1. The electric force of precession electrons exists in OCC but has the opposite direction to that in ICC. This is a relativistic effect of rotation; we term the Critical Cylinder Effect (CCE). CCE reveals the incompleteness of Coulomb's law and Newton's gravitational law.
2. The observed critical radius indicates the precession of electrons possesses definite axis and constant angular velocity, so it is real rotation. Since only a rotating object can create precession when an external torque is applied, the spin of electron must be real rotation, contrary to claims of "not being a real rotation." in quantum spin theory.
3. Furthermore, quantum field theory believes that the electric force is transferred by virtual photons, which means that electrons emit virtual photons and hit the negative ions, causing the momentum change of the negative ions; the rate of momentum change is the force on the negative ions. However, this fails to explain why photon exchanges would exert opposing forces on either side of the critical radius. Electrical force must interact with a medium rotating in sync, i.e. its electric field but not virtual photons. In fact, the strong and weak force, and gravity are the relativistic effect of electromagnetic force, that we will explain in following.
4. There is field force in OCC means the tangential velocity of electric field of the precessing electron does not exceed the speed of light. In OCC, the relation between v and of fixed axis rotation is no longer $v=r\omega$, but $v=c2/(r\omega)$, which has not yet been known for modern physics. Reference (4) has seriously proved it. Now let us give the simple theoretic proof.

b) Space-Time exchange and Tangential Velocity of a Rotation

Suppose frame A' is rotating with a constant angular velocity **ω** about a fixed axis z (z') relative to frame A. It is well known that substituting the local reference frames of event point P for inertial frames, i.e. substituting $(ds,d\rho,dz,dt)$ for (x,y,z,t) and $\rho\omega$ for v into the (inverse) Lorentz transformation of inertial frames (1), the (inverse) Lorentz transformation for rotational frames can be got for the area of Inside Critical Cylinder (ICC) as shown in (2):

$$\begin{cases} x = \gamma(x'+vt') \\ y = y' \\ z = z' \\ t = \gamma(t'+\frac{v}{c^2}x') \end{cases} \quad (1) \qquad \begin{cases} ds = \gamma(ds'+\rho\omega dt') \\ d\rho = d\rho' \\ dz = dz' \\ dt = \gamma(dt'+\frac{\rho\omega}{c^2}ds') \end{cases} \quad (2)$$

Now, let's extend them to OCC. The $d\rho=d\rho'$ and $dz= dz'$ are kept for OCC too, so we only consider the first and last equations of (2) only. They are:

$$\begin{cases} ds = \gamma(ds'+\rho\omega dt') \\ dt = \gamma(dt'+\frac{\rho\omega}{c^2}ds') \end{cases} \quad (3)$$

Note: $$\gamma = \frac{1}{\sqrt{1-\rho^2\omega^2/c^2}} = \frac{ic}{\rho\omega}\frac{\pm 1}{\sqrt{1-c^2/(\rho^2\omega^2)}} = \frac{ic}{\rho\omega}\gamma' \quad (4)$$

Where, $$\gamma' = \frac{\pm 1}{\sqrt{1-c^2/(\rho^2\omega^2)}} = \frac{\pm 1}{\sqrt{1-\rho_c^2/\rho^2}}, \; i=\sqrt{-1} \quad (5)$$

Thus, equation (3) can be written as: $$\begin{cases} ds = \gamma ds'+\gamma' icdt' \\ icdt = \gamma icdt'-\gamma' ds' \end{cases} \quad (6)$$

And can be denoted in complex form: $$[ds, icdt] = [(\gamma ds'+\gamma' icdt'), (\gamma icdt'-\gamma' ds')] \quad (7)$$

For ICC, γ is real, γ' is imaginary, $(\gamma ds'+\gamma' icdt')$ is real, $(\gamma icdt'-\gamma' ds')$ is imaginary. Taken the real and imaginary parts of the two sides of (7) to be equal respectively, equation (6), i.e. eq. (3) can be got.

For OCC, γ is imaginary, γ' is real, $(\gamma ds'+\gamma' icdt')$ is imaginary, $(\gamma icdt'-\gamma' ds')$ is real. Taken the real and imaginary parts to be equal respectively again, following equation (8) can be got.

$$\begin{cases} ds = \xleftarrow{ICC} = \gamma ds'+\gamma' icdt' = \xrightarrow{OCC} = icdt \\ icdt = \xleftarrow{ICC} = \gamma icdt'-\gamma' ds' = \xrightarrow{OCC} = ds \end{cases} \quad (8)$$

We call this natural law space-time exchange. which has not been recognized by academics till now, It means the space in frame A' will become to space in ICC but to time in OCC of frame A. And the time in frame A' will become to time in ICC but to space in OCC of frame A.

As the event point is fixed at frame A', i. e. ds'=0, these equations become to:

$$\begin{cases} ds \xleftarrow{ICC} = \gamma' icdt' = \xrightarrow{OCC} icdt \\ icdt \xleftarrow[ICC]{} = \gamma icdt' = \xrightarrow[OCC]{} ds \end{cases}$$

The tangential velocity of this fixed point of A' relative to frame A is:

in ICC: $$\frac{ds}{dt}=\frac{\gamma' icdt'}{\gamma dt'}=\frac{\gamma' ic}{\gamma' ic/(\rho\omega)}=\rho\omega=c\rho/\rho_c,$$

in OCC: $$\frac{ds}{dt}=\frac{\gamma icdt'}{\gamma' dt'}=\frac{\pm|\gamma'|ic}{\gamma'(\rho\omega)}ic=\begin{cases}c^2/(\rho\omega)=c\rho_c/\rho & \gamma'=-|\gamma'| \vee \\ -c^2/(\rho\omega)=-c\rho_c/\rho & \gamma'=|\gamma'| \times\end{cases}$$

Both ICC and OCC the direction of rotation must be same, so only $c^2/(\rho\omega)=c\rho c/\rho$ is the true tangential velocity at OCC. That means γ' must take its minus root.

100 years ago Stern and Gerlach found the electron was spinning, Ulenbeck and Goldsmith proposed that the angular momentum of electron's spin was $L=\pm\hbar/2$. Then, Lorentz pointed out: if $L=\hbar/2$, ω should be 10^{26}r/s, then at $\rho=10^{-14}$m., the tangential velocity would be $v=\rho\omega=10^{12}m/s$, which was10^4 times of light speed, that was impossible.

Several scientists measured the tangential velocity of electron's spin at the radial distance near $\rho=10^{-14}$m, and get the results in the level of 10^4 (m/s), which was one ten-thousandth of light speed only: $v\approx c/10^4$. In terms of these measured results they believed the angular velocity to be $\omega=v/\rho\approx10^{18}$r/s, which was far less than 10^{26}r/s, that can create $L=\pm\hbar/2$.

So, till now the Quantum Mechanics has thought: the spin of charged particle is not rotation, and the angular momentum doesn't come from rotation but intrinsic.

However, according to our equation: $v=c^2/(\rho\omega)=c\rho_c/\rho$ i.e.: $c\rho_c=v\rho/c$, as $\rho=10^{-14}$m, $v=c/10^4$ means $\rho_c=10^{-18}$m, $\omega=c/\rho_c=3\times10^{26}$r/s, that can just create $L=\hbar/2$. On the other hand, only rotational body can create precession as it suffered from external force. Our experiment proves the electron's precession is real rotation, so its spin must be real rotation too. Denying spin to be rotation, unknown the relativistic effect of rotation, quantum spin theory cannot touch the essence of particle world. This is the reason, why the research about particle physics no achievement during last century. Both six quarks model and super string theory cannot introduce the research go ahead. It's the time to correct it.

c) Unification Form of Lorentz Transformations for Rotational Frames

Now we know Outside Critical Cylinder the tangential velocity of a rotation is $v=c^2/(\rho\omega)=c\rho_c/\rho$, $1-v^2/c^2=1-\frac{c^2}{\rho^2\omega^2}=1-\frac{\rho_c^2}{\rho^2}$, so the Lorentz factor in OCC is:

$$-|\gamma'|=-(1-c^2/\rho^2\omega^2)^{-1/2}=-(1-\rho_c^2/\rho^2)^{-1/2}$$

Thus, let $$v(\rho)=\begin{cases}c\rho/\rho_c & \rho<\rho_c\\ c\rho_c/\rho & \rho>\rho_c\end{cases}\qquad \gamma(\rho)=\begin{cases}(1-\rho^2/\rho_c^2)^{-1/2} & \rho<\rho_c\\ -(1-\rho_c^2/\rho^2)^{-1/2} & \rho>\rho_c\end{cases}$$

The Lorentz transformations for both ICC and OCC can be uniformly denoted as follows:

$$\begin{cases}ds=\gamma(\rho)(ds'+v(\rho)dt')\\ d\rho=d\rho'\\ dz=dz'\\ dt=\gamma(\rho)(dt'+\frac{v(\rho)}{c^2}ds')\end{cases}$$

In terms of this equation, we can get the transformations of mass (m), energy (w), tangential momentum (p_s), radial force (F_ρ), axial force (F_z) and their resultant (F_R) as follows:

$$m = \gamma(\rho)m'[1 + u_s^{'}v(\rho)/c^2];$$

$$w = \gamma(\rho)(w' + v(\rho)p_s^{'});\ p_s = \gamma(\rho)(p_s^{'} + v(\rho)E'/c^2);$$

$$F_{\rho/z/R} = \frac{F_{\rho/z/R}^{'}}{\gamma(\rho)[1 + u_s^{'}v(\rho)/c^2]} = \gamma(\rho)F_{\rho/z/R}^{'}[1 - u_s v(\rho)/c^2]$$

At OCC $\gamma(\rho)$ taken minus root, so the mass, energy, tangential momentum and force have opposite sign against those at ICC. We call it Critical Cylinder Effect (CCE). The experiment given above proves the radial force in OCC is opposite against that in ICC. That means the relativistic effects of rotation, proposed by us, is correct.

On the other hand, the force transformations given above, related to u_s, which is the tangential component of the accepter charge's velocity relative to the doner charge's spin. Even if the accepter charge's velocity is fixed, the u_s is different for different spin axis direction of doner charge. So that the force is related to the direction of spin axis of the doner charge. Different spin axis direction creates different force, the movement of accepter is different. This is the source of uncertainty in Quantum Mechanics.

Part 3. How does Strong Interaction Create between Protons

a) Explanation of Experimental phenomenon

i. *Before magnetic field being excited*

The electron is only spinning with critical radius of: ρ_{ce}≈10^{-18}m. Take lab as reference frame A, relative to A take the spin of an electron as A'. In A' this electron is really at rest. The force exerted by this electron upon the anion of ink is the true electrostatic force F_R'. Transform F_R' into lab frame A by the force transformation, we get the force acted by electron on the anion of ink in lab frame:

$$F_R = \gamma_s(R)F_R'[1-u_s v_s(R)/c^2]$$

In our experiment: u_s=0; and $R \approx 10^{-2}$m, $\rho_{ce} \approx 10^{-18}$m, $\gamma_s(R)$=-(1-($\rho_{ce}/R)^2)^{-1/2}$=-1. Thus: $F_R = -F_R'$.

In terms of Coulomb's experiment: $F_R=k(-e)(-q)/R^2=keq/R^2$ where $-q$ is the charge of anion. So $F_R' = -keq/R^2$,

In general, if the spinning charge is q, the test charge is q_t, the real electrostatic force in the spinning frame of q is: $F_R' = -kqq_t/R^2$

It means the real rest charge attracts the charge with the same sign, which is opposite against the Coulomb's law.

And as u_s=0 the force in lab frame is: $F_R = \gamma(R)F_R'$, i.e.

$$F_R/F_R' = \gamma(R) = \begin{cases} [1-(R/\rho_c)^2]^{-1/2} & R < \rho_c \\ -[1-(\rho_c/R)^2]^{-1/2} & R > \rho_c \end{cases}$$

We call it the first kind of CCE, as shown in Fig. 3.1(left). It means as R is changed across the critical radius, the force not only change direction but also approach to infinity. This is the source of so-called strong interaction. The strong interaction of protons appears at the level of 10^{-15}m (femto meter: fm), so the critical radius of proton's spin is on the level of fm, we take it is 1fm=1×10^{-15}m to discuss.

More general, if $u_s \neq 0$, $F_R = \gamma_s(R)F_R' - \gamma_s(R)F_R' u_s v_s(R)/c^2 = F_e + F_m$ = electric force+ magnetic force.

So, the electrical field of a spinning charge q in lab frame is: $E_s = -\gamma_s(R)kq/R^2$"

And the magnetic field of a spinning charge q in lab frame is:

$$B_s = \gamma_s(R)[kq/R^2][v_s(R)/c^2] = q\gamma_s(R)v_s(R)\mu_0/(4\pi R^2)$$

For proton q=+e=1.602×10^{-19}C, its spin magnetic field distribution along radial $R=\rho$ is given in table 1

Table 3.1: The distribution of $\gamma(\rho)$ and spin magnetic field B of proton

$R=\rho=$	$0.9\rho_c$	$0.999\rho_c$	$\rho_c=10^{-15}$m	$1.001\rho_c$,	i.1ρ_c,	10^{-9} m (nm)
$\gamma(\rho)=$	2.3	22,3	±∞	−22. 4	−2. 4	−1
B(T)=	0.12×10^{14}	1.07×10^{14}	±∞	-1.08×10^{14}	-0.087×10^{14}	-4.8 ×10^{-7}

And the direction of both electrical and magnetic field E and B are given in Fig. 3.1(right)

Thus, we know the direction of both electric field and magnetic field of spinning charged particle in OCC is opposite against that in ICC. So, as put this particle in an external magnetic field B, after longitudinal relaxation, the external magnetic field can coincide with either the spin magnetic field in OCC or that in ICC. This is why they define spin quantum number to be s=±1/2 in quantum mechanics. And we know that how roughly it is to describe the spin magnetic property of proton by magnetic moment.

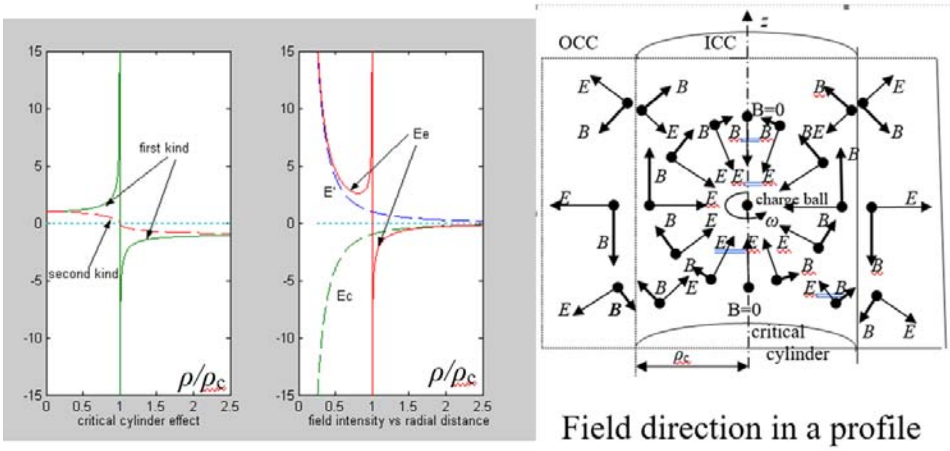

Fig. 3.1: Strength and direction distribution of spinning proton's field

ii. *As the magnetic field has been excited*

In this case, every electron has two rotations: spin in the angular velocity ω_s and precession with angular velocity of $\omega_m=\gamma B$. Take lab frame as A, the precession of an electron as A', then relative to A' take its spin as A", then in A" the force acted on anion of ink by the electron is the real electrostatic force: $F_R''=-keq/R^2$.Transform F_R" into A' we have:

$$F_R' = \gamma_s(R)F_R''[1-u_s'v_s(R)/c^2] \tag{3.1}$$

Note that both ω_s and ω_m are relative to lab frame A, so the angular velocity of A" relative to A' is: $\omega_s'=\omega_s-\omega_m$ i.e. $c/\rho_c'= c/\rho_c- c/r_c$, i.e. : $\rho_c'=\rho_c r_c/(r_c-\rho_c)$, so that in equation

$$\gamma_s(R) = \begin{cases} [1-(R/\rho_c')^2]^{-1/2} & R < \rho_c' \approx 10^{-18} m \\ -[1-(\rho_c'/R)^2]^{-1/2} & R > \rho_c' \approx 10^{-18} m \end{cases}$$

$$v_s(R) = \begin{cases} cR/\rho_c' & R < \rho_c' \\ c\rho_c'/R & R > \rho_c' \end{cases}$$

Then, transform F_R' into A we have:

$$F_R = \gamma_s(R)\gamma_m(R)F_R''[1-u_s'v_s(R)/c^2][1-u_m v_m(R)/c^2]$$

In our experiment $u_m=0$, (0,5cm<R<2cm)>>$\rho_c=10^{-18}$m. $v_s(R)=c(\rho_c/R)\approx 0$, we have:

$$F_R = \gamma_s(R)\gamma_m(R)F_R''$$

Where:

$$\gamma_m(R) = \begin{cases} [1-(R/r_c)^2]^{-1/2} & R < r_c = 1.5cm \\ -[1-(r_c/R)^2]^{-1/2} & R > r_c = 1.5cm \end{cases}$$

So, for $R<\rho_c=10^{-18}$m, F_R is attraction; for $\rho_c<R<r_c$, F_R is repulsion; for $R>r_c$, F_R is attraction, which we have observed in our experiment.

b) The strong interaction between two protons

Just like we can think the mass of earth is concentrated in its center, as we discuss the gravity of a body outside the earth, we can think the charge of proton is uniformly distributed in a ball with radius of b=0.9194fm, as we discuss the interaction between protons. We will give the detail in part 5 of this paper. Sometimes, for simple, we think the radius of charge ball is 1fm.

For the two protons system, every proton is spinning with critical radius of ρ_c, that creates spin magnetic field B_s, which makes the other proton precession with critical radius of r_c, that creates precession magnetic field B_m. As the spin and precession axis of every proton are coincide, and anti-parallel to the axes of the other proton, and the distance (R) between two protons is greater than both ρ_c and $2r_c$, the two proton will attract to each other Take lab as A, spin of p_1 as A' , relative to A' take precession of P_1 as A". The force exerted on p_2 by p_1 in frame A" is real electrostatic force $F_R" =-ke^2/R^2$. Transform it to A' and then to A, we get the force in lab frame as follows

$$F_R = F_R^{"}\gamma_s(R)(1-v_s(R)u_s/c^2)\gamma_m(R)(1-v_m(R)u_m'/c^2) \tag{3.2}$$

Where: u_s is the tangential component of the P_2's velocity relative to the spin of P_1 in lab frame A

u_m' is the tangential component of the P_2's velocity relative to the magnetic precession of P_1 in spin frame A'

$$\gamma_s(R) = -[1-(\rho_c/R)^2]^{-1/2}, \quad v_s(R) = c(\rho_c/R)$$

$$\gamma_m(R) = -[1-(r_c'/R)^2]^{-1/2}$$

$$v_m(R) = c(r_c'/R), \quad r_c' = r_c\rho_c/(\rho_c-r_c) \tag{3.3}$$

For keeping two protons attract to each other, R must be greater than both ρ_c and r_c', this means R must be greater than $2r_c$ (accurately $r_c<0.5002$fm). If $r_c>0.5003$fm, then $r_c'>$R, the two protons will repel to each other, the two protons system can not exist.

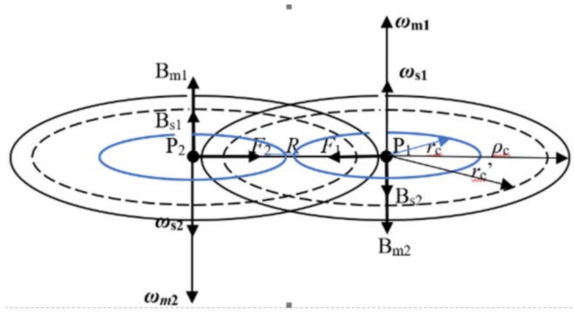

Fig. 3.2: Strong interaction between two protons

In terms of Eq. (3.2), we can get the spin and precession magnetic fields at $\rho=r=R$ as follows:

$$B_s = e[\gamma_m(R)\gamma_s(R)]v_s(R)\mu_0/(4\pi R^2)$$

$$B_m = e[\gamma_m(R)\gamma_s(R)]v_m(R)\mu_0/(4\pi R^2)$$

At the stable state, longitudinal relaxation ended, the spin and precession axes are almost coincided for every proton, and are anti-paralleled to the axes of the other proton, as shown in Fig. 3.1. In this case the magnetic field passing through every proton is:

$$B = (B_m + B_s) = e\gamma_m(r)\gamma_s(\rho)[v_s(\rho)+v_m(r)]\mu_0/(4\pi R^2). \tag{3.4}$$

In terms of Larmor equation: $\omega_m = -2\pi\gamma_p B$, where minus sign means the direction of $\boldsymbol{\omega}_m$ is opposite against the direction of passing magnetic field B, we can get the angular velocity of proton's precession and its critical radius:. $r_c = c/\omega_m$. Where, γ_p=4.257×10^7(Hz/T) is the gyromagnetic ratio of proto.

Note: e=1.602×10^-19(C), ρ_c=1×10^-15m (ω_s=3×10^23 r/s), The strongest interaction happens at $R=\rho_c+b$ =1.0009194×10^-15m. At that place $\gamma_s(R)$=-23.3363, $v_s(R)$=2.9972×10^8m/s are definite. If r_c=0.499×10^-15m (ω_m=6.012×10^23 r/s), then $\omega_m'=\omega_m-\omega_s$=3.012×10^23r/s, r_c'=0.996×10^-15m, $\gamma_m(R)=-[1-(r_c'/R)^2]^{-1/2}$=-10.01, $v_m(R)=cr_c'/R$=2.988×10^8m/s。The magnetic field passing through every proton is: $B=e\gamma_s(R)\ \gamma_m(R)[\ v_s(R)+v_m(R)]\mu_0/(4\pi R^2)$=2.2563×10^15T, which can create the precession of proton with angular velocity of $\omega_m=2\pi\gamma_p B$=6.035×10^23r/s, corresponding critical radius is $r_{cc}=c/\omega_m$ = 0.4971×10^-15m. That means r_c=0.499fm can not self-sustain, It will be decreased to 0.4971fm. As it is decreased to [0.49899063, 0.49899062, 0.49899061] fm, the system parameters are shown in table 3.2.

Table 3.2: The stable self-sustain state of two-proton system with strong interaction

$\gamma_s\gamma_m$	F/F"	B	r_c'	r_c set	$r_c$create
235.0	468.6	2.247727e+015	9.95971e-016	4.9899061e-016	4.989926e-016
235.0	468.6	2.247736e+015	9.95971e-016	4.9899062e-016	4.989906e-016
235.0	468.6	2.247745e+015	9.95971e-016	4.9899063e-016	4.989886e-016

This means r_c=0.4989906(2) fm can keep the two protons system self-sustain, as given by the middle row of table 3.2. And this self-sustain state is stable. That means as something makes r_c be changed from r_c=0.4989906(2) fm, the system can make it return, as shown in table 3.2 (The upper and lower rows). By the way, we always use the three rows table to give the stable self-sustain state in our works. We hope readers can follow it.

If the two protons are not shift in lab, then $u_s=0$, $u_m'=-c\rho_c/R$. The interaction between two protons is following:

$$F_R = F_R''\gamma_s(R)\gamma_m(R)(1-v_s(R)u_s/c^2)(1-v_m(R)u_m'/c^2)$$

$$= F_R''235(1-\rho_c r_c'/R^2) = 468.6F_R'' = -468.6ke^2/R^2$$

It is attraction of 468.6 times stronger than the electrostatic force, and appears at $R=\rho_c+b$ only. This is the so-called strong interaction between two protons and is given in table 3.2 by the term of *F/F*". However, the two-proton system cannot be without shift in lab frame. We talk it is just as a foundation of following discuss.

c) *Strong interaction between more protons*

Consider four protons distribute at the vertices of a square with side length of $R=\rho_c+b$=1.9194fm. After longitudinal relaxation, the spin axis and magnetic precession axis of every proton are coincided, and they are antiparallel to the axes of two adjacent protons as shown in Fig.3.3.

Thus, the magnetic field passing through every proton is as following:

$$B = 2\gamma_s(R)\gamma_m(R)e[v_s(R)+v_m(R)]\mu_0/(4\pi R^2) - \gamma_s(\sqrt{2}R)\gamma_m(\sqrt{2}R)e[v_s(\sqrt{2}R)+v_m(\sqrt{2}R)]\mu_0/(8\pi R^2)$$

The critical radius of magnetic precession, which can hold the system stable self-sustaining, is r_c=0.4953731×10^-15m. The stable self-sustain state is given in table 3.3.

Table 3.3: The stable self-sustain state of 4-proton system with strong interaction

$\gamma_s\gamma_m$	F/F"	B	r_c '	r_c set	r_c create
119.5	236.7	2.264148e+015	9.8166229e-016	4.9537315e-016	4.953736e-016
119.5	236.7	2.264150e+015	9.8166233e-016	4.9537316e-016	4.953731e-016
119.5	236.7	2.264153e+015	9.8166237e-016	4.9537317e-016	4.953726e-016

If only take $B=2\gamma_s(R)\gamma_m(R)e[v_s(R)+v_m(R)]\mu_0/(4\pi R^2)$, that means neglect the effect of diagonal proton. The stable self-sustain state is given in table 3.4, which is almost the same as table 3.3

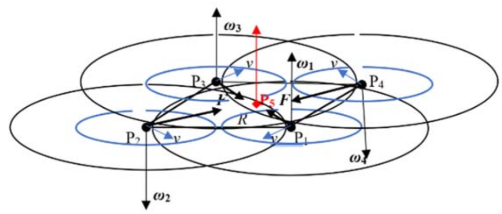

Fig. 3.3: Strong interaction in 4/5-proton system

$\gamma_s\gamma_m$	F/F"	B	r_c '	r_c set	r_c create
119.2	236.0	2.264276e+015	9.8155336e-016	4.9534541e-016	4.953456e-016
119.2	236.0	2.264278e+015	9.8155340e-016	4.9534542e-016	4.953451e-016
119.2	236.0	2.264281e+015	9 8155344e-016	4.9534543e-016	4.953446e-916

Fig. 3.4: The stable self-sustain state of even-proton system with strong interaction

This means that for the multi-proton system distributed in polygon, only the two adjacent protons gives the strong interaction. Thus, we get the force acted on every proton of multi-proton system is as follows

For the proton in 4-proton system $F=2\sin(\pi/4)\times 236F"=-334ke^2/R^2$

For the proton in 6-proton system $F=2\sin(\pi/6)\times 236F"=-236ke^2/R^2$

For the proton in 8-proton system $F=2\sin(\pi/8)\times 236F"=-181ke^2/R^2$

This force is pointed to the center of polygon, which holds the even-proton system stable.

If there is another proton (P_o) located at the center of this polygon, the resultant force exerted by the even protons on P_o is zero. The magnetic field at the center of polygon is zero, so there isn't magnetic precession for P_o. It is only spinning so the force exerted on other even protons is as follows:

For 5-proton system: $F_o=-2\gamma_s(\frac{\sqrt{2}R}{2})ke^2/R^2=-2.828\ ke^2/R^2$ attraction,

For 7-proton system: $F_o=-\gamma_s(R)ke^2/R^2=23.3363\ ke^2/R^2$ repulsion

For 9-proton system: $F_o=-\gamma_s(\frac{R/2}{\sin(\pi/8)})ke^2/R^2=1.5538\ ke^2/R^2$ repulsion

For the nuclei with even protons, the magnetic field and angular momentum are cancelled to each other, so there is no spin angular momentum and magnetic moment. And the nuclei with odd protons have only one proton's spin angular momentum and magnetic moment. This conclusion is confirmed by both classical theory and quantum theory. Now we have given its relativistic essence.

d) Sub-strong interaction between protons

As mentioned above, when $R=\rho_c+b>2r_c$, so that the distance (R) between two protons is greater than both ρ_c and $r_c'=\rho_c r_c/(\rho_c-r_c)$, the interaction between two protons is strong attraction. However, as $R=\rho_c+b$ is less than r_c, so that the magnetic field passing through every proton is in the same direction as its spin axis, and so that the precession axis of every proton is anti-parallel to its spin axis as shown in Fig.3.4.. In other words, the rotating direction of precession is opposite against that of spin. Thus, relative to spin frame A' the angular velocity of precession frame is $\omega_m'=\omega_s+\omega_m$ i.e.$r_c'=\rho_c r_c/(r_c+\rho_c)$. And no matter how much is $r_c(>R)$, the r_c' is always less than $\rho_c<R$. This means the force between the two protons is attraction too and can be denoted by following equation as well

$$F_R=F_R''\gamma_s(R)\gamma_m(R)(1-v_s(R)u_s/c^2)(1-v_m(R)u_m'/c^2)$$

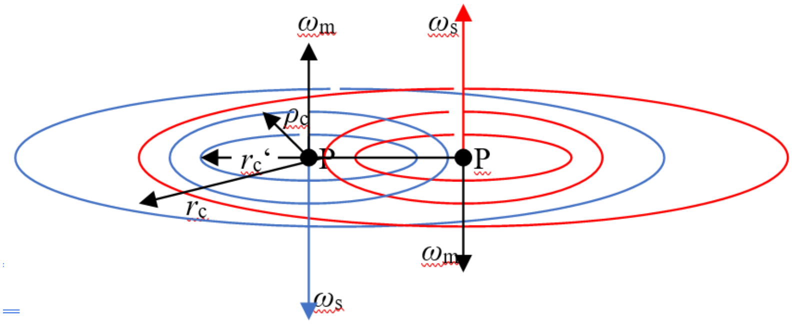

Fig. 3.4: Two protons with sub-strong interaction

Following is the stable self-sustain state of 4-proton system in this case

$\gamma_s\gamma_m$	F/F"	B	r_c'	r_c set	r_c create
32.0	10.1	5.1e+014	6.8602333e-016	2.18495e-015	2.18498e-015
32.0	10.1	5.1e+014	6.8602530e-016	2.18497e-015	2.18497e-015
32.0	10.1	5.1e+014	6.8602727e-016	2.18499e-015	2.18496e-015

Fig. 3.5: The stable self-sustain state of 4-proton system with substrong interaction

As the four protons are no shift in lab, then u_s=0, u_m'=-cρ_r/R, $v_m(R)$=-cr_c'/R The force between two protons is: $F_R = F_R^{''}\gamma_s(R)\gamma_m(R)(1-\rho_c r_c'/R^2) = -10.1ke^2/R^2$, that is given in table 3.5 by the term of F/F".

Thus, we get the force acted on every proton of multi-proton system is as follows

For the proton in 4-proton system $F=2\sin(\pi/4)\times 10.1F"=-14ke^2/R^2$。

For the proton in 6-proton system $F=2\sin(\pi/6)\times 10.1F"=-10ke^2/R^2$

For the proton in 8-proton system $F=2\sin(\pi/8)\times 10.1F"=-7.7ke^2/R^2$

They are pointed to the center of polygon but not so strong. We call them sub-strong interaction, that is unknown by modern physics.

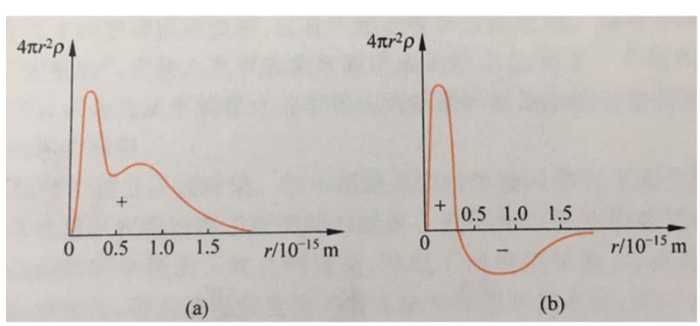

Fig. 4.1: The charge distribution in proton(a) and Neutron(b)

Fortunately. in the free radical oxygen and epoxide, the interaction between protons is sub-strong, but in the oxygen nuclei of normal tissue the interaction between protons is strong, which is dozens of times stronger than the sub-strong interaction. So the Magnetic Resonance Therapy (MRT) can kill cancer and no effect to normal tissue by decomposing epoxide but not oxygen.

Part 4 .Neutron and Weak Interaction

a) The Construction of Neutron

Modern quark theory proposed that the proton is consisted of u-d-u three quarks; neutron is consisted of d-u-d quarks, where u quark carries +2e/3 charge, d quark carries -e/3 charge. However, now we know the charge distribution in proton as shown in Fig. 4.1(a). There is not any negative charge in proton。This means there is not d quark in proton, and proton is not consisted by u-d-u quarks.

From Fig.4.1（a）we know that the charge density at 0.25 fm is twice of that at 0.75 fm. That means the proton is consisted of three same charged particles, everyone carries +e/3 charge, we call it q quark. And the q quark at 0.75 fm can move from 0.3fm to 1.5fm, that is caused by the measurement. As without measurement, this quark will go back to its original place of 0.3fm, and the three q quarks forms the charge distribution like the part inside 0.3 fm of Fig.4.1 (b). In other words, the part inside 0.3 fm of neutron is just a proton, and the negative charge in neutron must be given by an electron, because the neutron is electricity neutral. It is well known that the neutron can easily decay to proton + electron and neutrino, that is the proof of neutron is consisted of an electron plus a proton.

Now we propose: "the neutron is consisted of a proton and an electron, which is separated from proton by (0.4∽1.5)fm". We take it to be $R=0.8\times10^{-15}$m to discuss, and this is the difference from hydrogen atom. In hydrogen atom the distance between proton and electron is in the level of 10^{-10}m, which is far greater than the spin critical radius of both proton ($\rho_{cp}=10^{-15}$m, i.e. fm) and electron ($\rho_{ce}=10^{-18}$m, i.e. am). Outside the spin critical cylinders, the proton and electron attract to each other and create a rotation around their mass center called system precession with the angular velocity ω_g and critical radius of $l_c=c/\omega_g=7\times10^{-9}$m (we use l to denote the radial of system precession to distinguish from spin (ρ) and magnetic precession r).

However, for neutron the distance between proton and electron is $R=0.8\times10^{-15}$m, which is less than $\rho_{cp}=10^{-15}$m. If the critical radius of system precession $l_c>R$, the proton repels electron, system precession can't create. If $l_c<R$ the proton attracts electron, but the mass of electron becomes to negative, since it is outside critical cylinder (OCC) of system precession. Attraction acts on minus mass, the acceleration is centrifugal, the system precession can't create as well. Without system precession, $R=0.8\times10^{-15}\text{m}<\rho_{cp}=10^{-15}$m, the proton repels the electron with plus mass, the electron will go away. The state can't be stable, the neutron can not exist. However, as the critical cylinder of system precession pass through the charge ball of electron, so that its OCC part suffered from attraction and with minus mass but its ICC part suffered from repulsion and with plus mass. And only as the resultant force is repulsion and the resultant mass is negative, the acceleration of electron is centripetal, the system precession can create and the proton-electron system can be stable, the neutron can exist, as shown in Fig. 4.2.

Now let us give the detail, based on thinking the charge of both proton and electron is uniformly distributed in a ball with radius of $b\approx1\times10^{18}$m, although they are consisted of three quarks.

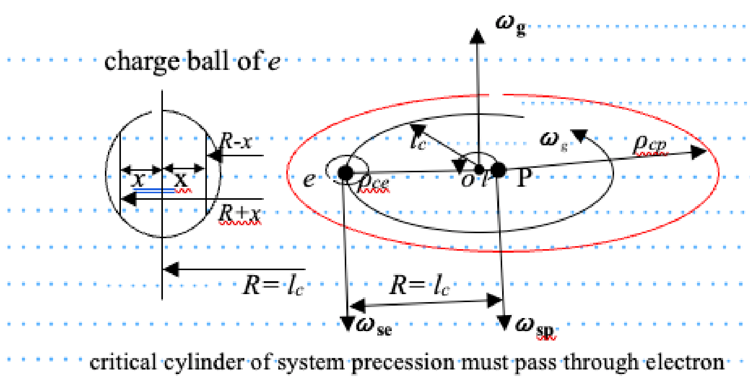

Fig. 4.2: The construction of neutron

Now, let us consider the possibility of this state. Since the critical cylinder of l_c pass through the charge ball of electron, the magnetic field in OCC is opposite against that in ICC, so the magnetic precession of electron can be neglected. On the other hand the critical radius of proton's magnetic precession is on the level of 10^{-13}m, which is far greater than both ρ_{cp} and l_c, and can be neglect as well. There are only spin and system precession two rotations for both proton and electron.

The mass of proton is 1800 times greater than the mass of electron, so the distance from mass center to proton is $l=R/1800=0.4\times10^{-18}$m, which is less than the radius of charge ball $b=1\times10^{-18}$m. This means the mass

Global Journal of Research in Engineering (J) XXV Issue I Version I Year 2025

center is almost coincided with the proton, the system precession of electron can be thought around the proton, And the R and l_c have the same origin O=P.

First let us consider the situation of $R= l_{c,}$ that means the critical cylinder of $l_{c,}$ pass through the charge ball of electron from its center. Take lab as A, system precession as A', in A 'the electron has only spin. Its mass must be distributed in axis symmetry that means the mass m_0 in cross-plate R-x is equal to that in R+x. In lab frame they are rotating with tangential velocity of $v(R\text{-}x)=c(R\text{-}x)/R$ and $v(R+x)=cR/(R+x)$, The mass becomes to

$$m(R-x) == m_0 / \sqrt{1-(R-x)^2 / R^2}\ ;$$

$$m(R+x) = -m_0 / \sqrt{1-R^2/(R+x)^2}\ ,$$

Since $R^2 > R^2 - x^2 = (R-x)(R+x)$, i.e., $R/(R+x) > (R-x)/R$,

So $m(R+x) + m(R-x) < 0$, i.e., the resultant mass is negative as $R=l_c$.

As $l_{c,}$ is increased from $l_{c,}=R$ the ICC part, i. e. , the positive mass is increased. As $l_{c,}=R+$b, the total mass is positive. So there must exist l_{c1}: $R< l_{c1} <R+b,$ where the resultant mass equals 0. Thus, keep $l_{c,} < l_{c,1}$ can keep the resultant mass to be negative.

b) How doe's weak interaction creates

As mentioned above in system precession frame A', both proton and electron are no shift, the force acted on the electron by spinning proton is $F_R' = \gamma_{sp}(R)ke^2/R^2$, Transform it into lab frame A, we have:

$$F_R=\gamma_{gp}(R) \qquad F_R'(1\text{-}u_g v_g(R)/c^2) \tag{4.1}$$

Where $\gamma_{gp}(R)= (1\text{-}v_g^{\,2}(R)/c^2)^{-1/2}$, u_g is the tangential velocity of electron in lab frame A .and it just is $u_g= v_g(R)$, since the electron is synchronously rotating with the system precession of proton. So the factor $(1\text{-}u_g v_g(R)/c^2) = (1\text{-}v_g^{\,2}(R)/c^2) =1/\gamma_{gp}^{\,2}(R)$. Thus, equation (4.1) becomes to,

$$F_R= F_R'/\gamma_{gp}(R), \text{ i.e. } F_R/ F_R'=1/\gamma_{gp}(R\_x).$$

We call it second kind CCE and shown in Fig. 3.1: As R is changed from less than $l_{c,}$ to greater than $l_{c,}$, the force will pass through 0 and change direction. Partly because second kind CCE, partly because the forces acted on the two sides of critical cylinder are cancelled to each other, the force acted on electron by proton is very weak. Now let us calculate the force as $R=l_{c,}$

The volume of charge ball is: $4\pi b^3/3$

The charge density in charge ball is: $-3e/(4\pi b^3)$

The volume element at R-x is $dv= \pi[b^2\text{-}x^2]dx$

The charge in this dv is

$$-3e/(4\pi b^3)\times\pi[b^2\text{-}x^2]dx=-(3/4)e[b^2\text{-}x^2]dx/b^3$$

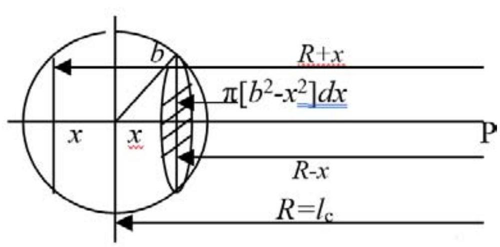

Fig. 4.3: Calculate the resultant force

The total repulsion exerted on electron by proton is:

$$F_i = \int_0^b [\frac{\gamma_s (\mathrm{R - x})}{\gamma_g (\mathrm{R - x})}][\frac{\mathrm{ke}^2}{(\mathrm{R - x})^2}][\frac{3(\mathrm{b}^2 - \mathrm{x}^2)}{4\mathrm{b}^3}]\mathrm{dx}$$

The total attraction exerted on electron by proton is:

$$F_o = \int_0^b [\frac{\gamma_s(R+x)}{\gamma_g(R+x)}][\frac{ke^2}{(R+x)^2}][\frac{3(b^2-x^2)}{4b^3}]dx$$

As $R=l_c$=0.8fm; $b=10^{-18}$m=1am The resultant force is: $F=F_i+F_o$=0.002197 (N), and it is repulsion.
As R=0.8fm the electrostatic force is $F_c=ke^2/R^2$=344.7419 (N), so $F\approx6/10^6\ F_r$ is very weak repulsion.

This is so-called weak interaction acted on electron (by proton). They found this repulsion, and could not think it came from proton, constrained by Coulomb's law. And though it came from lepton.

As l_c is decreased from $R=l_c$, the repulsion F_i is decreased and the attraction F_o is increased. There must exist l_{c2}: $R\text{-}b<l_{c2}<R$, where resultant force F=0. Keep $l_c> l_{c2}$ can keep the resultant force to be repulsion.

Thus, only if $l_{c1}> l_c> l_{c2}$ the system precession can create, the neutron can stably exist. The magnetic resonance therapy just makes l_c to beyond this scope, so that the neutron will decay and epoxide be damaged.

c) The Stable State of Neutron ($l_{c2}< l_c< l_{c1}$)

For proton: The force exerted on proton by electron is: $F=\frac{\gamma_{se}(R)}{\gamma_{ge}(l)}\frac{ke^2}{R^2}=-\frac{ke^2}{R^2}$ where l is the distance from mass center to proton, In terms of $F=ma=\frac{mv^2}{l}=\frac{mc^2l}{l_c^2}$ we have $l_c^2=\frac{mc^2l}{F}$ As l=1.532×10^{-18}m, R=0.8fm the l_{cp} is 0.8fm For electron: $F=ma=\frac{mv^2}{R}=\begin{cases} mc^2R/l_c^2 & R<l_c \\ mc^2l_c^2/R^3 & R>l_c \end{cases}$ We have $l_c^2=\begin{cases} mc^2R/F & R<l_c \\ R^3F/mc^2 & R>l_c \end{cases}$

We know the decreased force F but do not know the decreased mass m. Suppose the decreased force $F=aF_r$ (a<<1), the decreased mass $m=anm_e$ where $F_r=-ke^2/R^2$, is the electrostatic force $m_e=9.09\times10^{-31}kg$ is the rest mass of electron. Thus, we have

$$l_c^2=\begin{cases} nm_ec^2R/F_r & R<l_c \\ R^3F_r/(nm_ec^2) & R>l_c \end{cases}\quad \text{i.e.: } l_{ce}=\begin{cases} c\sqrt{(m_enR)/F} & R<l_{ce} \\ \sqrt{FR^3/(m_enc^2)} & R>l_{ce} \end{cases},$$

Then, take $F=-ke^2/R^2, m_e=9.09\times10^{-31}kg$, R=0.8fm we get following result:

n	l	ω_p	l_{cp}	l_{cei}	l_{ceo}
3.5170	1.532e-018	3.75e+023	8e-016	7.9999e-016	8.0001e-016
3.5171	1.532e-018	3.75e+023	8e-016	8e-016	8e-016
3.5172	1.532e-018	3.75e+023	8e-016	8.0001e-016	7.9999e-016

That means as n=3.5171 $l_{cp}=l_{cei}=l_{ceo}=0.8\times10^{-15}$ m =R, that is a stable self-sustain state

Different deep of critical cylinder passing though the charge ball, corresponding different n, the stable state is different. As n=2.3447 R=1.2fm the critical radius of stable state is $l_{cp}=l_{cei}=l_{ceo}=1.2\times10^{-15}$m as shown in follows:

n	l	ω_p	l_{cp}	l_{cei}	l_{ceo}
2.3444	1.532e-018	2.5e+023	1.2e-015	1.1999e-015	1.2001e-015
2.3447	1.532e-018	2.5e+023	1.2e-015	1.2e-015	1.2e-015
2.3450	1.532e-018	2.5e+023	1.2e-015	1.2001e-015	1.1999e-015

This is why the negative charge can distribute in $[0.5\sim1.5]\times10^{-15}$m so wide area in Fig. 4. 1.

d) The Strong Interaction between Neutrons

Knowing the neutron is consisted of a proton plus an electron, we know the strong interaction between neutrons just is the strong interaction between their protons. and the influence of the electron to other neutrons can be neglected. Consider four-neutron system, their protons distribute at the vertices of a square with side length of $R=\rho_{cp}+b$, as shown in Fig.4.4. Every proton locates Outside Critical Cylinders of both spin and system precession of the other protons, so the four protons attract to each other. The critical radius of magnetic precession of every proton must be greater than $R=\rho_{cp}+b$ for both r_c (relative to lab) and r_c' (relative to its spin), which is kept by electron's magnetic field and enough big of r_c.

Take lab as A, spin of P_1 is A' the magnetic precession of P_1 as A'', the system pres\cession of P_1-$e_1$as A'''

Then, in A''' P_1 is really at rest, the force acted by P_1 on other proton is the real electrostatic force $F'''=-ke^2/R^2$. Transform it into A'', then A', then A, we have:

$$F_R = F_R'''\gamma_s(R)\gamma_m(R)\gamma_g(R)(1-v_s(R)u_s/c^2)(1-v_m(R)u_m'/c^2)(1-v_g(R)u_g''/c^2)$$

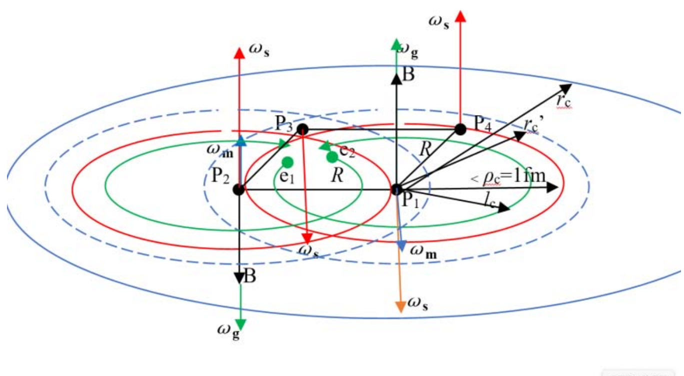

Fig. 4.4: The four-neutron system

The magnetic field passing through every neutron's proton is as follows

$$B_n = 2\gamma_s(R)\gamma_m(R)\gamma_g(R)e[v_s(R)+v_m(R)-v_g(R)]\mu_0/(4\pi R^2))]-ec\mu_0/(4\pi l_c^2)$$

Where the last term come from: $-\gamma_{se}(l_c)\gamma_g(0)ev_{se}(l_c)\mu_0/(4\pi l_c^2)$, that is the obit magnetic field of electron

The stable self-sustaining state is as follows:

$\gamma_s\gamma_m\gamma_g$	B	l_c'	r_c'	r_c set	r_c create
35.4749	3.656e+014	5.1974e-016	1.484e-015	3.0678e-015,	3.0680e-015
35.4753	3.656e+014	5.1974e-016	1.484e-015	3.0679e-015,	3.0679e-015
35.4757	3.656e+014	5.1974e-016	1.484e-015	3.0680e-015,	3.0679e-015

As the four proton are no shift in lab, $u_s=0$, $u_m'=-c\rho_c/R$, $u_g''=c(\rho_c+r_c)/(1+r_c\rho_c)$,

The attraction between two neutrons is as follows:

$$F_R = F_R'''\gamma_s(R)\gamma_m(R)\gamma_g(R)(1-v_s(R)u_s/c^2)(1-v_m(R)u_m'/c^2)(1-v_g(R)u_g''/c^2)$$

$$F_R = 35.5F_R^{'''}(1+\rho_c / r_c')(1-\frac{l_c'}{R}(\frac{r_c'+\rho_c}{1+\rho_c r_c'})) = 29F_R^{'''}$$

Thus, we get the force acted on every neutron's proton of multi-neutron system is as follows

For the proton in 4-neutron system $F=2\sin(\pi/4)\times 29F''=-41ke^2/R^2$。

For the proton in 6-neutron system $F=2\sin(\pi/6)\times 29F''=-29ke^2/R^2$

For the proton in 8-neutron system $F=2\sin(\pi/8)\times 29F''=-22ke^2/R^2$

This is the strong interaction between multi neutrons. Obviously, it is not so strong as that between multi protons. However, the strong interaction between, say, the system consisted of two protons and two neutrons is in the same level as that of four protons. Following is the stable self-sustain state with strong interaction for 2-proton2-neutron system.

γ_p	γ_n	r_{cp}'	r_{cp} (set)	r_{cp}(create)	r_{cn}'	r_{cn}	l_c'
117.6	153.5	9.81e-16	4.95209355e-16	4.95212e-16	1.0157e-15	5.03892e-16	4.475e-16
117.6	153.5	9.81e-16	4.95209356e-16	4.95207e-16	1.0157e-15	5.03892e-16	4.475e-16
117.6	153.5	9.81e-16	4.95209357e-16	4.95204e-16	1.0157e-15	5.03891e-16	4.475e-16

As the four protons are no shift in lab frame, the force exerted on every proton by every neutron is as follows:

$$F_p = 153.5F_R^{'''}\left(1+\left(\frac{\rho_c}{R}\right)\left(r_{cp}'\frac{}{R}\right)\right) = 304F_R^{'''}$$

The force exerted on every neutron by every proton is as follows:

$$F_n = 117.6F_R^{'''}(1+\rho_c/r_{cn}')(1-\frac{l_c'}{R}(\frac{r_{cn}'+\rho_c}{1+\rho_c r_{cn}'})) = 127F_R^{'''}$$

And their stable self-sustain state with sub-strong interaction is as follows

γ_p	γ_n	r_{cp}'	r_{cp} set	r_{cp} create	r_{cn}'	r_{cn}	l_c'
49.0	89.4	8.802e-16	7.34920e-15	7.34923e-15,	9.64518e-16,	2.71829e-14	4.69016e-15
49.0	89.4	8.802e-16	7.34922e-15	7.34922e-15,	9.64518e-16,	2.71830e-14	4.69016e-15
49.0	89.4	8.802e-16	7.34924e-15	7.34921e-15,	9.64518e-16,	2.71830e-14	4.69016e-15

As the four protons are no shift in lab frame, the force exerted on every proton by every neutron is as follows:

$$F_p=89.4\ F_R''(1-(\rho_c/R)\ (r_{cp}'/R))=10.7\ F_R''$$

The force exerted on every neutron by every proton is as follows:

$$F_n=49\ F_R''(1-(\rho_c/R)\ (r_{cn}'/R))(1+(l_c'/R))=3\ F_R''$$

Thus, we know the force acted on neutron is less than that on proton, The MRT just make neutron decay to damage the epoxide to treat cancer. We will give the detail in another paper.

Part 5. How Does Quantum Property Create

a) Quantum Property Comes from the CCE of Field Energy

Now, let us discuss the critical cylinder effect (CCE) of Energy and Mass (E-M) of spinning charged particle, based on thinking its charge *q* to be uniformly distributed in a charge ball of radius *b*, even though the particle may possess complex internal structure.

For the spinning charged particle, take the laboratory as reference frame *A* and the spin of the particle as reference frame A'. In frame A', the particle is indeed at rest, and its electric field is the true electrostatic field. The value of this electrostatic field at a distance *r* from the center of charge ball is:

$$E_r' = \begin{cases} -kqr/b^3, & r < b \\ -kq/r^2, & r > b \end{cases} \tag{5.1}$$

where $k = 1/(4\pi\varepsilon_0)$.

The field energy w' at that point is:

$$w'(r) = (\varepsilon_0/2)E_r'^2 = \begin{cases} (\varepsilon_0/2)k^2q^2r^2/b^6 & r < b \\ (\varepsilon_0/2)k^2q^2/r^4 & r > b \end{cases} = \begin{cases} (1/8\pi)kq^2r^2/b^6 & r < b \\ (1/8\pi)kq^2/r^4 & r > b \end{cases} \tag{5.2}$$

The total field energy of the charged particle in its spinning reference frame is obtained by integrating the energy density $w'(r)$ over the entire three-dimensional space. When this integral is calculated in the (r, φ, θ) sphere coordinate system, the energy inside charge ball, W_i', is:

$$W_i' = \frac{\varepsilon_0 k^2 q^2}{2b^6}\int_0^{2\pi} d\varphi \int_0^{\frac{\pi}{2}} sin\theta d\theta \int_b^{\infty} 2r^4 dr = \frac{kq^2}{10b} \# \tag{5.3}$$

The energy outside charge ball, W_o', is:

$$W_o' = \frac{\varepsilon_0 k^2 q^2}{2}\int_0^{2\pi} d\varphi \int_0^{\frac{\pi}{2}} sin\theta d\theta \int_b^{\infty} \frac{2}{r^2} dr = \frac{kq^2}{2b} \# \tag{5.4}$$

Similarly, the energy outside the ball with radius of *a* (*a*>*b*), W_{ao}', is:

$$W_{ao}' = \frac{kq^2}{2a} \# \tag{5.5}$$

If *a* = 1000*b*, then $W_{ao}' = 0.001W_o'$.This indicates that 99.9% of the energy outside the charged ball is contained within a sphere of radius *a* equals 1000*b*. Conversely, if *a*=2*b*, then $W_{ao}' = W_o'/2$, meaning that half of the energy outside the charged ball is located within the spherical shell defined by *b*<*r*<*2b*. The total field energy in the spinning frame, denoted as W' is given by:

$$W' = W_i' + W_o' = \frac{1.2kq^2}{2b} \# \tag{5.6}$$

For a proton, the charge *q* is 1.602*10^{-19}C. If the radius *b* is 0.9194×10^{-18}m, then the total field energy W' is 1.5053*10^{-10} J. This energy corresponds to the rest mass of $m' = \frac{W'}{c^2} = 1.67252 * 10^{-27}$ Kg, which just is the rest mass of a proton. This leads to the idea that "mass arises from its field energy." This result denotes that the particle's field energy in the spinning frame is a single, definite value, lacking quantum property Thus, we can think the charge of proton (*e*=1.602*10^{-19}C) is uniformly distributed in a ball with radius of *b*=0.6*ke*²/W' = 0.9194*10^{-18} m, that has been used in part 3 and 4.

In terms of energy-momentum transformation:

$$w = \gamma(\rho)\left(w' + v(\rho)p_s'\right) \# \tag{5.7}$$

Global Journal of Research in Engineering (J) XXV Issue I Version I Year 2025

Since the momentum in the spinning frame is zero ($p_s'=0$), Consequently, the field energy at $r=\sqrt{\rho^2+z^2}$ from the center of the charged ball in the laboratory frame A can be expressed as follows:

$$w(\rho)=\begin{cases}\frac{\gamma(\rho)\left(\frac{\varepsilon_0}{2}\right)k^2q^2r^2}{b^6} & r<b\\ \frac{\gamma(\rho)\left(\frac{\varepsilon_0}{2}\right)k^2q^2}{r^4} & r>b\end{cases} \quad \# \tag{5.8}$$

where
$$\gamma(\rho)=\begin{cases}\frac{1}{\sqrt{1-\left(\frac{\rho}{\rho_c}\right)^2}},\rho<\rho_c\\ -\frac{1}{\sqrt{1-\left(\frac{\rho_c}{\rho}\right)^2}},\rho>\rho_c\end{cases}$$

The total field energy of a spinning charged particle in the laboratory frame is obtained by integrating the energy at each point: $w(\rho)$, over the entire three-dimensional space. However, since $w(\rho)$ depends on $\gamma(\rho)$ and the expression of $\gamma(\rho)$ in ICC differs that in OCC, this integration must be divided into four distinct parts:

(A) W_1 for the region where $b<\rho<\rho_c$

(B) W_2 for the region where $\rho_c<\rho<\infty$

(C) W_3 for the region where $\rho<b, z>\sqrt{b^2-\rho^2}$

(D) W_4 for the region where $\rho<b, z<\sqrt{b^2-\rho^2}$

These regions are illustrated in Figure 5.1.

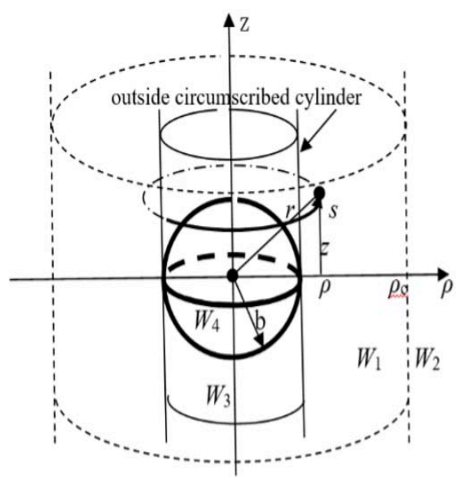

Fig. 5.1: Charge Ball and Critical Cylinder

For the location of $b<\rho<\rho_c$, the energy W_1 is given by

$$W_1=\frac{\varepsilon_0k^2q^2}{2}\int_b^{\rho_c}\frac{d\rho}{\sqrt{1-\rho^2/\rho_c^2}}d\rho\int_0^{2\pi\rho}ds\int_0^{\infty}\frac{2dz}{(\rho^2+z^2)^2} \tag{5.9}$$

Note that: $\int_0^{\infty}\frac{dz}{(\rho^2+z^2)^2}=\left[\frac{z}{2\rho^2(\rho^2+z^2)}+\frac{\arctan\left(\frac{z}{\rho}\right)}{2\rho^3}\right]_0^{\infty}$

$$=\frac{\pi(n\pm\frac{1}{2})}{2\rho^3},n=0,1,2,\cdots$$

Thus,
$$W_1=\frac{kq^2}{4}\pi\left(n\pm\frac{1}{2}\right)\int_b^{\rho_c}\frac{\rho_c d\rho}{\rho^2\sqrt{\rho_c^2-\rho^2}}d\rho$$

$$= \frac{kq^2}{2b}\frac{\pi}{2}\left(n \pm \frac{1}{2}\right)\sqrt{1 - \frac{b^2}{\rho_c^2}}, \mathrm{n} = 0,1,2,\cdots \# \tag{5.10}$$

For the location of OCC where $\rho_c < \rho < \infty$, we have:

$$W_2 = \frac{\varepsilon_0 k^2 q^2}{2}\int_0^{2\pi\rho} ds \int_{\rho_c}^{\infty} -(1-\rho_c^2/\rho^2)^{-1/2}\, d\rho \int_0^{\infty} \frac{2dz}{(\rho^2+z^2)^2}$$

$$= \frac{kq^2}{4}\pi(n \pm \frac{1}{2})\int_{\rho_c}^{\infty} \frac{-d\rho}{\rho\sqrt{\rho^2-\rho_c^2}} = -\frac{kq^2\pi(n \pm \frac{1}{2})}{4}\left(\frac{arccos(\rho_c/\rho)}{\rho_c}\right)\Big|_{\rho_c}^{\infty}$$

$$W_2 = -\frac{kq^2\pi^2}{4\rho_c}\left(n \pm \frac{1}{2}\right)\left(m \pm \frac{1}{2}\right), \quad n = 0,1,2,,\cdots, m = 0,1,2,\cdots \# \tag{5.11}$$

The total energy outside the circumscribed cylinder of the charge ball in the laboratory frame A is:

$$W_1 + W_2 = \frac{kq^2}{2b}\frac{\pi}{2}\left\{\sqrt{1-\frac{b^2}{\rho_c^2}} - \frac{b\pi}{\rho_c}\left(m \pm \frac{1}{2}\right)\right\}\left(n \pm \frac{1}{2}\right),$$

$$n = 0,1,2,\cdots, m = 0,1,2,\cdots \# \tag{5.12}$$

This implies that the energy of a spinning charged particle in the laboratory frame has multiple values, leading to the mass also having multiple values. This characteristic is referred to as the quantum property of a spinning charged particle. Clearly, this quantum property arises from the critical cylinder effect (CCE). The factor ($n\pm1/2$), $n=0$, 1, 2…. represents both the principal quantum number n and the spin quantum number $s=\pm1/2$. Meanwhile, the factor ($m\pm1/2$), $m=0$, 1, 2, …, accounts for the Zeeman splitting .

Similarly, the energy within the circumscribed cylinder of the charge ball, but outside the charge ball itself, is described by the following expression.

$$W_3 = \frac{\varepsilon_0 k^2 q^2}{2}\int_0^b \gamma(\rho)d\rho \int_0^{2\pi\rho} ds \int_{\sqrt{b^2-\rho^2}}^{\infty} \frac{2dz}{(\rho^2+z^2)^2} \tag{5.13}$$

Unfortunately, this expression does not have an analytic solution. However, it must be multivalued because it includes the integral of $\int_{\sqrt{b^2-\rho^2}}^{\infty}\frac{2dz}{(\rho^2+z^2)^2}$:

The total energy within the charge ball is given by the following expression, which lacks an analytic solution:

$$W_4 = \frac{\varepsilon_0 k^2 q^2}{2b^6}\int_0^b \frac{2d\rho}{\sqrt{1-\frac{\rho^2}{\rho_c^2}}} d\rho \int_0^{2\pi\rho} ds \int_0^{(b^2-\rho^2)^{\frac{1}{2}}} (\rho^2+z^2)dz \# \tag{5.14}$$

In addition to spin, charged particles can exhibit other types of rotation, such as magnetic precession and system precession. Each type of rotation has its own CCE, which can result in the energy having multiple values. These variations in energy are the sources of what are known as the magnetic and angular quantum numbers. The presence of these quantum numbers reflects the complex rotational dynamics of charged particles, contributing to their unique quantum properties.

b) The Field Energy and Mass of Proton

For proton, where $\rho_c=10^{-15}$m>>$b=0.9194\times10^{-18}$m, neglecting b/ρ_c, following Eq. (5.12)

$$W_1 + W_2 = \frac{kq^2}{2b}\frac{\pi}{2}\left\{\sqrt{1-\frac{b^2}{\rho_c^2}} - \frac{b\pi}{\rho_c}\left(m \pm \frac{1}{2}\right)\right\}\left(n \pm \frac{1}{2}\right)$$

can be expressed as follows:

$$W_1 + W_2 = \frac{kq^2}{2b}\frac{\pi}{2}\left(n \pm \frac{1}{2}\right), n = 0,1,2,\cdots,$$

The difference between n=1 and n=0 is called quantum interval, and is $\Delta W = \frac{kq^2}{2b}\frac{\pi}{2}$

Substituting b=0.9194×10^{-18}m, K=8.988×10^{9}, q=1.602×10^{-19}C the quantum interval of energy for proton is as follows: $\Delta W = \frac{kq^2}{2b}\frac{\pi}{2} = 1.9705 \times 10^{-10}(J)$

Note that ρ_c=c/ω_s=10^{-15}m means the spin angular velocity is ω_s= c/ρ_c=3×10^{23} (r/s), we have.

$$\Delta W / \omega_s = 6.5683 \times 10^{-34}(Js)$$

This indicates that the energy quantum interval ΔW is proportional to ω_s, with a proportionality constant of 6.5683×10^{-34} (Js), which corresponds to Planck's constant: h=6.6256×10^{-34}(Js),.

The critical radius associated with the spin of a proton is approximately $\rho_c = 10^{-15}$ m, which is thousand times larger than b. As result, over 99.9% of the proton's energy or mass is contained within ICC. This significant concentration allows us to neglect the mass present in the OCC and the multivalued property given by m=0,1,2,3….

c) *The Energy-Mass of electron and Dark Mass*

In contrast, the critical radius of an electron's spin is closely aligned with the charge ball's radius. This proximity necessitates considering the field energy of the electron in both ICC and OCC. The total energy in the OCC is not only multivalued but also negative, allowing it to cancel the positive energy in the ICC. Assuming the radius of the electron's charge ball is the same as that of the proton, due to their identical absolute charge, the critical radius for the electron's spin should be ρ_c=1.16×10^{-18} m.

In this scenario, for the state characterized by n=0, s=1/2, and take (m±1/2) to be 1/2, the total energy in the OCC is:

$$W_2 = -\frac{kq^2\pi^2}{16\rho_c} = -12.266 * 10^{-11}\ (J)$$

The energy outside circumscribed cylinder of charge ball but within critical cylinder is:

$$W_1 = \frac{kq^2}{2b}\frac{\pi}{4}\sqrt{1 - b^2/\rho_c^2} = 5.91145 * 10^{-11}(J)$$

The energy within the charge ball can be determined through numerical integration, $W_4 = \frac{\varepsilon_0 k^2 q^2}{2b^6}\int_0^b \frac{2d\rho}{\sqrt{1-\rho^2/\rho_c^2}} d\rho \int_0^{2\pi\rho} ds \int_0^{(b^2-\rho^2)^{1/2}} (\rho^2 + z^2)dz$ =3.01*10^{-11}(J)

Using numerical integration, the energy within the circumscribed cylinder of the charge ball but outside the charge ball itself is calculated as follows:

$$W_3 = \frac{\varepsilon_0 k^2 q^2}{2}\int_0^b \gamma(\rho)d\rho \int_0^{2\pi\rho} ds \int_{\sqrt{b^2-\rho^2}}^{\infty} \frac{2dz}{(\rho^2 + z^2)^2} = 3.35 * 10^{-11}\ (J)$$

Thus, the total energy of a spinning electron in the laboratory frame for the state characterized by m=0, n=0, s=1/2 is as follows:

$$W = W_1 + W_2 + W_3 + W_4 = 8.2 \times 10^{-14} \text{J}.$$

This energy corresponds to a mass of m=W/c^2=9.1×10^{-31} Kg that is well known electron's mass.

In spin frame, the mass of an electron is calculated as 0.6ke^2/b= 1.6725×10^{-27}Kg, However, in the laboratory frame, it is 9.1×10^{-31}Kg. The difference of 1.6716×10^{-27}Kg is referred to as "dark mass," which can be partially "relit" by other types of rotations, such as magnetic precession or system precession.

This understanding not only reveals the source of quantum properties but also elucidates the origins of mass and dark mass. In the laboratory frame, mass is distributed on either side of the critical cylinder with opposite signs, effectively canceling each other out. The so-called rest mass of charged particles in the laboratory frame is merely the remainder after this cancellation, rather than the true rest mass in the spin frame. Therefore, what is termed "dark matter" is simply the portion of mass that is canceled out in the laboratory frame; it exists in spinning frame but remains undetectable in the laboratory frame.

It should be pointed out that the dark matter mentioned here is not the same thing as that mentioned by the academic community.

According to Newton's law, the gravitational pull of a galaxy with mass M on a planet with mass m is $F=GMm/R^2$. The centripetal acceleration produced by the planet under this gravitational pull is $a=v^2/R$, where v is the tangential velocity of the planet. According to $F=ma$, $v=(GM/R)^{1/2}$ can be obtained, that is, the farther the distance, the slower the velocity.

However, when observing the rotation of spiral galaxies, it is found that the tangential velocity of the planets at the edge of the galaxy increases with distance, and according to $v=(GM/R)^{1/2}$, scholars believe that this indicates that the mass M increases with distance, so they propose that there is a kind of "dark matter" that we cannot see around the galaxy. This material exerts an additional gravitational pull on the planets at the edge of the galaxy, causing them to rotate faster.

We don't think such dark matter exists. The original reason of the rotation speed of the planet does not decrease but rises with distance, not the existence of dark matter, but the relativistic effect of rotation. To simplify the discussion, let's consider the force of a central planet with mass M on a marginal planet with mass m, when the central planet spins with ρ_c and rotates with the marginal planet around their mass center with the critical radius of lc. Take lab as frame A, system precession as A', the spin of central planet as A", then in A" the force acted by M on m is $F''=GMm/R^2$, but in lab frame it becomes follows

$$F = \gamma_s(R)/\gamma_g(R)\frac{GMm}{R^2} = \frac{\sqrt{1 - R^2/l_c^2}\,M}{\sqrt{1 - R^2/\rho_c^2}}\frac{Gm}{R^2}$$

where R is the distance between two planets and when it is far less than lc, this equation can be simplified as:

$$F = \gamma_s(R)\frac{GMm}{R^2} = \frac{M}{\sqrt{1 - R^2/\rho_c^2}}\frac{Gm}{R^2} \quad \cdots\cdots\cdots \quad v=(\gamma_s GM/R)^{1/2}$$

When R increases and approaches ρ_c, M does not change but the Lorentz factor γ_s increases, causing the rotational velocity of the marginal planets to increase. This is relativistic effect but not dark matter.

d) How Does Gravitation Create

Mass comes the field energy; the gravitation must be related to electromagnetic force. It comes from the CCE of electron's spin, i.e.: the electron attracts the other electron inside critical cylinder and repels the electron outside critical cylinder.

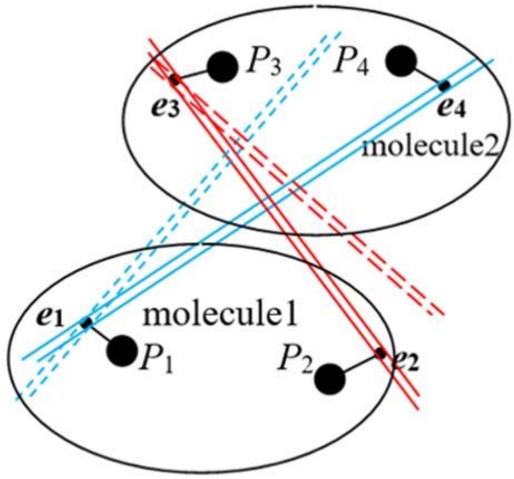

Fig. 5.1: Gravity comes from CCE

Consider the four proton-electron (p-e) pairs located in two molecules as shown in Fig. 5.1 As the spin critical cylinder (SCC) of e_1 doesn't include p_3-e_3 and p_4-e_4, it attracts p_3p_4, repels e_3e_4 , the resultant force is F=0. As the SCC of e_1 includes, say, e_4, it attracts p_3 p_4 and e_4, repels e_3, the resultant attraction is $F=-2ke^2/R^2$

Similarly, as the spin critical cylinder (SCC) of e_3 includes e_2, molecule 2 attracts molecule1 with the same $F=-2ke^2/R^2$. These two attractions are the source of gravitation.

The distance between molecules is on the level of $R=10^{-9}$m, and the critical radius of electron's spin is $\rho_{ce}=10^{-18}$m, the probability by which the SCC of e_1 includes e_4 is:

$$\pi\rho_{ce}^2/(4\pi R^2)=10^{-36}/(4\times10^{-18})=0.25\times10^{-18} .$$

Similarly, the probability by which the SCC of e_3 includes e_2 is the same 0.25×10^{-18}. The probability of these two events happens in the same time is 6.25×10^{-38}. That means the gravitation is only on the 10^{-38} level of electromagnetic interaction, which is known by modern physics.

Obviously, the gravitation is proportional to the number of electrons in a body. And in the natural body the number of electrons is equal to the number of protons (the neutron is consisted of a proton and an electron), so the number of electrons is proportional to the mass of the body. That made Newton thought the gravitation came from mass.

II. Conclusion

1. Cancer and cardio- and brain-vascular diseases are top two killers of mankind. MRT can not only treat but also prevent them. Besides, MRT can treat lots of other diseases caused by oxidation. Once it is popularized into every family, the level of health will be increased.
2. The Relativity for Rotational Frames reveals lots of natural laws, which are unknown for modern physics, such as space time exchange, the tangential velocity for OCC is $c^2/(\rho\omega)$, the critical cylindrical effects, which indicate the force will change direction, as the acceptor is changed from ICC to OCC, and is verified by our experiment
3. Strong, weak and gravity are all electromagnetic interaction suffered from different Critical Cylinder Effects (CCE).
4. Only based on relativity for rotational frames the research about both astronomy and basic particles can touch the essence.
5. The quantum property comes from the CCE of field energy The uncertainty of particle world comes from the stochastic direction of donor's spin axis. We open a way to unify the quantum mechanics with relativity.

Acknowledgements

A special acknowledgment is due to our Guides and teachers and Dr. C.N. Yang, Dr. H. T. Nieh and Dr. P. Lauterbur in the State University of New York at Stony Brook, and Dr. R. A. Scheuing, Dr. T. C. Fang in the Grumman Aerospace Corporation for their kindly inviting and supporting me to do some research work in the SUNY at Stony Brook. A special acknowledgment is due to Prof. B. Nordenström in Karolinska Medical Institute and Prof. Y. L. Xin in Chinese-Japanese Friendship Hospital for their kindly inviting me to do some research work about Electric-Chemical Therapy of cancer. I wish to thank Prof. S. Zhou and Prof. Y. C. Chi in Chinese-Japanese Friendship Hospital for their kindly helping us to do the cells and animals experiments of MRT. I wish to thank Prof. D. C. Tao in Analogic Corporation and Prof. J. Z. Hoang in Hang Zhou Railroad Central Hospital for their kindly supporting us to do the clinical experiments of MRT. A special hallow is due to the volunteers. At last thanks editorial department of AJBSR and editor Elena Moore for their work in publishing this booklet.

References Références Referencias

1. James D. Watson, Molecular Biology of the Gene, W. A. BENJAMIN INC. 1977.
2. Yin Rui, Rotating Lorentz Transformation and Unification of Forces, B.U.A.A. Press, Beijing, 1997.
3. Yin Rui, Unification of Forces According to Relativity for Rotations, H Adronic Journal, Volume 23, Number 5, October 2000, pp. 487-549. (Note: page 497 should be between 492 and 493).
4. C. Møler, THE THEORY OF RELATIVITY, Clarendon Press Oxford 1972.
5. Zhang San-Hui, Physics in University Tzing-Hua UniversityPress 2009.
6. Yin Rui, Yin Ming, Wang Yang: Critical cylindrical Effect and space-time exchange in rotational reference frames of special relativity; World Academy of Science, Engineering and technology (Physical and Mathematical Sciences) Online ISSN 1307 6892.
7. Yin Rui, Yin Ming, Wang Yang: Magnetic Resonance Therapy (MRT) and Relativity America Journal of Biomedical Science & Research 2024, Tissue 5.
8. Yin Rui, Yin Ming, Wang Yang: Magnetic Resonance Therapy (MRT) Treat cardio- and brain-vascular diseases America Journal of Biomedical Science & Research 2024, Tissue 6.

This page is intentionally left blank

Global Journal of Researches in Engineering: J
General Engineering
Volume 25 Issue 1 Version 1.0 Year 2025
Type: Double Blind Peer Reviewed International Research Journal
Publisher: Global Journals
Online ISSN: 2249-4596 & Print ISSN: 0975-5861

Impact of Cost Overruns on Infrastructure Projects Failures and Effective Cost Management to Reduce Overruns

By Ahmed Mohamed Nabil
Cairo University

Abstract- This research is to investigate and analyze the reasons behind cost overruns in infrastructure projects compared to the planned costs. It also delves into establishing procedures for effectively monitoring and controlling project costs and measuring cost performance indicators throughout the project lifecycle. To achieve these goals, the research addresses three key questions that provide clarity on the research objectives. The research questions primarily focus on the estimation of risk costs for construction and infrastructure projects as an integral part of project knowledge areas. Additionally, the study analyzes the actual cost estimation methods employed by construction organizations and seeks to develop project cost management as an integrated part of all project knowledge areas, thereby enhancing the procedures for monitoring and controlling costs.

Keywords: cost overrun, cost management, infrastructure projects, faulted projects, water and wastewater projects, root cause of failure project, cost management, water & wastewater.

GJRE-J Classification: LCC Code: TA190

IMPACTOFCOSTOVERRUNSONINFRASTRUCTUREPROJECTSFAILURESANDEFFECTIVECOSTMANAGEMENTTOREDUCEOVERRUNS

Strictly as per the compliance and regulations of:

Impact of Cost Overruns on Infrastructure Projects Failures and Effective Cost Management to Reduce Overruns

Ahmed Mohamed Nabil

Abstract- This research is to investigate and analyze the reasons behind cost overruns in infrastructure projects compared to the planned costs. It also delves into establishing procedures for effectively monitoring and controlling project costs and measuring cost performance indicators throughout the project lifecycle. To achieve these goals, the research addresses three key questions that provide clarity on the research objectives. The research questions primarily focus on the estimation of risk costs for construction and infrastructure projects as an integral part of project knowledge areas. Additionally, the study analyzes the actual cost estimation methods employed by construction organizations and seeks to develop project cost management as an integrated part of all project knowledge areas, thereby enhancing the procedures for monitoring and controlling costs.

To ensure comprehensive findings, the research employs the descriptive statistical analytical approach. The quantitative method involves a survey questionnaire administered to 462 respondents, while the qualitative approach involves analysis for case studies. By utilizing a descriptive approach, the research provides an in-depth exploration of the research questions from various perspectives. Based on a thorough literature review, three research hypotheses were formulated and subsequently validated during the discussion and analysis of the research questions. The results of the study affirm the positive validation of these hypotheses. The empirical findings reveal the following:

Accurate study of project costs during the initial stages of the project has a positive impact on controlling cost overruns.

Effective management of the project risk plan, including the identification, analysis, and control of risks, positively contributes to controlling cost overruns.

The utilization of the Earned Value Management (EVM) method throughout the project lifecycle serves as a strong indicator that assist in monitoring and controlling project cost overruns.

In conclusion, this research provides valuable insights into the reasons for cost overruns in construction projects and infrastructure. It also offers practical procedures for monitoring and controlling project costs, as well as essential cost performance indicators throughout the project lifecycle. The research findings confirm the importance of managing project risk, conducting accurate cost estimations, and utilizing effective project management methods to prevent cost overruns.

Author: *PhD, MSc, PMP. Faculty of Graduate Studies for Statistical Research, Cairo University. e-mail: ahmed_nabil6@hotmail.com*

Keywords: cost overrun, cost management, infrastructure projects, faulted projects, water and wastewater projects, root cause of failure project, cost management, water & wastewater.

I. Introduction

Project cost management is the backbone of project completion within the scope of the contract, which the project costs aim at estimating the financial resources required for the project, aggregating those cost estimates, and working on monitoring and controlling the budget of the project so that the project is completed within the specified budget to control the variables that would affect the cost at different stages of the project. Infrastructure and construction projects evolve rapidly regarding their diversity, size, and financial budget, and to keep up with that development need to adapt to contemporary changes, e.g. (dynamic project performance, flexibility to change, quality assurance, and human resource performance). The impact of this development is illustrated in project processes from initiation to close. Therefore it should be used dynamic project management tools to analyse the cost elements for these projects.

The importance of this research is to study and analyse the radical reasons for exceeding the actual cost of construction and infrastructure projects compared with the planned cost, and then find adequate procedures capable of controlling the costs of projects within the specified framework and without cost overrun, and measure the performance of these costs throughout the project lifecycle, and to reveal gaps and deviations from the planned cost. According to Vrijling & Redeker (1993), there are many projects where actual costs exceed planned costs, especially infrastructure projects.

Based on the foregoing, where the infrastructure projects are the core of all construction projects, so it is should be to shed light closely on the infrastructure projects that have been affected, either by suspensions or by failures as a result of cost overruns for these projects.

II. Study Background

Completing the project on time and within budget is a primary goal for all projects. The purpose of project cost management is to provide management team better and more effectively estimate, monitor, and control project costs.

The research has two main types of variables, as following:

1. The dependent variable, which is (Infrastructure Projects Failures).
2. The independent variable, which is (Cost Overrun).

The independent variables are related to three dimensions, which are and according to The Project Management Book of Knowledge (PMBOK).

- The First dimension: Project costs
- The Second dimension: Managing the project risk plan paragraphs.
- The Third dimension: Earned value management (EVM) paragraphs.

The dependent variables are related to Infrastructure Projects Fail.

III. The Primary Objectives of the Research

The research aims to study the root causes for increasing the planned cost compare with the actual costs for construction and infrastructure projects. As well as recommendations for procedures that are recommended to be followed in order not to fall into cost overruns. The status quo of cost estimation methods for several infrastructure projects will be analyzed and develop the best practice manner by achieving integration and incorporating cost management tools in a way that contributes to achieving effective control on cost overruns and rational decision-making. Consequently, the primary objectives of the research will address that:

1. Analyzing the actual cost estimation methods in construction organization and developing project cost management as an integrated part of all project knowledge areas, e.g. (Schedule, Resource, Risk, Procurement) thus contributing to the achievement of effective control and monitoring over cost elements and making rational decisions.
2. Cost estimation of risk for construction and infrastructure project where is an embedded of project knowledge areas, which aims at estimating the total cost of construction projects and according to project scope, time, quality, which is usually close to the actual cost.
3. Monitoring and measuring projects performance with an effective tool and develop a proposed procedure to improve the process of monitoring the performance of project costs and make some recommendations and proposals.

IV. The Research Questions

The research aims to study the causes for increasing the planned cost compare with the actual costs for construction and infrastructure projects. The research will discuss and answer three main questions, and that will be through subsidiaries questions will be exposed in detail by questionnaire, so the three main questions are:

A. What is the effect of cost estimating a rough order of magnitude (ROM) during the roll-out phase on final project budget cost?
B. What is the effect of estimated costs of risk on project budget cost and their relation to a cost overrun?
C. Is the Earned Value Management (EVM) method used to monitor and measure the performance of project costs and detect cost overruns early during all project processes?

V. Research Hypothesis (Assumption)

a) Development of Main-Hypothesis (H0)

There is no Statistical relation between the Cost Overruns (Project costs, managing the project risk plan, Earned value management (EVM)) and Infrastructure Projects Failures).

b) Development of Sub-Hypothesis (H1)

H1: Study of project costs accurately during the roll-out phase will contribute positively to controlling cost overruns.

c) Development of Sub-Hypothesis (H2)

H2: Managing the project risk plan, e.g., (identify, analysis, and control risks) of each project will contribute positively to controlling cost overruns.

d) Development of Sub-Hypothesis (H3)

H3: Using Earned value management (EVM) method during the project lifecycle will provide strong indicators that contributed to monitor and control project cost overruns.

VI. Research Methodology (Research Design and Approach)

Based on the nature of the study and the objectives it seeks to achieve, the researcher has used the descriptive statistical analytical approach, which depends on the study of the phenomenon as it exists in reality, is interested as an accurate description, and expresses it qualitatively and quantitatively. This approach is not satisfied with collecting information related to the phenomenon in order to investigate its various manifestations and relationships, but goes beyond it to analysis, linking and interpretation to reach conclusions on which the proposed perception was built and the field study method has been relied upon to achieve the study objectives. A quantitative approach is based on statistical and estimate processes. Therefore, it is concerned with the variables that include the measurement of the characteristics. A quantitative approach aims to test and validate hypotheses; this is performed by defining the hypotheses that already exist in the previous literature, where the relations between the variables are assumed, and the data are collected and analysed statistically, and based on the results obtained, the hypotheses are accepted or rejected. According to Kothari, C. R. (2004) who indicated that the quantitative approach seeks to obtain the causes and facts and the relationships between variables so that these variables can explain cause-and-effect relationships, and it becomes possible to arrive at accurate predictions about phenomena under study. The data will be presented by using statistical programs such as (SPSS, Excel Sheets, Smart-PLS).

VII. The Literature Review

Estimating project costs requires proper planning which contributes to estimating the cost of each activity in the project accurately, specifying the control thresholds for the variables that occur in the project cost management and the permitted flexibility limits associated with the variables e.g. (construction risk, cost reserve) that take place in the project during the different stages of the work. Based on that, the poor planning, and the inability to meet the needs of projects on time within the project budget cost will lead to cost overrun.

Accordingly, the researchers have studied the impact of independent and dependent factors and diversity variables on the project cost management; The research review a number of the literature of these researchers and studies among years (1996-2023) as shown in summary in table No. 1 as shown below:

Table No. (1): Summary of Literature Review

Year	Author's	Research Title	Approach	Research Dimension	Results	Critical Analysis the Studies
1996	Fleming & Koppelman	Forecasting the final cost and schedule results	Statistical Analysis	Cost Performance Measure	The result of the research was that two tools could be used to measure the project's performance time and cost critical path method (CPM), despite the limited use of the Earned Value.	Due to the ever-changing nature of the industry, these techniques may not accurately predict the final outcomes.
2002	Flyvbjerg et al.,	Cost Underestimation in Public Works Projects	Statistical Analysis	Technical, economic, psychological, and political	Decision making, tender, and the contract should be accurately studied during the planning process	Love et al., (2002) criticized Flyvbjerg's research, where they indicated that the cons of the research approach which did not include different management cultures, inflation, and market volatility factors were not considered, as well the pros were an Experimental study of the theory, which ensures confirmation of the hypotheses.

Global Journal of Research in Engineering (J) XXV Issue I Version I Year 2025

2004	Reilly & Brown	Management and Control of Cost and Risk for Tunnelling and Infrastructure Projects	Method for estimating project risks	Cost Estimate Validation Process	There is potential to realize cost savings and reduce risks	Although this approach noted the critical role of risks costs in infrastructure projects, this approach did not illustrate how to use risk analysis and assessment in other construction projects.
2007	L Bergkvist and B Johansson's	Evaluating Motivational Factors Involved at Different Stages in an IS Outsourcing Decision Process	Qualitative method	Decision Making, tendering, contract	Decision making is a key factor in ensuring that projects reach their goals and objectives	The research did not recommend a clear structure of decision-making powers, which is considered the only way to influence the success of the project in a positive way.
2007	Zwikael & Sadeh	Risk Management	Constructionist epistemology	Risk	Risk has direct impact can have a crucial effect on the productivity of work	Therefore, one of the research weaknesses is that did not address how to estimate risk costs.
2010	Love et al.,	Rework in Civil Infrastructure Projects	Questionnaire survey	Rework	§ Lack of defined working procedure. § Changes made at the request of the customer. § The inefficient use of information technology. § Lack of transparent contractor procedures to improve quality. § Effective Participation of stakeholders in the project	No recommendation about how to budget cost control should be considered in the early stages of project planning in order to ensure that the project is completed on time and within the allocated budget.
2010	Olawale & Sun	Cost and Time Control of Construction Projects	Quantitative and qualitative methods	Design, time, resources	Explore the relationship between project budget and schedule, as well as their impact upon results	The research did not indicate what type of skills are necessary to control project budget.
2010	Ahsan K and I Gunawan	Analysis of Cost and Schedule Performance of International Development Projects	Qualitative method	Cost, Schedule	Cost and Schedule should be managed effectively to achieve successful project results	The research did not elucidate what an effective method of cost management means.

2011	Doloi H.	Cost Overruns and Failure in Project Management	Qualitative	Project Document	Tender and contract processes are also critical	The research does not highlight the appropriate tools and procedures for studying and analyzing bids that ensure cost control
2011	Zwikael & M. Ahn,	Risk management process	Quantitative	Risk	Risk has direct impact and can have a crucial effect on the productivity of work	The research does not provide guidance into calculating and estimating the cost of risk, as well as the types of risk to be taken into consideration
2012	Chen and Zhang	Accuracy of cost and schedule forecasting in construction projects.	Quantitative	Schedule	§ Complexity of construction § Unpredictability of external factors	The research does not indicate that this is what means the risks of the project can be controlled if they are studied more deeply during the planning process.
2012	Doloi H.	Cost Overruns and Failure in Project Management	Survey and case study	Cost Baseline	Communication between the project management team and key stakeholders should be activated to reduce cost Overruns	The research lacks a vision of the effective structure for managing communication between stakeholders, as well elucidate communication channels and levels of powers and responsibilities.
2012	Lopez et al.	Design Error Costs in Construction Projects	Survey	Design	Significant relationship between the design error costs and the types of procurement methods	The research did not indicate any effective methods necessary to manage project planning within the specified budget
2014	Gul Polat et al.,	Factors Affecting Cost Overruns in Micro-scaled Construction Companies	Qualitative methods	Design important factors that may cause cost overruns in construction projects	Design problems and delays in design approvals.	The design cannot represent the essential element for cost overrun. The cost had to be taken into consideration as the design changed after another, which is the effective management and risks
2016	Swapnil P. Wanjari and Gaurav Dobariya	Identifying factors causing cost overrun of the construction projects in India	Survey	The impact of raw material prices on cost overruns	Raw material prices have a direct impact on cost overruns	The research doesn't refer to the inflation expected for raw materials as a negative risk, so it should be considered as an embedded essential knowledge area from the cost baseline
2017	Flyvbjerg	The Iron Law of Megaproject Management	Qualitative methods	External Factors	Cultural, inflationary, and volatile market factors	The research does not address the necessary procedures to control such factors.

2017	Nabil Al Hazem et al.,	Delay and cost overrun in infrastructure projects in Jordan	Quantitative	External Factors	Terrain conditions, weather conditions, variation orders, and unavailability of laborer's	But the research has limited the place in which the causes of cost overruns have been studied, and the research has not concluded what are the effective method to address cost overruns in similar projects, even if they are similar in nature of the location.
2018	Flyvbjerg et al.,	Planning Fallacy or Hiding Hand: Which is the Better Explanation	Quantitative	Risks	Unaccounted factors could lead to increased costs and delays	The research did not consider different management cultures, inflation, and market volatility factors, and thus overlooked potential cons. As well the research does not provide comprehensive insight into project performance and its analysis may be missing important factors. Therefore, research should include a wide range of factors to provide a more thorough understanding of the implications of major projects.
2020	Marey-Perez et al	Delays and cost Overrun Causes in Construction Projects of Oman	Quantitative	Change Scope, Decision Making	Change Scope, delay in decision Making	Project delays are a frequent occurrence in the world of project management; Therefore, the research did not address what are the root causes that delayed the project, and it is expected that costs will be exceeded due to them.
2023	Osama A. et al.,	Investigation of critical factors affecting cost overruns and delays in Egyptian mega construction projects	Survey	Suspension of works, Low experience of design firm, delay between procurement phase and design phase, variation order, force majeure, and lack of supervision	It was found that 24 refined main factors are responsible for cost overrun and delays	The dataset may not cover the entire spectrum of construction projects in Egypt, which could limit the generalizability of the findings.

a) Cost Baseline and Cost Control

The process of aggregating the estimated costs of individual activities or work packages to establish an authorized cost baseline. Cost control is the process of monitoring the status of project expenses, updating project budgets, and managing budget-based changes. Budget updates include a monthly record of actual costs incurred to date and tracking of approved but not yet realized costs (accrued and deferred). Adjustments to the baseline budget to address overspending should only be made through an integrated change control process. Inputs to cost management include project management plans, project funding requirements, performance information, and organizational process resources.

VIII. Importance of Water and Wastewater Projects

In the 20th century, water and wastewater infrastructure projects became more standardized and regulated. Governments and international organizations started taking a more active role in providing clean water and improved sanitation to their citizens. As shown in Fig. 1.1 the impact of lack of water and wastewater on citizens.

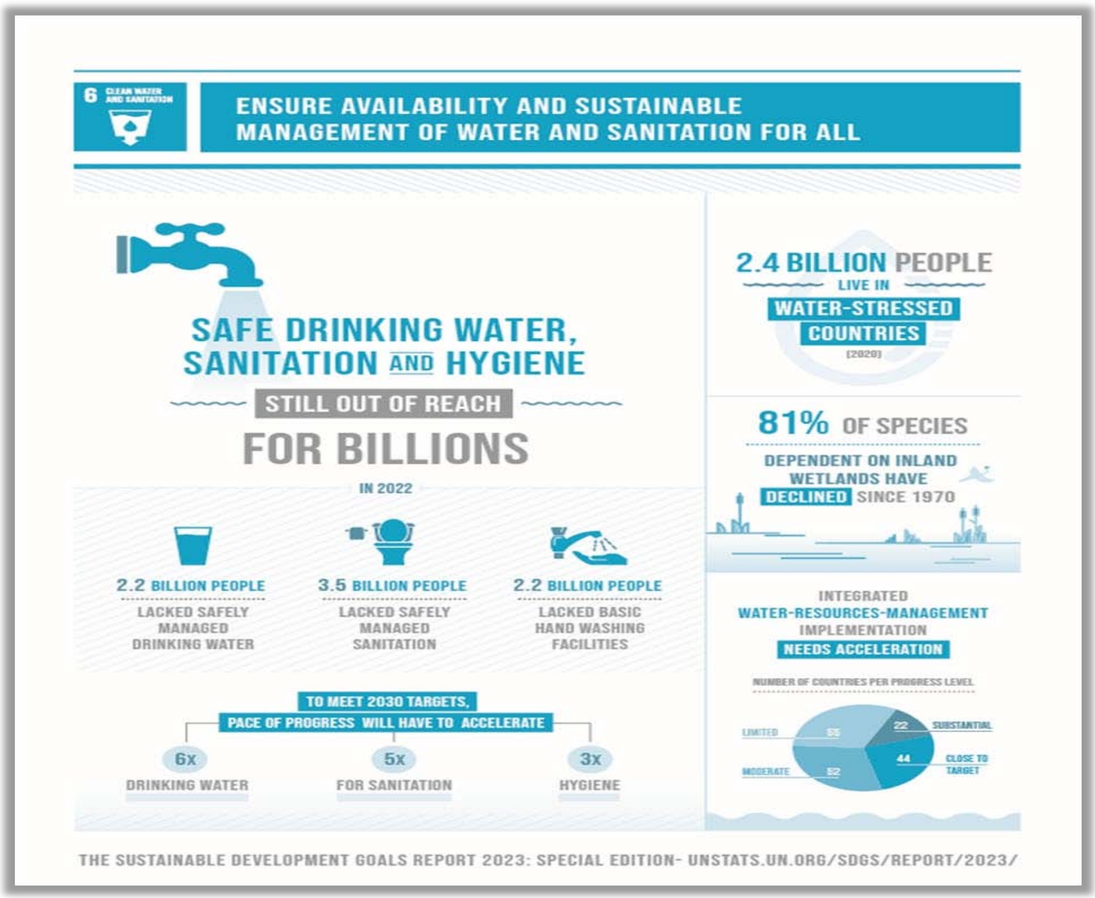

United Nation- Report 2023

Figure 1.1: Impact of Lack of Water and Wastewater Projects

In today's world, water and wastewater projects play a crucial role in sustaining thriving communities and ensuring the well-being of its residents. However, these projects often face significant challenges, with cost overruns being a recurring issue that hinders their success. This research aims to delve into the complexities of faulted water and wastewater projects, specifically focusing on the detrimental effects of cost overruns. Through a comprehensive analysis, it becomes evident that faulty planning and execution are the primary factors contributing to these financial setbacks. With a determined purpose to convince, this research seeks to shed light on the root causes of cost overruns in infrastructure projects, emphasizing the utmost importance of effective project management in mitigating such issues. By exploring these critical aspects, we can pave the way for the successful completion of future endeavors in the water and wastewater industry.

IX. Performance Analysis for Water and Wastewater Projects

To ensure the successful implementation of these ambitious goals, it was imperative to thoroughly analysis the performance indicators of these projects and develop urgent and radical solutions. The performance indicators of water and wastewater projects serve as valuable tools for evaluating the effectiveness and efficiency of these initiatives. By closely monitoring and analyzing these indicators, it becomes possible to identify areas of improvement, address challenges, and optimize resource allocation. Such a comprehensive assessment enables the development and implementation of innovative solutions that can contribute to the realization of the United Nations' coverage targets. The analysis of these projects encompasses various aspects, including infrastructure development, technological advancements, environmental impact, and financial considerations. Therefore, it was necessary to analyze the performance indicators of several projects and come up with urgent and radical solutions to implement those goals, The indicators of these projects can also be measured through the criteria shown in Table 2.1 below.

Table 2.1: National Water Company Projects Performance Criteria

Project Criteria	Performance
Regular	0 > (EV- PV) ≥- 10 %
Delayed	-10 %> (EV- PV) ≥- 25%
Faulted	(EV– PV) < - 25%
Ahead of Schedule	EV > PV

Referring to Figure 1.2, which illustrates the total of project from 2018 to 2023. This dynamic chart not only reveals the total number of projects each year but also highlights the intriguing percentages of troubled projects, those currently under implementation, and those successfully handed over.

Delving into the data, we find that 2018 stands out as a remarkable year, boasting a staggering 1,010 projects with budget 38.8 billion SAR. Fast forward to 2021, a year that faced significant challenges, as it recorded the highest percentage of troubled projects at a concerning 27.2%. However, by 2023, and by innovative recovery strategies and proactive measures, the rate of troubled projects dramatically dropped to just 4.9%, marking it as the best year yet.

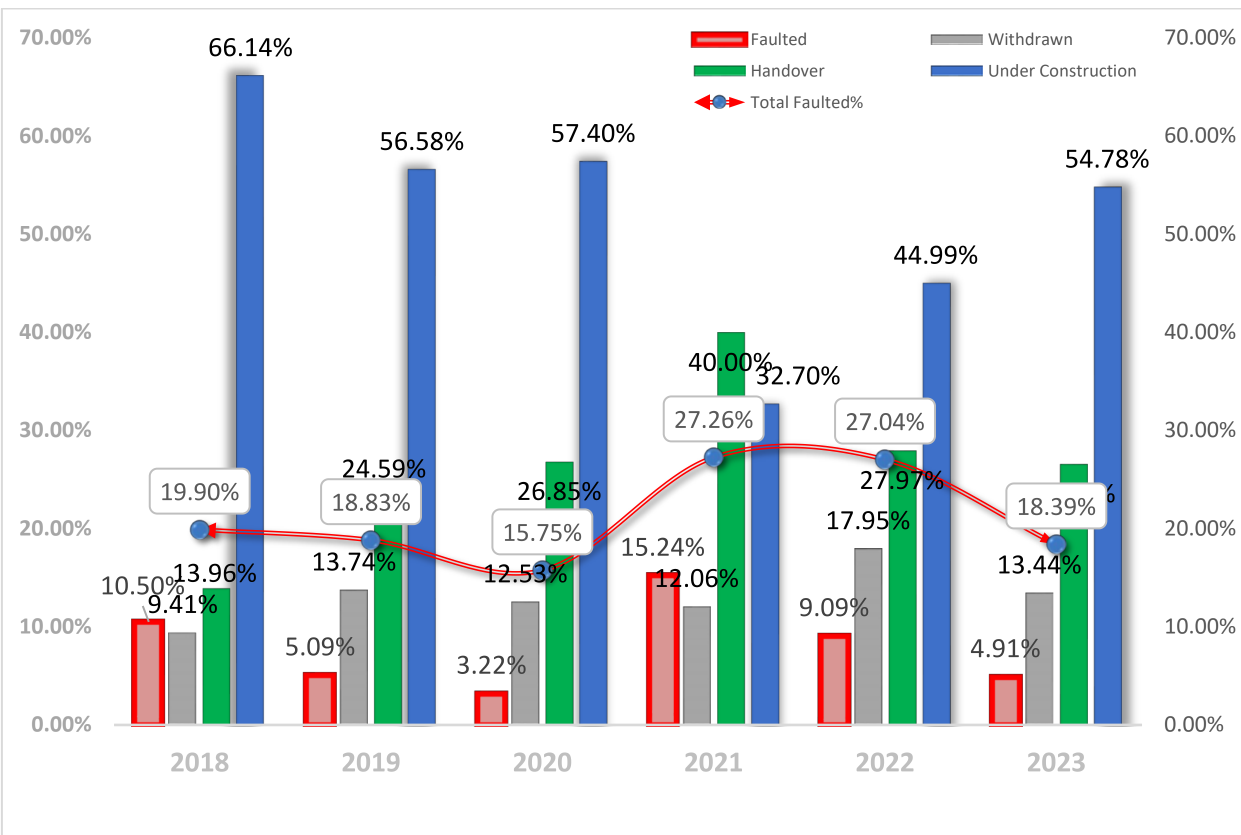

Figure 1.2: Projects portfolio status - Year (2018-2023)

Table (2.2): Projects Portfolio and KPI (2018-2023)

Year	Total No. of Projects	Budget Billion	No. of troubled Projects	No. of Withdrawn Projects	Total No. of Handover Projects	Total No. of troubled Projects (withdrawn + troubled)
2018	1010	38.8	106	95	141	201
2019	1041	51.2	53	143	256	196
2020	838	40.3	27	105	225	132
2021	631	33.5	96	76	252	172
2022	429	27.6	39	77	120	116
2023	386	25.8	19	52	103	71

a) *Covid-19 Negative Impact*

As the relentless march of Covid-19 continued unabated into 2021, its grip on projects tightened, reaching its peak in the early months of the year. Our recovery plan valiantly battled to stem the tide of setbacks, adapting, and refining itself with newfound expertise. However, the halt in logistics and travel proved to be an insurmountable hurdle. Delays in supplies became the norm, causing material prices to skyrocket and inflation to soar. The burden of processing, already a formidable challenge, intensified twofold, (shown in Fig. 1.3), which vividly portrays the impact of Covid-19 on defaulted projects, Where according to NWC-PMO Report, December 2021, 2022, Saudi Arabia, shows that the number of troubled projects reached its peak in mid-2020 with a number of 91 and 10.8% of the project portfolio during the year 2020, which represents a large percentage of the total project portfolio. Then it reaches its peak at the beginning of the year 2021, becoming 143 projects, representing 22.6% of the total project portfolio for that year. Embarking on a mission to revive struggling projects, the plan for 2022 and 2023 is unwavering in its determination to overcome various global challenges, particularly in the wake of the disruptive Covid-19 pandemic. As the year 2022 unfolds, the number of defaulted projects reaches its climax, standing at 98, accounting for a substantial 22.84% of the entire project portfolio. However, armed with the implementation of the aforementioned treatment plan, a glimmer of hope emerges. Extensive research indicates that by year-end, the number of faltering projects is expected to dwindle to 39, representing a noteworthy 9.1% of the total portfolio.

Fast forward to the onset of 2023, and the count of faltering projects stands at 25, with a faltering percentage of 10.6%. Yet, through unwavering dedication and collaborative efforts, the

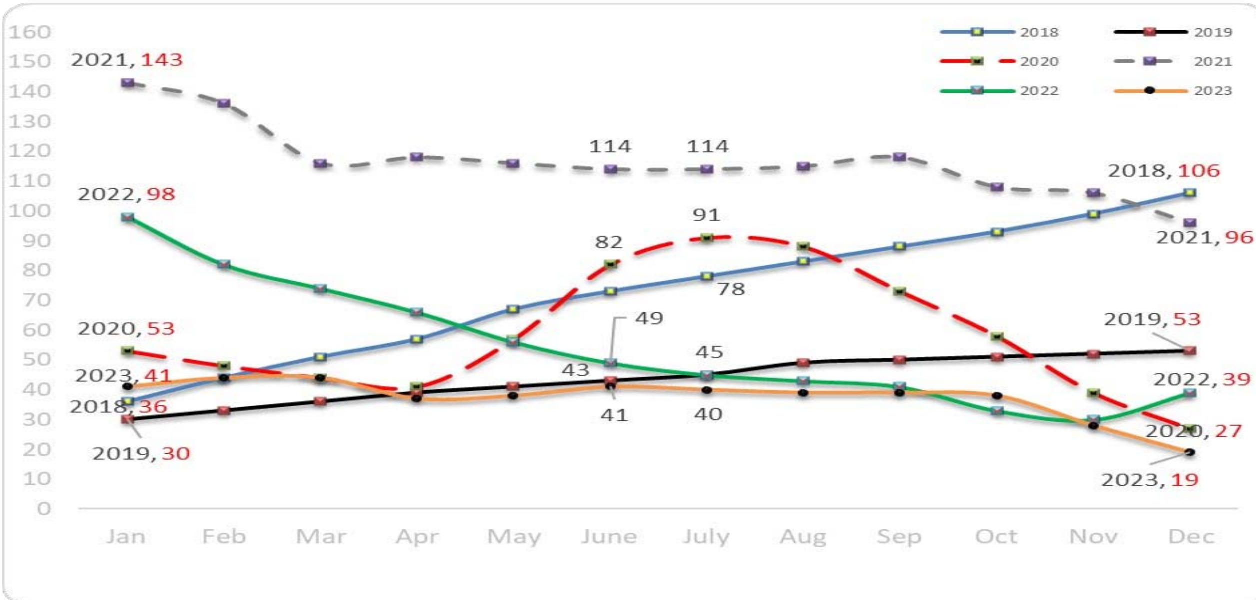

Figure 1.3: Troubled Projects during years (2018 to 2023)

As a result, the projects a remarkable turnaround, generating impressive gains as shown in Fig. 1.4 where each project now plays a pivotal role in community service by spearheading the construction of strategic reservoirs, water purification plants, sewage treatment plants, and operational tanks. Furthermore, millions of lengths of water and sewage networks have been added to enhance citizen services and improve water efficiency.

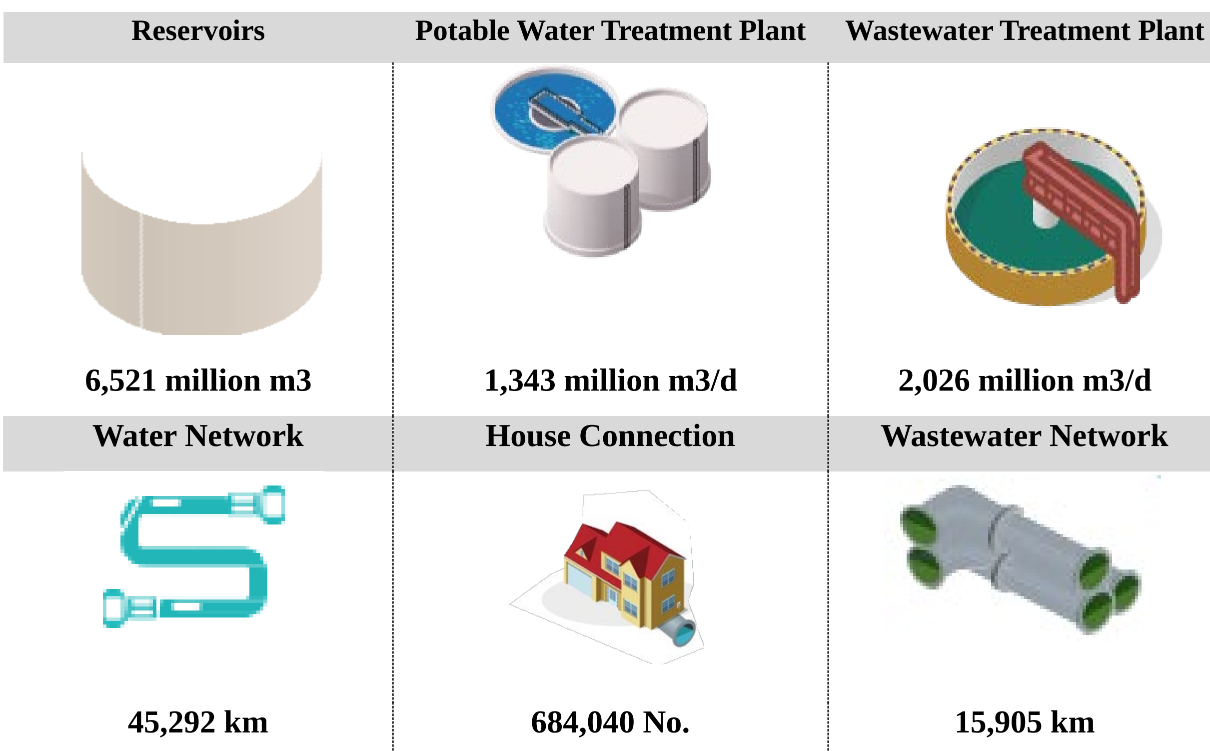

Figure 1.4: Projects Deliverables during years (2018 to 2023)

X. Statistics Results, Analysis and Evaluation of Findings

The research data collection methods consist of two parts: a survey questionnaire based on the quantitative approach.

a) Questionnaire Questions

The research questionnaire contained an independent variable (Cost Overruns) which consists of 3 dimensions of the number of total (16) paragraphs, and dependent variable (Infrastructure Projects Failures) consists of (5) paragraphs, all that evaluated by 5-point Likert Scale which illustrated below:

Table No. 9.1: Likert Scale Pentameter

Response	Strongly agree	Agree	Uncertain	Disagree	Strongly disagree
Score	5	4	3	2	1

The Independent variable (Cost Overruns) consists of 3 dimensions as follows:

- The First dimension: Project costs which contain (4) paragraphs.
- The Second dimension: Managing the project risk plan which contains (6) paragraphs.
- The Third dimension: Earned value management (EVM) which contains (6) paragraphs.

The Dependent Variable (Infrastructure Projects Failures) contain (5) paragraphs.

Descriptive Analysis:

Descriptive Analysis of demographic data

Job Position:

Table No. 9.2: Frequency and relative percent distributed for (Job Position)

Job Position	Frequency	Percent
Project Manager	172	37.23%
Project Engineer	109	23.59%
Project Control Manager	25	5.41%
Construction Manager	24	5.19%
Planning Manager	23	4.98%
Planning Engineer	22	4.76%
Director	18	3.90%
Engineering Manager	17	3.68%
Procurement Manager	14	3.03%
Cost Manager	13	2.81%
Contract Manager	11	2.38%
Risk Manager	8	1.73%
Quality Manager	6	1.30%
Total	462	100

The table No. 9.2 shows the Frequency and relative percent distributed according to (Job Position), it has been shown that the first set (Project Manager) with percent 37.23%, and the second set (Project Engineer) with percent 23.59%, and third set (Project Control Manager) with percent 5.41%, Construction Manager with percent 5.19%, and Planning Manager with 4.98%.

Resident Country:

Table No. 9.3: Frequency and relative percentage distributed for (Resident Country)

Resident Country	Frequency	Percent
Saudi	310	67.10%
Egypt	135	29.22%
Emirates	8	1.73%
Canada	6	1.30%
Oman	1	0.22%
Kuwait	1	0.22%
Qatar	1	0.22%
Total	462	100

The table No. 9.3 show the Frequency and relative percent distributed according to (Resident Country), it has been shown that the first set (Saudi) with percent 64.1%, the second set (Egypt) with percent 29.22% and third set (Emirates) with percent 1.73%.

Job Description

Table No. 9.4: Frequency and relative percentage distributed for (Job Description)

Experiences Years	Frequency	Percent
More Than 20	357	77.27%
(10-20)	98	21.21%
(5-10)	6	1.30%
Less Than 5	1	0.22%
Total	462	100

Table No. 9.4 show the Frequency and relative percent distributed according to (Experiences Years), it has been shown that the first set (More Than 20) with percent 77.27%, the second set (10-20) with percent 21.21%, third set (5-10) with percent 1.3%, and (Less Than 5) set with percent 0.22%.

b) Hypothesis Test

The research Confidence Interval of the Difference is 95%, which mean α =0.05 If (P-Value > α =0.05), that means the research will approve H0, and Reject the H1, and Vice-Versa.

i. *Main Hypothesis H0*

There is no Statistical relation between the Cost Overruns (Project costs, managing the project risk plan, Earned value management (EVM)) and Infrastructure Projects Failures).

Figure (9.1): Modeling the structural equations of the main hypothesis

It is clear from the previous figure (9.1) that:

- There is a statistically significant effect from Cost Overruns on Infrastructure Projects Failures at a level of confidence of 95%, as the significance of the path reached 0.000, which is less than the error level of 5% with a coefficient of 0.911.

R-square

Table No. 9.5: The coefficient of determination for main hypothesis

	f-square	R-square	R-square adjusted	Path coefficients
Cost Overruns -> Infrastructure Projects Failures	4.850	0.829	0.827	0.911
Cost Overruns -> Project costs	1.763	0.638	0.634	0.799
Cost Overruns -> Managing the project risk plan	2.494	0.714	0.711	0.845
Cost Overruns -> Earned value management (EVM)	2.316	0.698	0.695	0.836

The table shows that the coefficient of determination for (Cost Overruns -> Infrastructure Projects Failures) equal 0.829, this means that Cost Overruns explain 82.9% from any change occur in Infrastructure Projects Failures, the unexplained percentage may be due to other factors that were not considered.

ii. *Sub-Hypothesis H1*

There is no Statistical relation between the Project costs and Infrastructure Projects Failures.

H0: No significance, where the project budget is accurate estimate.

$$\mu 1 = \mu 2$$

H1: There is a level of significance where the project budget doesn't accurately estimate.

$$\mu 1 \neq \mu 2$$

Table No. 9.6: Goodness of fit for main hypothesis

Model fit	Saturated model	Estimated model
SRMR	0.075	0.075
NFI	0.808	0.804

It is clear from the table that the square root mean error for the actual model was 0.075, while it was 0.075 for the estimated model. It was also shown that the quality index (NFI) was 0.808, and then it is possible to judge the quality of the results obtained.

So, we reject the null hypothesis and accept the alternative hypothesis that there is statistical relation between the Project costs and Infrastructure Projects Failures.

$$\boldsymbol{\mu 1 \neq \mu 2}$$

According to the above, P-Value (Level of Sig. (2-tailed)) = 0 which is < (**α** =0.05), that means the first research hypothesis (H1) has been verified positively, which is "*Study of project costs accurately during the roll-out phase will contribute positively to controlling cost overruns.*"

iii. *Sub-Hypothesis H2*

There is no Statistical relation between Managing the project risk plan and Infrastructure Projects Failures.

H0: No significance, where estimated costs of risk on project budget cost and doesn't impact cost overrun.

$$\mu 1 = \mu 2$$

H2: There is a level of significance, Managing the project risk plan, will contribute positively to controlling cost overruns.

$$\mu 1 \neq \mu 2$$

Table No. 9.7: Goodness of fit for sub-hypothesis2

Model fit	Saturated model	Estimated model
SRMR	0.062	0.062
NFI	0.854	0.854

It is clear from the table that the square root mean error for the actual model was 0.062, while it was 0.062 for the estimated model. It was also shown that the quality index (NFI) was 0.854, and then it is possible to judge the quality of the results obtained.

So, we reject the null hypothesis and accept the alternative hypothesis that there is statistical relation between Managing the project risk plan and Infrastructure Projects Failures.

$$\mu 1 \neq \mu 2$$

According to above, P-Value (Level of Sig. (2-tailed)) = 0 which is < (**α** =0.05), that is mean the second research hypothesis (H2) has been verified positively, which is "*Managing the project risk plan, will contribute positively to controlling cost overruns."*

iv. *Sub-Hypothesis H3:*

There is no Statistical relation between the Earned value management (EVM) and Infrastructure Projects Failures.

H0: No significance, where Earned Value Management will not provide strong indicator for monitor & control project cost overrun.

$$\mu 1 = \mu 2$$

H3: There is level of significance, Using Earned value management (EVM) method during the project lifecycle will provide strong indicators that contributed to monitoring and control project cost overruns.

$$\mu 1 \neq \mu 2$$

Table No. 9.8: Goodness of fit for sub-hypothesis3

Model fit	Saturated model	Estimated model
SRMR	0.065	0.065
NFI	0.853	0.853

It is clear from the table that the square root mean error for the actual model was 0.065, while it was 0.065 for the estimated model. It was also shown that the quality index (NFI) was 0.853, and then it is possible to judge the quality of the results obtained.

So, we reject the null hypothesis and accept the alternative hypothesis that there is statistical relation between the Earned value management (EVM) and Infrastructure Projects Failure.

$$\boldsymbol{\mu 1 \neq \mu 2}$$

According to above P-Value (Level of Sig. (2-tailed)) = 0 which is < (**α** =0.05), *that means the third research hypothesis (H3) has been verified positively, which is" Using Earned value management (EVM) method during the project lifecycle will provide strong* *indicators that contributed to monitoring and control project cost overruns".*

XI. Conclusion and Recommendations

a) Root Cause of Failure Projects

The root causes of failure in water and wastewater projects which often lead to cost overruns that create a heavy financial burden for both the public and private sectors. The research analysis revealed a major reasons behind these cost overruns: inadequate initial cost estimation. Insufficient evaluation of project requirements and a limited understanding of potential risks can result in unrealistic budgeting, dramatically increasing the likelihood of cost overruns. Delays in project completion due to unforeseen circumstances, such as adverse weather conditions or logistical challenges, also contribute to cost overruns. These delays bring with them additional expenses related to extended construction periods, increased labor costs, and the need for extra resources. It's a vicious cycle that drains resources and exacerbates the problem. Poor project management and ineffective communication between stakeholders leading to further delays and cost overruns.

It is, therefore, of utmost importance for project managers and stakeholders involved in water and wastewater projects to conduct thorough cost estimations, identify potential risks, and establish effective communication channels to mitigate the impact of cost overruns. By addressing these issues head-on, the water and wastewater industry can significantly improve project delivery, ensure the efficient use of resources, and alleviate the financial strains on both public and private entities. Various other factors contribute to cost overruns in water and wastewater projects. One such factor is the lack of comprehensive asset management strategies. This lack of foresight leads to cost overruns during the project implementation phase. To combat this, project stakeholders must invest in comprehensive asset management strategies that encompass regular inspections, condition assessments, and long-term planning. By gaining a clear understanding of the condition and performance of their assets, utilities can accurately estimate the level of investment required, thereby minimizing the risk of cost overruns.

- Design flaws also play a significant role in driving up costs in water and wastewater projects. These flaws can range from errors or omissions in the engineering design to inadequate consideration of operational requirements.
- Construction delays are yet another major contributor to cost overruns in water and wastewater projects. These delays can be caused by a multitude of factors, such as adverse weather conditions, logistical challenges, or poor project management. When projects experience delays, additional expenses are incurred due to extended construction periods, increased labor costs, and the need for supplementary resources. To mitigate the risk of construction delays, project managers should develop realistic project schedules, account for potential risks and uncertainties, and implement effective project management techniques. This includes regular monitoring and reporting of project progress, proactive identification and resolution of issues, and seamless coordination and communication among all stakeholders involved.

By tackling these issues head-on, the water and wastewater industry can pave the way for successful projects and alleviate the financial strains imposed on both public and private entities.

b) Recommendation

Based on the research results, the following recommendations are made, which directly affect controlling the project costs and their impact on project management:

- The contracting companies should delegate authority to the competent authorities to distribute and allocate the resources for work package, and the planning department of the company should allow the experienced employees to participate in the development of the plans.
- The laws, regulations, and circulars that affect the cost planning and control process for construction and infrastructure projects should be studied and identify the procedures to be applied to control costs.
- The terms of the contract must be reviewed and audited. Also, the executive regulations of the procurement procedures should be considered, because of its binding clauses for the contractor.
- Familiarity with the prices of raw materials used according to the approval of the owner to procurement plan, taking into consideration the difference in prices of raw materials from one area to another.
- The price of the project items should be determined according to the specified profit margin, taking into consideration the nature of the project, size, and location, so that the profit margin is realised in all the items in a balanced manner.
- The project risk plan should take importance regarding project risk identification in advance and then estimate the costs of these risks within the overall project costs.
- Monitoring and control of project costs should be determined from the initiation process for the project and during the project life cycle, and use of appropriate measurement indicators to monitor and measure the cost plan.

Global Journal of Research in Engineering (J) XXV Issue I Version I Year 2025

Enhancing Cost Accuracy: Activity-based Costing (ABC)

- *Better Cost Control:*

Through the detailed insights provided by ABC, organizations can exercise better control over their costs. This includes identifying cost-saving opportunities, optimizing resource allocation, and improving overall operational efficiency.

- *Enhanced Budgeting and Planning:*

ABC facilitates more accurate budgeting and planning by providing a realistic breakdown of costs associated with each activity. This helps organizations set more realistic budgets and allocate resources more effectively.

- *Adaptability to Changes:*

ABC is adaptable to changes in business processes. If there are changes in activities or resource requirements, the ABC model can be adjusted to reflect these changes, ensuring ongoing accuracy in cost allocation.

- *Benchmarking and Performance Measurement:*

ABC enables organizations to benchmark the performance of different activities and departments. This information is valuable for identifying areas of improvement and making strategic decisions to enhance overall organizational efficiency. While ABC offers numerous advantages in enhancing cost accuracy, it's important to note that its implementation may require a significant investment in data collection and analysis.

References Références Referencias

1. Ahsan, K. and Gunawan, I. (2010) Analysis of Cost and Schedule Performance of International Development Projects. International Journal of Project Management, 28, pp. 68-78.
2. Al-Hazim N. & Abu Salem Z. & Ahmad H. (2017). Delay and Cost Overrun in Infrastructure Projects in Jordan. Procedia Engineering 182 (2017) 18-24.
3. C. R. Kothari. (2004). Research Methodology: Methods and Techniques, second. Revised. Ed., New Age International Limited, Publishers.
4. Crowther, D. & Lancaster, G. (2008). Research Methods: A Concise Introduction to Research in Management and Business Consultancy. Butterworth-Heinemann.
5. Doloi, H. (2011). Cost Overruns and Failure in Project Management: Understanding the Roles of Key Stakeholders in Construction Projects. May 2013, Journal of Construction Engineering and Management 139(3): pp. 267-279.
6. Doloi, H. (2012). Cost Overruns and Failure in Project Management Understanding the Roles of Key Stakeholders in Construction Projects. Journal of construction engineering and management, 139(3), pp. 267-279.
7. Fleming, Q. W. & Koppelman, J. M. (1996). Forecasting the final cost and schedule results. PM Network, 10(1), pp. 13–18.
8. Flyvbjerg, B., Holm, M. K. S., and Buhl, S. R. L. (2002). Underestimating Costs in Public Works Projects: Error or Lie?, Journal of the American Planning Association, vol. 68, no. 3, pp. 279-295.
9. Flyvbjerg, B. (2017). The Iron Law of Megaproject Management, The Oxford Handbook of Megaproject Management, Oxford University Press, Chapter 1, pp. 1-18.
10. Flyvbjerg, B. (2018). Planning Fallacy or Hiding Hand: Which is the Better Explanation, World Development, Vol. 103, 2018.
11. Love P.E.D. (2002). Influence of project type and procurement methods on rework costs in building construction projects. J. Constr. Eng. Manag., 1.
12. Love P.E.D. (2002a). Influence of project type and procurement methods on rework costs in building construction projects. J. Constr. Eng. Manag., 128(1), pp. 18-29.
13. Love, P. E. D & Tse, R. Y. C. & Edwards, D. J. (2005). Time-cost relationships in Australian building construction projects, J. Constr. Eng. Manage., 131(2), pp. 187–194.
14. L Bergkvist., B Johansson. (2007). Evaluating motivational factors involved at different stages in an IS outsourcing decision process.
15. Love, P. E. D & Edwards, D. J. & Watson, H. & Davis P. (2010). Rework in Civil Infrastructure Projects-Determination of Cost Predictors. Journal of Construction Engineering and Management, 136 (3), pp.275-282.
16. Lopez, R. & Love, P.E.D. (2012). Design Error Costs in Construction Projects. Journal of construction engineering and management. J. Constr. Eng. Manage., 138(5), pp. 585-593.
17. M. Easterby-Smith, M., Thorpe, R. & Jackson, P. (2012). Management Research, fourth. Edition, London: SAGE Publications.
18. Marey-Perez M. & Al Amri T. (2020). Delays and cost Overrun Causes in Construction Projects of Oman. Project Management Journal, 5(2020), pp. 87-102.
19. NWC. (2021). Project Management Offices Report, National Water Company, Saudi Arabia.
20. NWC. (2022). Project Management Offices Report, National Water Company, Saudi Arabia.
21. NWC. (2023). Project Management Offices Report, National Water Company, Saudi Arabia.
22. Olawale, Y., and Sun M. (2010). Cost and time control of construction projects: Inhibiting factors and mitigating measures in practice. Construction Management, and Economics, 28 (5), pp. 509–526.
23. Project Management Institute (2011). Practice Standard for Earned Value Management. 2nd.

Edition, Newtown Square, PA: Project Management Institute.

24. Project Management Institute. (2013). A Guide to Project Management Body of Knowledge, (PMBOK® Guide), fifth. Edition, Newtown Square, PA USA: Project Management Institute.
25. Project Management Institute. (2017). A Guide to Project Management Body of Knowledge, (PMBOK® Guide), Sixth. Edition, Newtown Square, PA USA: Project Management Institute.
26. Polat, G., Okay, F. & Eray, E. (2014). Factors affecting cost overrun in micro scaled construction companies. Procedia Engineering 85 (2014), pp. 428-435.
27. Reilly, J. J. & Brown, J. (2004). Management and Control of Costs and Risk for Tunneling and Infrastructure Projects, Proceedings, World Tunneling Conference, International Tunneling Association, Singapore, pp. 1-11.
28. UNICEF/WHO (2012). Progress on drinking water and sanitation, 2012 update. New York, UNICEF; Geneve, World Health Organization.
29. Vrijling, J. K. & Redeker. (1993). The risks involved in major infrastructure projects. Options for Tunneling. Ed H Burger.
30. World Bank (2012). Online indicators database. Washington, DC, The World Bank.
31. Wanjari P. S., and Dobariya G. (2016). Identifying factors causing cost overrun of the construction projects in India.Sadhana Vol.41, No. 6, June 2016, pp. 679-693.
32. Zwikael, O. & Sadeh, A. (2007). Planning effort as effective risk management tool. Journal of Operations Management, 25 (4), pp. 755-767.
33. Zwikael, O., & M. Ahn, (2011). The Effectiveness of Risk Management: An Analysis of Project Risk Planning across Industries and Countries. Risk Analysis, 31 (1), pp. 25-37.

Global Journal of Researches in Engineering: J
General Engineering
Volume 25 Issue 1 Version 1.0 Year 2025
Type: Double Blind Peer Reviewed International Research Journal
Publisher: Global Journals
Online ISSN: 2249-4596 & Print ISSN: 0975-5861

Automation of Gas Leak Detection: AI and Machine Learning Approaches for Gas Plant Safety

By Godsday Idanegbe Usiabulu, Ifeanyi Eddy Okoh & Ndidi Lucia Okoh

University of Port Harcourt

Abstract- Safety and protection of the environment involve real-time gas leak detection. The paper discusses the improvement in the accuracy and speed of gas leak detection using AI based on pressure-based monitoring. The model will be performing a flow consistency check using machine learning techniques for instantaneous detection at distinct stages in flows.

Extensive exploratory data analysis was performed to assess the data and to choose the right machine learning models. The findings showed a significant evolution of pressure differences over time; hence, refining the tolerance level for leakage detection down to a fractional ± 0.166 window was necessary. The gas flow data was divided into training and testing datasets, which consisted of 80% and 20%, respectively. Several AI models were tested, such as linear regression, logistic regression, SVM, and Random Forest-all had a test accuracy of over 99%. This AI-powered monitoring system could trigger an alarm or immediate notification in the case of a pressure drop beyond the defined tolerance window, improving upon the traditional methods of inspection. All of these contribute to improved safety, operational efficiency, and even cost savings.

Keywords: test score, training, test dataset, split dataset, tolerance, lag time.

GJRE-J Classification: *LCC Code: TJ930*

AUTOMATIONOFGASLEAKDETECTIONAIANDMACHINELEARNINGAPPROACHESFORGASPLANTSAFETY

Strictly as per the compliance and regulations of:

Automation of Gas Leak Detection: AI and Machine Learning Approaches for Gas Plant Safety

Godsday Idanegbe Usiabulu [α], Ifeanyi Eddy Okoh [σ] & Ndidi Lucia Okoh [ρ]

Abstract- Safety and protection of the environment involve real-time gas leak detection. The paper discusses the improvement in the accuracy and speed of gas leak detection using AI based on pressure-based monitoring. The model will be performing a flow consistency check using machine learning techniques for instantaneous detection at distinct stages in flows.

Extensive exploratory data analysis was performed to assess the data and to choose the right machine learning models. The findings showed a significant evolution of pressure differences over time; hence, refining the tolerance level for leakage detection down to a fractional ±0.166 window was necessary. The gas flow data was divided into training and testing datasets, which consisted of 80% and 20%, respectively. Several AI models were tested, such as linear regression, logistic regression, SVM, and Random Forest-all had a test accuracy of over 99%. This AI-powered monitoring system could trigger an alarm or immediate notification in the case of a pressure drop beyond the defined tolerance window, improving upon the traditional methods of inspection. All of these contribute to improved safety, operational efficiency, and even cost savings. Furthermore, the scalability of the model holds great promise for other industrial scenarios. The animated simulation of the proposed solution was demonstrated.

Keywords: test score, training, test dataset, split dataset, tolerance, lag time.

I. Introduction

The gas industry necessitates accurate and timely leak detection to ensure safety and mitigate environmental hazards. Traditional methods of leak detection in gas plants are often manual and time-consuming, leading to potential risks and inefficiencies (Usiabulu et al., 2021; 2022; 2023; Appah et al., 2021). Due to these challenges, there has been a growing interest in leveraging artificial intelligence to develop instantaneous leak detection systems that can automate and streamline the monitoring process (Zukang et al., 2021).

Author α: World Bank African Center of Excellence, Center for Oilfield Chemicals and Research, University of Port Harcourt, Port Harcourt, Nigeria. e-mail: godsdayusiabulu@gmail.com

Author σ: First Hydrocarbon Nigeria Limited FHN 26 Block W Shell Estate Edjeba, Delta State.

Author ρ: Department of Environmental Pollution and Control, Federal University of Petroleum Resources Effurun, Delta State.

Most of the existing systems lack real-time analysis and decision-making despite the advancements in AI and ML techniques. This paper fills this knowledge gap by proposing a sophisticated algorithm in AI/ML that would analyze complicated data patterns in real time to quickly find and locate gas leaks within a plant. Contrary to the usual methodologies, this approach avoids much human interference, which in turn will reduce errors and increase speed and accuracy in detection.

In this work, AI was used to enable continuous monitoring of the modeled JK-52 gas plant with minimum human intervention. Integration of recording sensors and pressure-measuring devices enabled us to develop a real-time surveillance system powered with our AI/ML algorithm that will act on anomalies in an instant, like pressure drops beyond allowable tolerance levels, probably signaling a leak.

Simulations of the proactive detection mechanism were performed at different stages of gas injection, from residual phase to ramp-up and then to the plateau stage. Such automation will raise safety and reduce the possible effects of gas leakage on the environment and public health. Besides, AI-driven predictive maintenance will reduce potential downtime from undetected leaks, promising significant cost savings.

This work, therefore, contributes to better operational efficiency and prolongs the life of equipment by enabling gas plant operators to identify a problem before it escalates. The study also looks into the possibility of integrating IoT devices for further enhancement of data collection and communication in real time. This research will likely set a new standard in leak detection systems, emphasizing both environmental sustainability and societal health concerns.

The objectives of this application of artificial intelligence for instantaneous leak detection in gas plants were as follows:

1. Develop a system for instantaneous and accurate gas leak detection using artificial intelligence and machine learning techniques.

2. Automate the modeling process for leak detection to enable rapid identification of gas leaks in real-time.
3. Enhance the speed, accuracy, and efficiency of leak detection while minimizing reliance on manual intervention.
4. Establish continuous and proactive monitoring of gas plants using sensors and monitoring devices adapted for AI solutions.
5. Contribute to cost savings by reducing potential downtime through AI-driven predictive maintenance.
6. Improve safety measures, minimize environmental impact, and enhance operational efficiency in gas plants through the application of AI for leak detection.

These objectives aim to address the inefficiencies and potential hazards associated with traditional manual gas leak detection methods while leveraging AI to enhance safety, minimize environmental impact, and optimize operational processes.

a) Data and Methods

The process of gas leak detection in gas plants involves a number of efficiencies and hazards that must be addressed. For this purpose, an effective data acquisition process is needed to provide instantaneous identification of the leaks. The traditional methods of gas leak detection employ limited observational data that are non-instantaneous and liable to human error. These can pose serious risks to the safety of personnel and the environment, apart from causing financial losses to the plant operators.

In this work, the acquisition of data necessary for the automation and improvement of the modeling process, using artificial intelligence for the detection of gas leaks, is in focus. The main data sources consisted of pressure and time measurements, which were obtained from sensors placed at strategic points in the gas plant. These sensors had a sampling frequency of 99Hz, which allowed high-resolution data to be captured in different operation conditions. The temperature and humidity levels were measured, too, as environmental factors to contextualize the pressure readings.

A number of phases of gas pumping were covered in this dataset, including the initiation phase residual, the buildup phase, and the optimal or plateau stage. Other metrics derived aside from raw pressure and time data are tolerance levels, lag time, and alarm notifications. Tolerance levels were calculated based on the trend of historical data, whereas lag time was determined by analyzing the response time of the system against changes in pressure. Notifications of alarms were triggered when pressure values fell outside the predefined limits of tolerance.

Data preprocessing was carried out to make it robust; hence, cleaning of outliers and normalization was performed. Further, missing data was treated using interpolation methods, maintaining continuity in the dataset. Feature engineering was also applied to the raw data for the extraction of meaningful variables, which improved the model's predictive power.

The AI/ML model used for this work included the type, such as support vector machines and neural networks, and was chosen because of their potentiality in analyzing patterns in complex data in real time. Modelling involved the training of the algorithm using, say, of the gathered data; the remaining are reserved for testing to gauge the performances of the models. It thereby integrates methodologies to construct a wide framework for real-time gas leak detection with minimum human intervention and maximum safety and operational efficiency.

These data were recorded in an ascii file, extracted as iESogV1.csv for the purpose of this study. The structure of the columns is as below:

1. *Time (s):* Represents time in seconds.
2. *Pr_final:* Final pressure value.
3. *Pr_initial:* Initial pressure value.
4. *Events:* Describes significant events during the process (e.g., "Residual stage").
5. *Tolerance:* Tolerance level during the process.
6. *Min:* Minimum threshold.
7. *Max:* Maximum threshold.
8. *Diff_Pres (bar):* Difference in pressure (in bar).

The data was loaded using the commands below:

```
# Load the data from the 'in' sheet to inspect its content
df = pd.read_excel(file_path, sheet_name='in')
# Show the first few rows of the data to understand its structure
df.head()
```

The results were as shown in Table 1, for the first rows and columns.

Table 1: Result showing first rows and column of dataset

	Time (s)	Pr_final	Pr_initial	Events	Tolerance	Min	Max
0	4005	3.5	1.5	Residual stage	0.428571	0.8	1.2
1	4010	3.5	1.5	NaN	0.428571	0.8	1.2
2	4015	3.5	1.5	NaN	0.428571	0.8	1.2
3	4020	3.5	1.5	NaN	0.428571	0.8	1.2
4	4025	3.5	1.5	NaN	0.428571	0.8	1.2

	Diff_Pres (bar)
0	2.0
1	2.0
2	2.0
3	2.0
4	2.0

(Note that similar or same reading for first few data is normal for large data at initiation of recording)

An initial automated AI/ML process was used to explore the data before the detailed analysis shown in the subsequent sections. By leveraging AI and machine learning, the goal was to use these data and develop an advanced system that can accurately and rapidly detect gas leaks, thereby improving safety, minimizing environmental impact, and optimizing operational efficiency in gas plants. The methods used in this work were:

- Data collection is essential, where sensors recorded data from the gas plants and was gathered for the analysis.
- Data preparation, which involved data cleaning, preprocessing, and ensuring the data is in a format suitable for modeling.
- Selecting appropriate machine learning algorithms.
- Training the model using the prepared data, and fine-tuning the model to achieve optimal performance.
- The machine learning techniques were applied to build the model for leak detection.
- Automation of the modeling process, which was necessary to ensure efficient and accurate detection of leaks in real time.
- The developed model is tested and validated to assess its performance and reliability.

The final delivery involved simulating different leak scenarios and evaluating how well the model detected and responded to these scenarios. The model was compared with against existing manual detection methods to demonstrate its effectiveness. These validation tests were vital to ensure the AI-powered leak detection system met the necessary performance standards for deployment in other real-world gas plant environments.

b) Challenges with Traditional Methods of Gas Leak Detection

Traditional methods for detecting gas leaks can be categorized into three main groups: manual methods, fixed detection systems, and acoustic methods.

i. *Manual Methods*

Manual detection methods include gas sniffers, flame ionization detectors, and bubble testing. Gas sniffers are handheld devices that measure gas concentrations, while flame ionization detectors burn gas samples to detect ions. Bubble testing involves applying a soapy solution to suspected leak areas; bubble formation indicates escaping gas. Visual inspections and periodic maintenance further supplement these methods.

ii. *Fixed Detection Systems*

In industrial settings, fixed gas detection systems continuously monitor for hazardous gases (Pablo et al., 2018; Tan & Tan, 2019; Todd et al., 2024). These systems include point gas detectors, which are strategically placed to detect leaks, and open-path gas detectors that use infrared technology to monitor larger areas. Sampling systems analyze air pulled into detectors (Baker, 2002; Bear, 1972).

iii. *Acoustic Methods*

Acoustic leak detection utilizes listening devices to identify the sound of escaping gas, providing an additional layer of monitoring in certain scenarios.

c) Limitations of Traditional Methods

Despite their widespread use, traditional gas leak detection methods present several significant limitations:

- *Manual Inspection Delays:* Reliance on manual inspection is inherently time-consuming and labor-intensive, leading to potential delays in detecting leaks. Human error can further compromise the effectiveness of these inspections, resulting in missed or incorrectly identified leaks.

- *Sensitivity Issues:* Many traditional methods lack the sensitivity required to detect small leaks or those in hard-to-reach areas. For instance, visual inspections may not effectively identify leaks in underground pipelines, risking undetected emissions.
- *Applicability Constraints:* Techniques such as bubble testing may not be suitable for certain gases or environments, limiting their effectiveness in diverse industrial contexts.
- *Lack of Real-time Monitoring:* Traditional methods often fail to provide continuous surveillance of gas pipelines, creating gaps in detection that may lead to critical safety hazards or environmental damage (Bhattacharya et al., 2019; Boujema et al., 2019).

These limitations highlight the pressing need for more effective detection methods. This work introduces Artificial Intelligence and Machine Learning techniques for gas leak detection, utilizing pressure-based observations instead of volume-based methods. This approach allows for programmable data analysis, where pressure readings over time serve as the primary input for detection, significantly improving response times and accuracy.

II. Gas Leak Detection using Artificial Intelligence and Machine Learning

Artificial Intelligence involves creating algorithms and models that enable machines to learn from data, recognize patterns, and make decisions. It can be designed for a specific task, which has the ability to perform any intellectual task that a human being can do, in this case, gas leak detection. It is important to consider its impact on the economy, the job market, privacy, and ethics, where personnel carrying out manual inspection of gas leakages may be affected by being replaced by the AIML solutions (Pablo et al., 2018; Tan and Tan, 2019). The responsible development and deployment of AI systems requires careful consideration of these factors to ensure that the benefits of AI are maximized while minimizing potential risks on interchanging human roles.

To determine the best model for predicting leakage, we followed a machine learning pipeline that included:

1. *Data Preprocessing:* Handle missing values, encode categorical variables, and scale the data if necessary.
2. *Feature Engineering:* Analyze which features are most relevant to predict the target
3. *Model Selection:* Compare various models such as:
   - Linear Regression
   - Decision Trees/Random Forests
   - Support Vector Machines
   - Gradient Boosting (e.g., XGBoost)
4. *Model Evaluation:* Use metrics like Mean Squared Error (MSE), R-squared, etc., to evaluate performance.

a) *Gas Plant Flow Data Input and Coding using Python*

The flow data from the gas plant was obtained by recording the input pressure, known as initial pressure, resulting from the upstream pressure reading. The upstream pressure gauge is the first point the processed gas flow rate is recorded before piping and running to the delivery point of the gas point. At the delivery point, another gauge records the out-flow pressure, which is the downstream gauge. The tendency for leakage to occur is more common between the two gauge points, due to increasing pressure meant to pump the gas out of the processing section to the delivery area.

The flow phases undergo two processes (Figure 1):

Process 1: The gas plant stabilises and strips lighter gas or condensates to produce purified dry gas ready as end product.

Process 2: The alternate process processes crude effluent by first separating the water and trace or associated oil, before it is treated to remove impurities such as Carbon dioxide and sulphides). The resulting gas is then compressed or liquified (Liquified Natural Gas – LNG) for storage and eventual supply.

In both cases, initial sensors and gauges are placed at the upstream (sourcing section) and at the downstream (receiving section) of the products. Inlet and outlet pressure gauges are placed across intervals with tendency of gas leak.

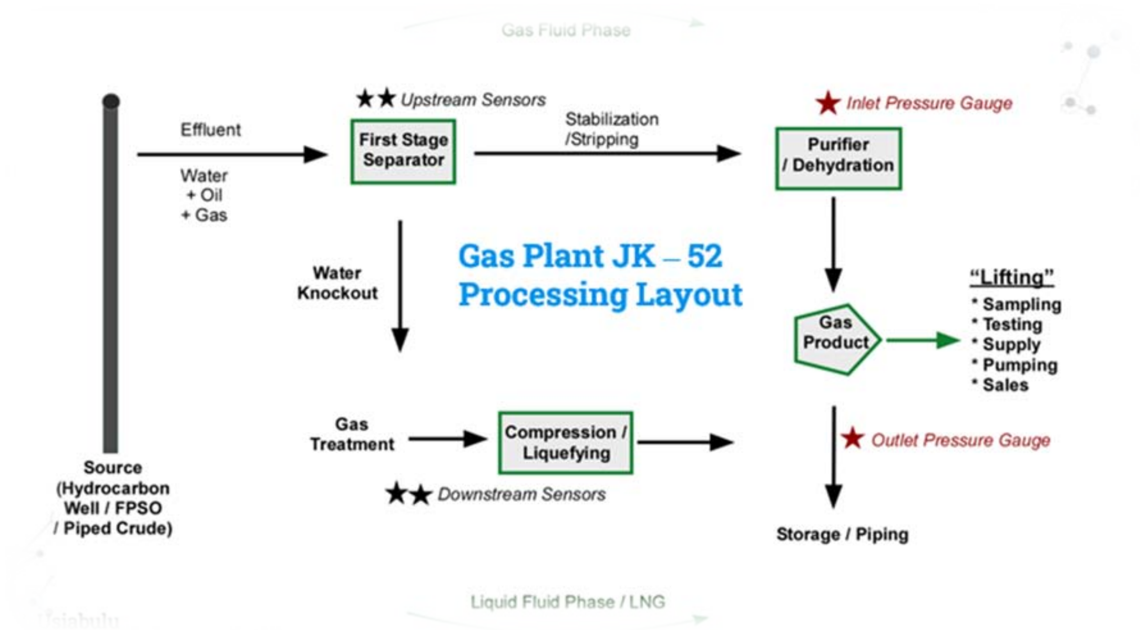

Figure 1: Gas flow Process in a Gas Plant showing the position of the inlet and outlet pressure gauges

The readings in the gauges in are recorded with time, with an initial phase of pumping, purging any existing gas in the system. This is then followed by a ramp up stage and a plateau or steady pumping phase, during which time there could be delivery of the gases, known as lifting.

Rate of flow, estimated as quantity passing over time, is directly related to the pressure recorded on the gauge. This is one of the variables used to determine volume changes and eventually leakage. The pressure is a measure of quantity or volume of gas (rate) pumped over a certain time.

The process of using AIML methods involved data collection, recording of pressure and time data, and recording other events during the flow. The collected data was different formats, such as numerical, categorical, or textual. It was important to ensure the data collected is accurate, complete, and representative of the events occurring during the flow process. The data collection involved using specialized tools and techniques for data scraping, logging, or monitoring from well gauges and computer system in which they are saved. Once the data was collected, the next step was data preprocessing.

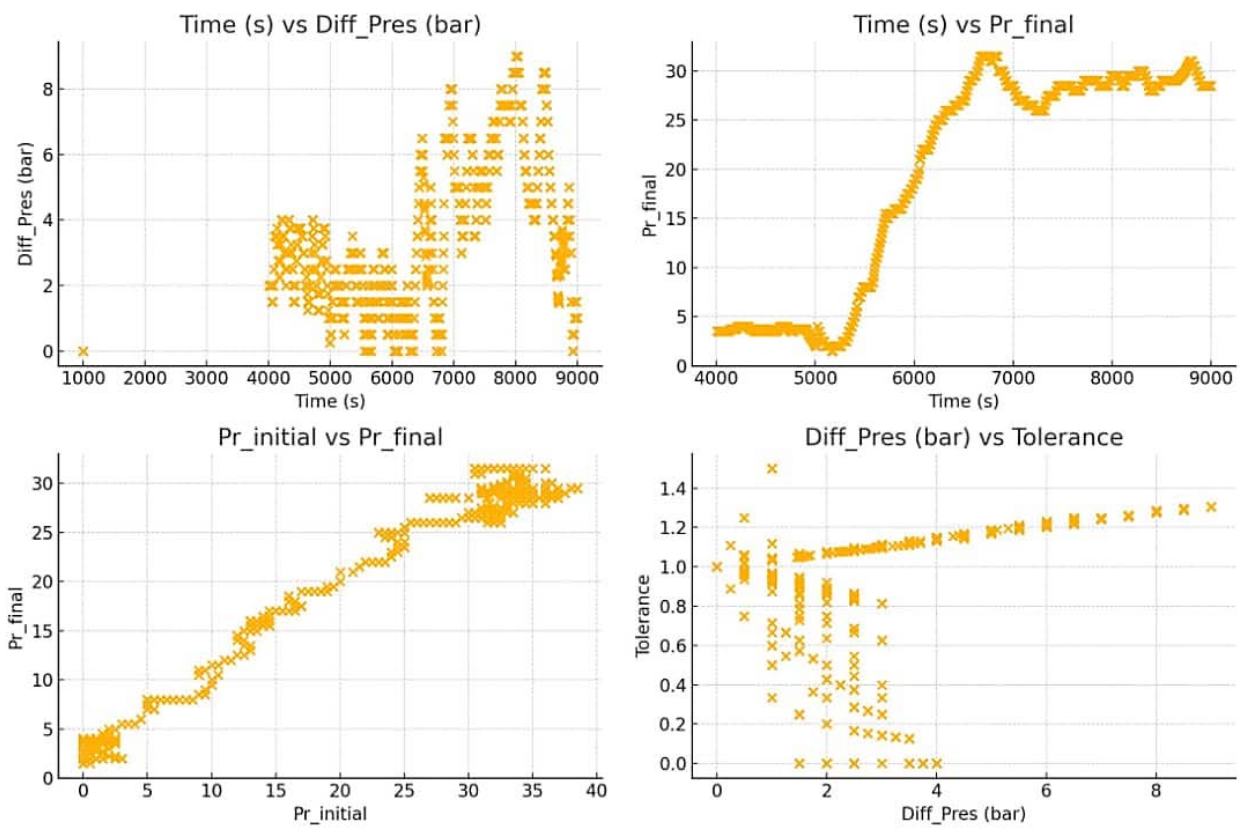

Figure 2: Analytical Plots showing relationships among variables

Initial analytical plots (Figure 2) were automated to show the trends of the data. The analytical plots above illustrate the relationships among different variables in your dataset:

1. *Time (s) vs Diff_Pres (bar):* This scatter plot shows the difference in pressure as a function of time. There seems to be a constant difference in pressure over time, suggesting stability in this aspect of the system, such that a deviation would indicate an event such as leakage.
2. *Time (s) vs Pr_final:* This plot demonstrates the final pressure value over time, showing that pressure evolution increased with time. Like the pressure difference, this variable also appears stable over time with only significant fluctuations being the three (3) stages of initiation, ramp-up and higher plateau or flow pressures.
3. *Pr_initial vs Pr_final:* The relationship between initial and final pressures shows a relative difference. Both values seem to be consistent, potentially reflecting that input and output pressure are the same, unless leakage or other events occur.
4. *Diff_Pres (bar) vs Tolerance:* The difference in pressure and tolerance seems to have a linear relationship, indicating that the tolerance might increase proportionally as the pressure difference grows, as such an anomaly will be based on local deviation outside the tolerance window.

b) Exploratory Data Analysis

The acquired data are usually structured in an excel file, with columns and rows, which may be extracted in a.CSV format. The file is then loaded in a python programing language interpreter. The development environment used for this study was Pycharm and Jupyter Notebook, where the Exploratory Data Analysis (EDA)/data wrangling were performed. Some of them were automated and compared with basic EDA charts. Examples of their Visualisation are shown in Figure 3. The Exploratory Data Analysis (EDA) reveals the following insights:

1. *Correlation Heatmap:* The heatmap shows a high correlation between the pressure variables:
   - o There is a strong positive correlation between Pr_final and Pr_initial, which is expected as they likely follow similar trends.
   - o The correlation between Diff_Pres (bar) and Tolerance is moderate, indicating some relationship between the pressure differential and tolerance.
2. *Distribution of Diff_Pres (bar):* The distribution plot for Diff_Pres (bar) suggests that the pressure difference is concentrated around a particular value,

Global Journal of Research in Engineering (J) Volume XXV Issue I Version I Year 2025

with a narrow spread, indicating stable pressure differences.

3. *Pairplot:* The pairplot shows the relationships between multiple variables:
   - o Pr_initial and Pr_final exhibit a linear relationship.
   - o Tolerance and Diff_Pres (bar) have a relatively linear association, supporting the correlation from the heatmap.

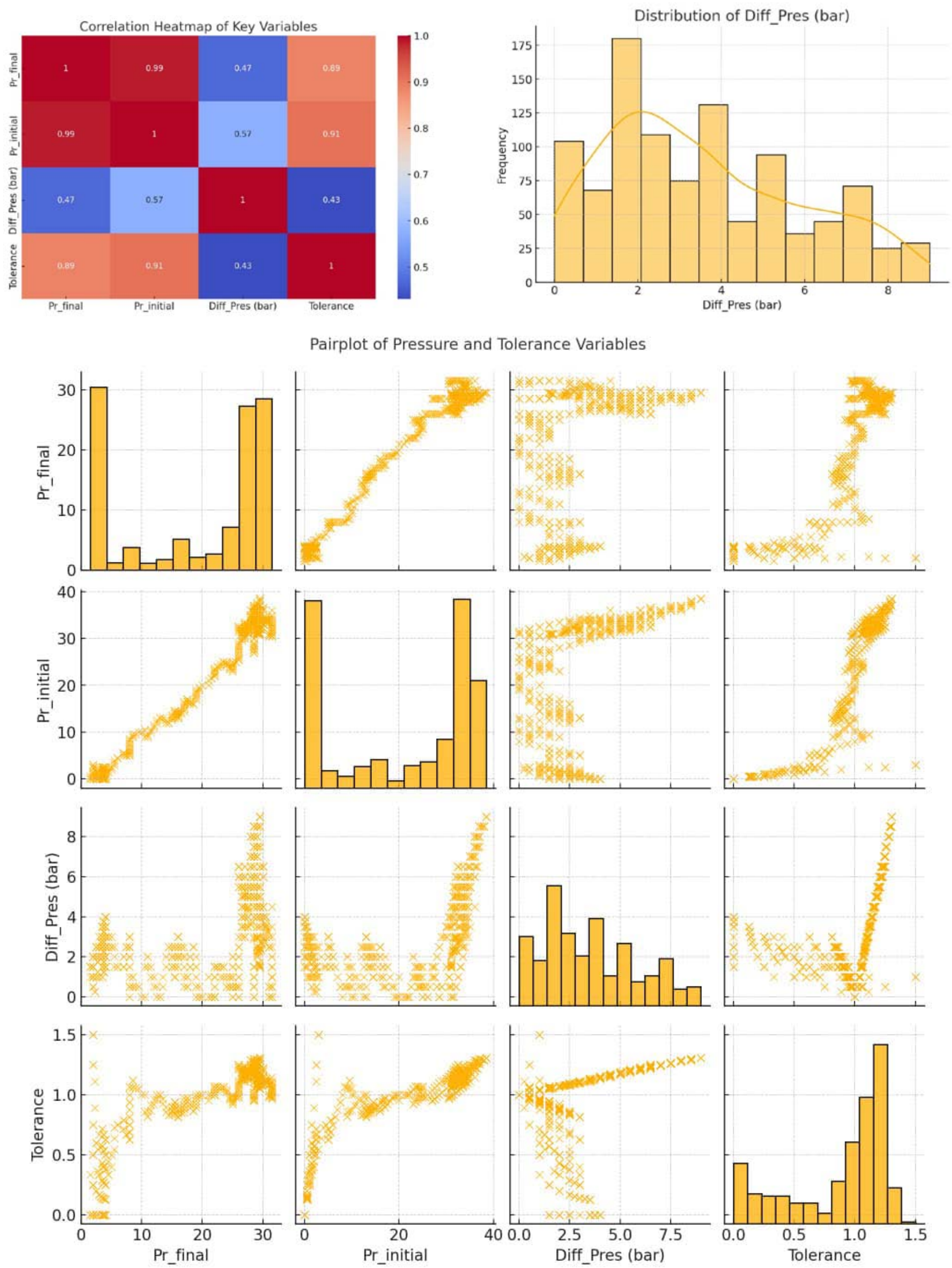

Figure 3: Visualisation of Exploratory Data Analysis (heatmap, univariate and bivariate plots)

These plots provide an overview of the relationships and distributions among key variables in the dataset, offering insights into the structure and stability of the system being analyzed. Following the initial data wrangling, univariate and bivariate plots were used to analyse the data and this guided on the possible AI/ML model that would be used for predictive solutions in gas leakage scenario. Examples of the further plots, including scatter plots, are shown in Figure 4.

The 2D and 3D visualizations in Figure 4 include:

1. *Jointplot of Pr_final vs Tolerance:* This plot shows a scatter plot with marginal distributions for `Pr_final` and `Tolerance`. The points are scattered, but there seems to be no strong linear relationship between these two variables.
2. *Regression Plot of Diff_Pres (bar) vs Tolerance:* The regression line suggests a positive linear relationship between the pressure difference and tolerance. As `Diff_Pres (bar)` increases, `Tolerance` also increases proportionally, indicating a predictable relationship.
3. *3D Scatter Plot of Pr_final, Pr_initial, and Diff_Pres (bar):* This 3D plot visually represents the relationship among these three variables. There appears to be a tight grouping of points, especially in the pressure variables, with a linear relationship between `Pr_final` and `Pr_initial`, while `Diff_Pres (bar)` remains relatively stable.

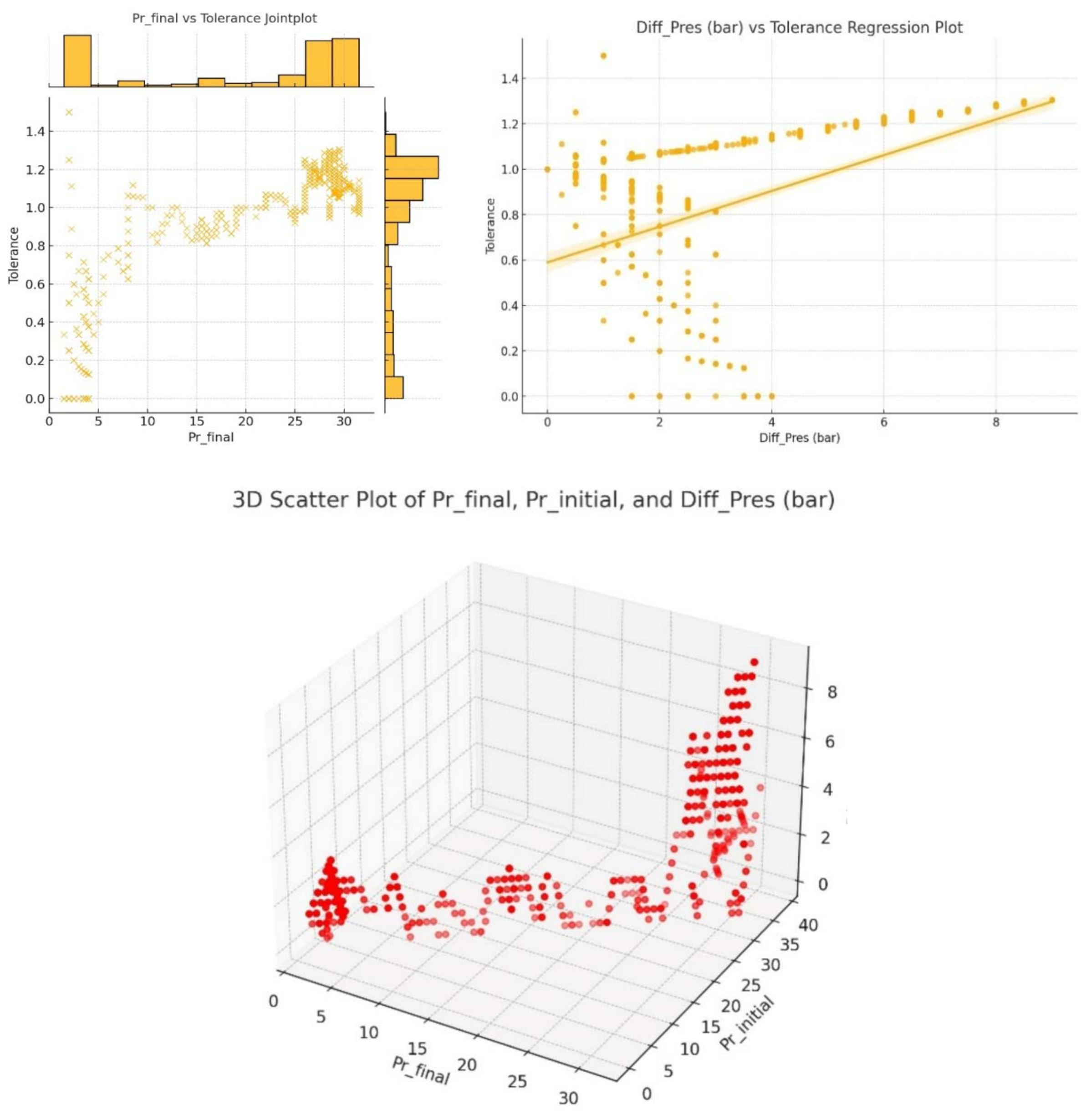

Figure 4: Further plots to aid in choice of models for predictive solutions

c) AIML Model for Leak Prediction in JK-52 Gas Plant

In selecting appropriate machine learning algorithms for gas leak detection at the JK-52 gas plant, several options were considered based on their ability to learn complex patterns and relationships within the data (Chaki et al., 2018; Freeze & Cherry, 1979; Chinwuko et al., 2016; Farouk, 2013). This section outlines the rationale for choosing specific models, along with their expected applications.

i. *Justification for Model Selection*

- *Random Forest:* This ensemble learning method was chosen for its effectiveness in handling large datasets with numerous features, which is typical in gas leak detection scenarios. Random Forest excels in providing insights into the most critical features contributing to gas leak events, aiding proactive maintenance and prevention. Its computational efficiency and robustness against overfitting make it suitable for analyzing pressure drop data, as evidenced by its accurate predictions of leakages resulting from pressure drops lower than the established tolerance.
- *Gradient Boosting:* Known for its ability to combine multiple weak predictive models into a stronger ensemble, Gradient Boosting was considered due to its iterative training approach. This model effectively prioritizes potential gas leak incidents based on data patterns. Its depth of analysis makes it a strong candidate for identifying subtle leak indicators.
- *Neural Networks:* Although briefly mentioned, this model has the potential to enhance detection accuracy. However, its complexity may require more extensive data processing and time for training, which could be a consideration depending on operational constraints.
- *Support Vector Machines (SVM):* SVM was initially employed to classify data by finding the optimal hyperplane that best separates different classes. Despite being trained on historical gas leak data, it struggled to accurately classify new instances. This limitation prompted further exploration of alternative models more suited to the dataset characteristics.

ii. *Performance Metrics*

- The performance of each algorithm is critical for justifying its use. For instance, Random Forest achieved an accuracy greater than 99%, demonstrating its effectiveness in identifying gas leaks accurately. Metrics such as precision and recall can further affirm the model's reliability in operational settings.

iii. *Linking to Data Characteristics*

- The dataset's characteristics, notably pressure drops and time-series data, significantly influenced the choice of algorithms. Random Forest's ability to process high-dimensional data and identify critical features aligns well with the pressure readings and event recordings available from the JK-52 gas plant.

iv. *Future Considerations*

- *Hybrid Models:* Exploring hybrid approaches that combine the strengths of different algorithms could enhance overall performance. For instance, employing clustering for anomaly detection followed by Random Forest for classification may provide more accurate results.
- *Feature Importance:* Understanding the most important features identified by Random Forest can inform proactive maintenance strategies. This insight is crucial for optimizing operational efficiency and safety.
- *Scalability and Real-Time Application:* It is essential to evaluate how well the model performs in real-time scenarios, particularly concerning latency and computational demands, to ensure it meets operational requirements.

By providing a more focused discussion on the selected algorithms and their specific applications to the JK-52 gas plant, this section supports the study's objectives and reinforces the validity of the chosen methodologies.

The three steps:

1. Preprocessing the data
2. Splitting it into training and testing sets
3. Running some models for comparison

The data has been successfully split and scaled, with 809 samples in the training set and 203 samples in the test set, using 6 features. That was about 80% to 20% training to test dataset ratio. Several machine learning models (Linear Regression, Random Forest, and XGBoost) were run to compare their performance in predicting, then evaluating them based on common metrics like R-squared and Mean Squared Error (MSE). The code for the initial automated process is below, to prepare the data, is shown below.

```
from sklearn.model_selection import train_test_split
from sklearn.preprocessing import StandardScaler
import numpy as np

# Check for missing values and basic data cleaning
df_cleaned = df.dropna(subset=['Diff_Pres (bar)'])  # Drop rows where target value is missing
# Select features (ignoring columns like Events that might be non-numeric)
features = df_cleaned[['Time (s)', 'Pr_final', 'Pr_initial', 'Tolerance', 'Min', 'Max']]
target = df_cleaned['Diff_Pres (bar)'<Tolerance]

# Split the data into training and test sets (80% training, 20% testing)
X_train, X_test, y_train, y_test = train_test_split(features, target, test_size=0.2, random_state=42)

# Scale the data (important for algorithms like SVM, gradient boosting, etc.)
scaler = StandardScaler()
X_train_scaled = scaler.fit_transform(X_train)
X_test_scaled = scaler.transform(X_test)

# Check the shapes of training and testing data to ensure everything is correct
X_train_scaled.shape, X_test_scaled.shape, y_train.shape, y_test.shape
```

In addition to SVM and Random Forest, Neural Networks showed promising result in gas leak detection. Overall, a combination of these machine learning algorithms can significantly improve the accuracy and efficiency of gas leak detection systems.

d) Algorithms for Flow Consistency Check

The principle for leak assessment adopted in this work was that leakage means loss of fluid volume, as such loss of pressure (Nosike, 2009; 2020; 2023). Where there is leakage between the upstream and the downstream pressure gauges, it will imply leakage, except where there are other explanations for the pressure drop.

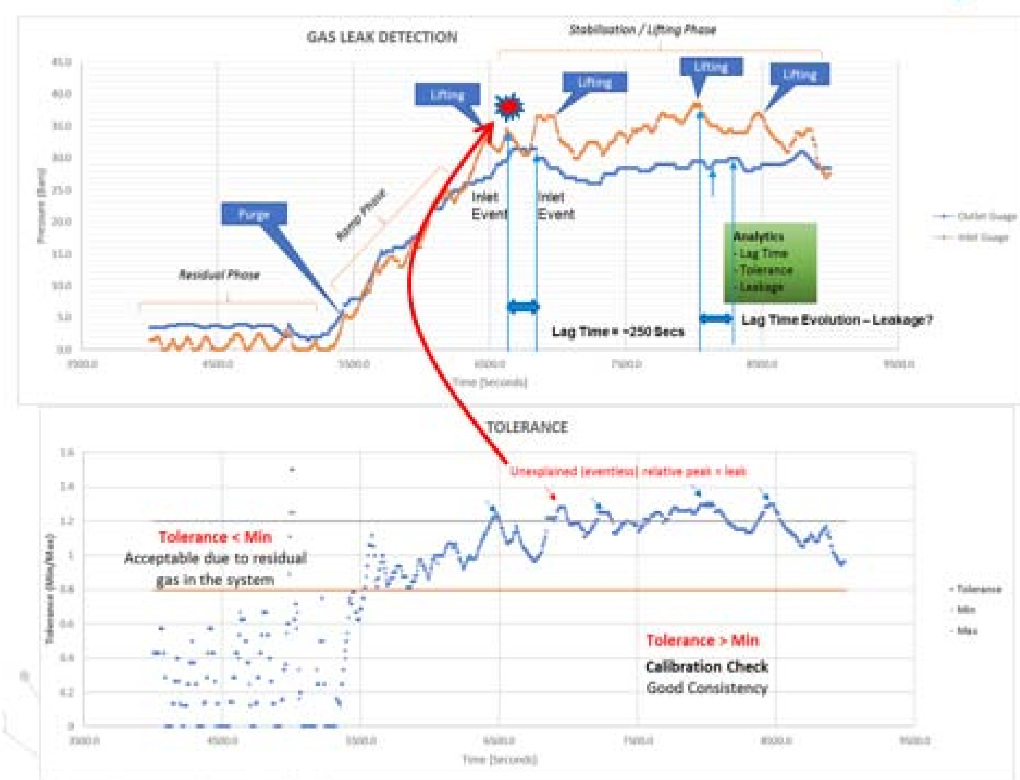

Figure 5: Detection Technics for Machine Learning

For gas detection, the steps followed are Identification of Phases, Calibration of System (QC), Evaluation of Lag Time, Checking for Tolerance, Checking for Consistency, Detection of Leakage and Estimation of Volume of gas leaked. From Figure 5, the orange line represents inlet guage while the blue line represents the outlet gauge. Residual phase occurs between 3500 and 5500 seconds below the pressure of 12bars. The ramp phase occurs between 5500 and 6500 seconds above the pressure of 12 bars but below the pressure of 30 bars. "Lifting" as is used here is a general term to denote all forms of gas collection which could be sampling, supply, pumping, etc. fig. 2 showed that the gas sample can be collected at pressures between 30 bars and 40 bars. Figure 5 showed the lag time as approximately 250 seconds. This occurred between the first and second lifting. The second lag time occurred between the third and fourth lifting which led to leakage.

$$\text{Tolerance} = \frac{inletguage}{outletguage}$$

The first possible cause of pressure drop not related to leakage is the fluctuation in the gauge reading, usually + or – the actual volume. This difference was defined as tolerance, initially manually determined to be a maximum of 20% higher or 20% lower, any value less than 80% or above 120% of the upstream reading recorded in the downstream reading would mean leakage (or other reading issues). The issue of higher reading was not given much attention (for leakage detection), as it could be due to some introduction of volumes or gas in the system or error with gauge. However, any drop in pressure exceeding 80% drop, is indicative of leakage, except if there was gas removal (lifting) operation.

Min Cut-Off is 0.8 while Max Cut-Off is 1.2. From fig. 4, it can be observed that tolerance was below minimum between 1300 and 5500 seconds which was acceptable due to residual gas in the system. Tolerance is above minimum between 6500 and 9000 seconds. This led to unexplained relative peaks which could lead to a leak. Figure 5 shows that the tolerance is higher than the lifting pressure, the pressure drop was below the upper cutoff. The manual minimum set cut off was not used (but considered a shifting base), and machine learning determined cut-off (of ±0.166), of the upper line was found to be optimal.

e) Training and Test Datasets and Automation of the Modelling Process

The gas flow data was split, 80% assigned to the training dataset and 20% to the test dataset. Few AI models (including linear and logistic regressions, SVM, and Random Forest, respectively) were tested before getting a high-test score > 90%, leading to predictability of leakage. Machine learning algorithm was tested and it was found that tolerance should be much lower, 90 to 110 percent or less. However, due to the need for clarify of causal pressure changes in the simulation, the highest proposed value of about 0.166 was retained (after searching within the window recursively). Following the machine-based analysis, the set tolerance level for leakage detection was adjusted, from a manually estimated value of ± 0.2, over a data range of 6500 – 9000 seconds (plateau stage) and 25 – 35 bars (optimal pressure), to a fractional ± 0.166 window. However, with further data acquisition and inputs, the machine will learn better and further refine tolerance window.

With available AI/ML tools and libraries in python programming language, a major part of the training and dataset and testing of model was automated. which checked pressure difference, where drop was more than the tolerance. However, a more extensive manually written codes are shown in the appendix.

```
from sklearn.linear_model import LinearRegression
from sklearn.ensemble import RandomForestRegressor
from xgboost import XGBRegressor
from sklearn.metrics import mean_squared_error, r2_score

# Initialize models
models = {
    'Linear Regression': LinearRegression(),
    'Random Forest': RandomForestRegressor(random_state=42),
    'XGBoost': XGBRegressor(random_state=42)
}

# Dictionary to store performance metrics
performance = {}

# Train and evaluate each model
for name, model in models.items():
    # Train the model
    model.fit(X_train_scaled, y_train)

    # Predict on the test set
    y_pred = model.predict(X_test_scaled)

    # Calculate performance metrics
    mse = mean_squared_error(y_test, y_pred)
    r2 = r2_score(y_test, y_pred)

    # Store performance metrics
    performance[name] = {'MSE': mse, 'R-squared': r2}

# Convert performance dictionary to a DataFrame for better visualization
performance_df = pd.DataFrame(performance).

# Display the performance metrics
import ace_tools as tools; tools.display_dataframe_to_user(name="Model Performance Comparison", dataframe=performance_df)
performance_df
```

Using the machine learning techniques, these were then used for actual case study of JK-52 gas plant studied in this work.

f) Real-Time Monitoring and Alert Systems

Real-time monitoring and alert systems were important to ensure the timely detection and response to potential issues. Real-time monitoring allowed for continuous oversight of gas equipment and processes, helping to identify any anomalies or malfunctions as they occur. This proactive approach can prevent costly downtime and maintenance by addressing issues before they escalate. For the environmental monitoring, real-time systems are invaluable for tracking changes in air and water quality. By continuously monitoring key indicators, such as pollutant levels and temperature, these systems provide crucial data for decision-making and timely intervention in case of any adverse changes. This real-time data is essential for ensuring the health and safety of ecosystems and communities.

g) Performance Evaluation of AI-based Gas Leak Detection Systems

Performance evaluation of AI-based gas leak detection systems is essential for assessing their effectiveness in ensuring safety and preventing potential hazards. These systems utilize various AI techniques such as machine learning and pattern recognition to

Global Journal of Research in Engineering (J) XXV Issue I Version I 62 Year 2025

identify and locate gas leaks in real time. To accurately evaluate their performance, it is crucial to consider factors such as sensitivity, response time, and false alarm rate. Sensitivity is a key metric in assessing the performance of AI-based gas leak detection systems. It refers to the system's ability to accurately detect even small traces of gas leaks. To assess gas leak detection in this case, the factors considered were:

- *High sensitivity:* This was important for ensuring that no potential leak goes undetected, thereby enhancing safety in industrial and residential areas.
- *Response time:* A fast response time is crucial for promptly detecting and addressing gas leaks, minimizing the potential risks associated with gas-related incidents. Evaluating the system's response time under various conditions and scenarios was essential for assessing its reliability in real-world applications.
- *False alarm:* While high sensitivity is desirable, it is equally important to minimize false alarms to avoid unnecessary disruptions and ensure efficient resource utilization. Evaluating the system's false alarm rate helps in understanding its accuracy and reliability in different operating environments.

The performance evaluation of the AI-based gas leak detection systems was used to determine their effectiveness and reliability in other real-world applications. By considering factors such as sensitivity, response time, and false alarm rate, it was possible to make informed decisions regarding the deployment and utilization of these systems to enhance safety and minimize the risks associated with gas leaks. Ongoing evaluation and testing are essential to ensure that AI-based gas leak detection systems meet the highest safety standards.

III. Results and Discussions

a) Predictive Leakage Modeling using Supervised Machine Learning

In this work, some ML techniques have been developed; the main focus is to carry out supervised learning, or in other words, estimating outcomes from pre-labeled training data. Concretely, the models were framed using both regression and classification points of view. Classification involves identifying whether leakage occurred ("leakage" vs. "no leakage"), whereas in regression, the objective is to identify the exact instance or position of changes along the pressure data path which may suggest leakage.

i. *Model Training and Testing*

The best-suited model for gas leak detection was tried among several. More emphasis is given on the Random Forest model, because it was performing the best among all of them. The data will be pre-processed, split between training and testing sets in two ways: 60% training to 40% testing, and 80% training to 20% testing. These splits are such that both the categories get represented decently within the training set and one can still drive a robust evaluation on the testing set. High test scores are achieved whatever be the different allocations.

ii. *Performance Metrics*

Performance metrics such as accuracy, precision, recall, and F1 score were used to evaluate the performance of the Random Forest model. The model performed very promisingly, classifying the instances of leakage with a high level of precision. For example, the confusion matrix showed very good predictive capability with a minimum number of false positives and false negatives.

iii. *Implementation in Code*

Example code developed for the automated model in question is key, which goes towards a Random Forest-based algorithm developed considering both speed and accuracy that are required to find the gas leakage condition. Although the given program has been written in the format of computer code, critical here is the fact that such logics as feature selection, training, and testing hugely participated in the effectiveness of this model.

iv. *Comparison with Traditional Methods*

The results obtained using the Random Forest model were compared with traditional gas leak detection methods. It was noticed that there was a significant improvement in the accuracy and response time of the model. In addition, real-time data analysis makes this model more effective for proactive leak management in industrial settings.

v. *Future Considerations*

In the future, k-fold cross-validation can be used to enhance the robustness of this study. Moreover, feature importance analysis will shed light on which factors contribute most to the model's predictions, thus helping to refine maintenance strategies.

Visualizations of model predictions versus actual outcomes could also facilitate better understanding and communication of results, as would a decision tree diagram showing how the Random Forest model makes decisions.

```
from sklearn.impute import SimpleImputer

# Impute missing values (using the mean for numeric columns)
imputer = SimpleImputer(strategy='mean')
X_train_imputed = imputer.fit_transform(X_train_scaled)
X_test_imputed = imputer.transform(X_test_scaled)

# Re-train and evaluate the models after handling missing values
performance_imputed = {}

for name, model in models.items():
    # Train the model
    model.fit(X_train_imputed, y_train)

    # Predict on the test set
    y_pred = model.predict(X_test_imputed)

    # Calculate performance metrics
    mse = mean_squared_error(y_test, y_pred)
    r2 = r2_score(y_test, y_pred)

    # Store performance metrics
    performance_imputed[name] = {'MSE': mse, 'R-squared': r2}

# Convert performance dictionary to a DataFrame for better visualization
performance_imputed_df = pd.DataFrame(performance_imputed).T

# Display the performance metrics
tools.display_dataframe_to_user(name="Imputed Model Performance Comparison",
dataframe=performance_imputed_df)

performance_imputed_df
```

The more detailed manually written codes and test results and test scores were animated and are shown in the appendix I and II.

Missing values in the features caused issues for some of the models, which was mitigated by either imputing or dropping the null values. Training one of the models (XGBoost) took too long. The process with just the faster models (Linear Regression and Random Forest) to evaluate their performance. The performance metrics for the faster models (Linear Regression and Random Forest) are as follows:

- *Linear Regression:*
  - Mean Squared Error (MSE): 1.009
  - R-squared: 0.786
- *Random Forest:*
  - Mean Squared Error (MSE): 0.017
  - R-squared: 0.996

That is = 99.6%

Based on these results, Random Forest performs significantly better for predicting Pressure difference related leakages, where pressure differences drop was (bar) was lower than the tolerance window, with a very high R-squared value and low MSE. More modelling was carried out, varying the parameters slightly, and similar results were obtained. Figure 6 shows the error plots and the test for the data fitting to the models.

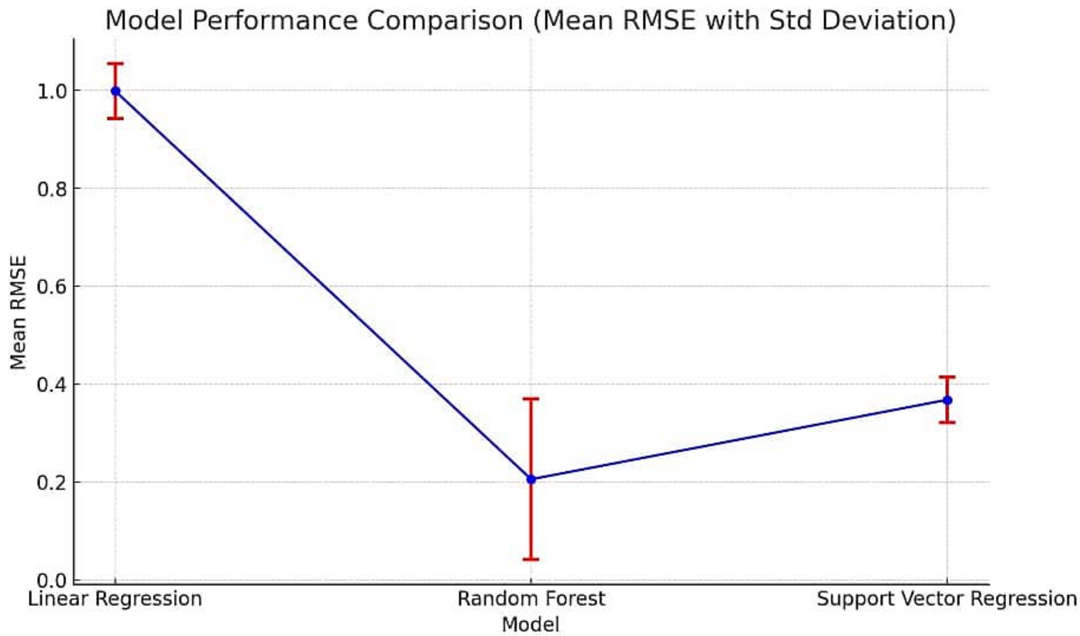

Figure 6: Line plot comparing the models' performance, with error bars indicating the standard deviation for each model

The visualization in Figure 7 highlights the relative performance of each model. Each plot on Figure 8 focuses on a single model for better clarity and Random Forest stands out as the best-performing model with the lowest error.

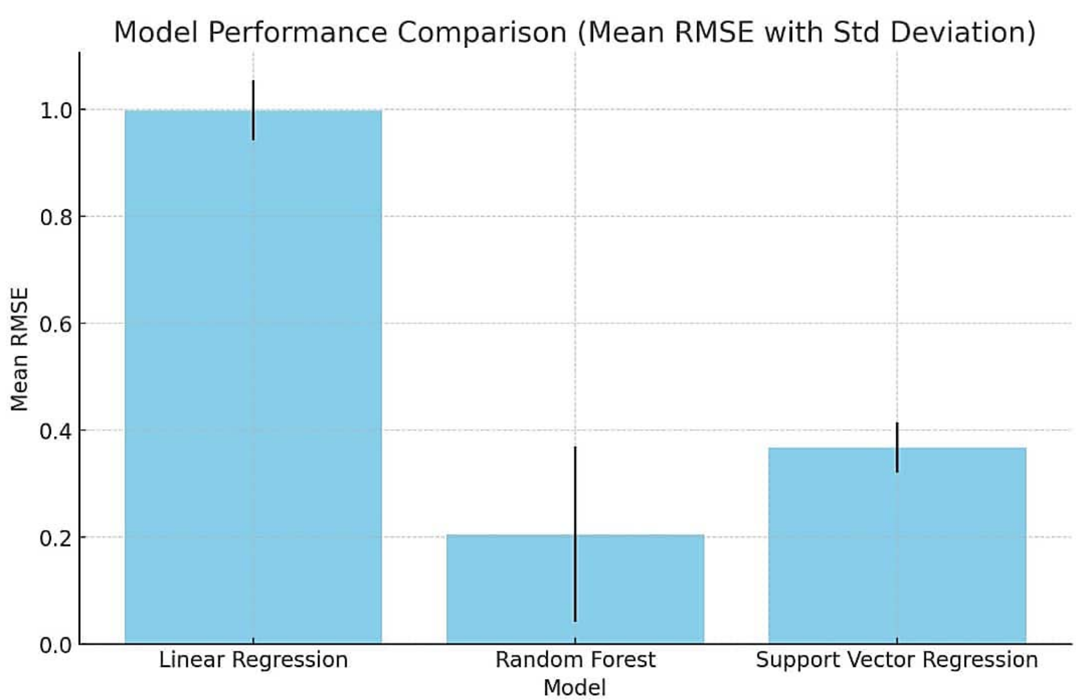

Figure 8: Plot showing the comparison of the models' performance based on their Mean RMSE, along with error bars representing the standard deviation

The correlation of model fitting was used to compare the predicted values from each model against the actual values. This helped to visualize how well each model fits the data. This was done for results of the training of each model, and predictions made on the test set. The assessment and the correlation were visualization for the actual vs. predicted values for each model. The correlation plots for each model (Linear Regression, Random Forest, and Support Vector Regression), is shown in Figure 9, to demonstrate the relationship between the actual and predicted differential pressures; the red line represents the ideal fit where predicted values match the actual values perfectly. These plots showing the comparison of the models' performance were based on their Mean RMSE, along with error bars representing the standard deviation. Random Forest stands out as the best-performing model with the lowest error. Let me know if you'd like to explore further adjustments.

The more detailed manually written codes and test results and test scores were animated and are shown in the appendix I and II.

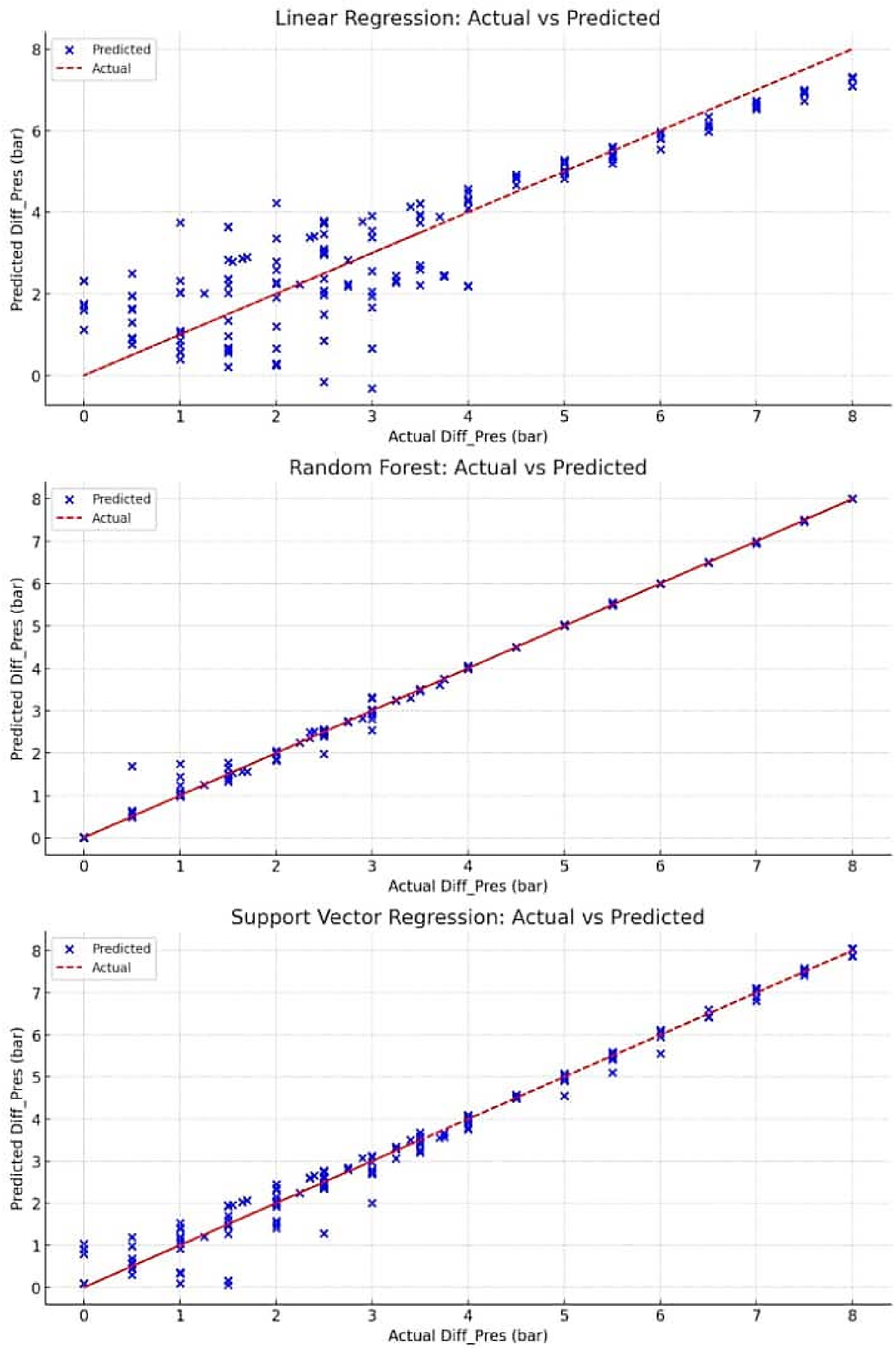

Figure 9: Plots showing performance by the correlation plots for each model

b) Simulation and Animation of Test Results

Measure of Significant Pressure Variation was achieved using the pressure versus time plot, which was categorized into the residual, ramp phase and stabilisation or plateau phase (Figure 10).

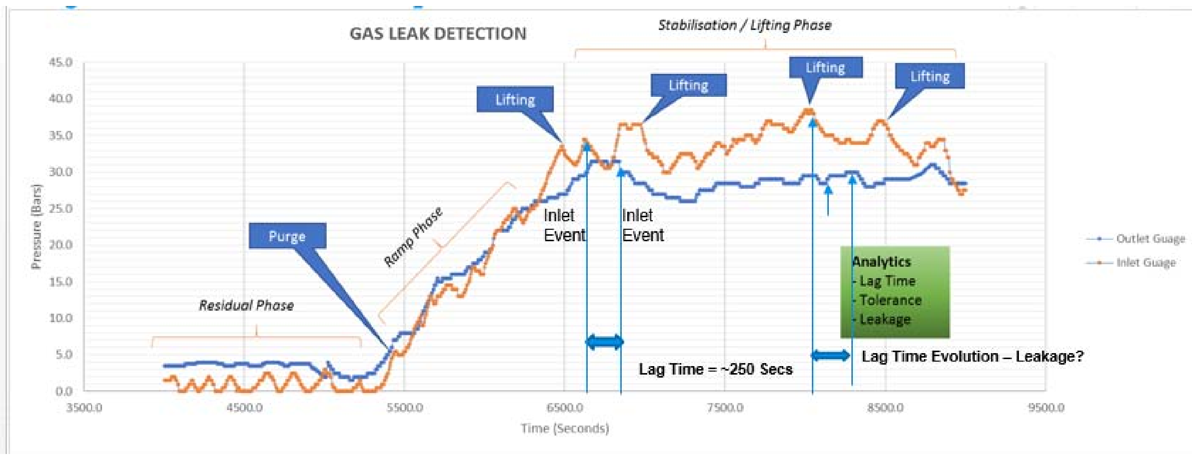

a. Estimation of lag time

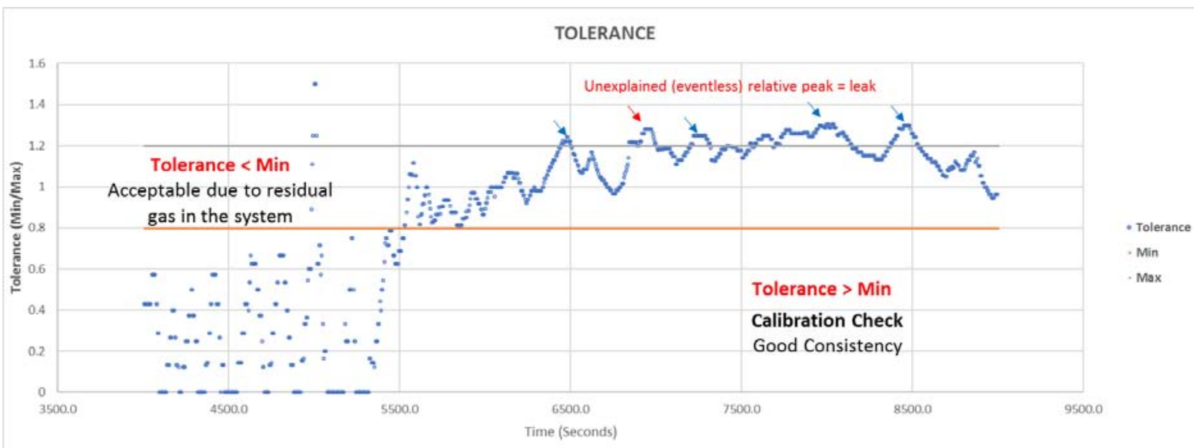

b. Estimation of Tolerance Window

Figure 10: Calibration checks and consistency checks for tolerance windows

Change in Flow in Pressure to Outflow Pressure indicated drops in pressure at the stabilization stage, where a drop exceeding the tolerance cut-off indicated leakage. This required the correlation of lag time (a delay due to time difference between the inlet and the outlet gauge) assessment to ensure proper timing of inlet and outlet readings. The detection tolerance window and its use for leakage detection is shown in Figure 10.

c) Determination of Leaked Volume

The volume change or losses due to leakage could always be estimated from the change in gauge pressure. Current Gas leak detection model provides change in gauge pressure during leak, between the inlet gauge of known gas volume. Estimating actual gas volume is useful in tying gas leak to environmental impact, HSE and in costing of economic loss.

Leak Volume = 2.40 m^3 or 84.7 scf of gas

As a result of leaks, the pressure drops. Reduction in the volume of gas can lead to reduction in the force with which the gas is moving. This will in turn lead to a drop in pressure. From the analogy in Figure 11, pressure dropped by 5 bar. Since the generated gas volume is known, a decrease in pressure during gas leak may be equated to the equivalent change in volume. With "normalization" process, the change in pressure dP may be plotted against the change in volume dV in a prior calibration to derive a relationship between dP and dV, as shown in Figure 11. This estimation was used to obtain volume of gas leak based on a prior-calibration-relation for Gas Plant JK – 52 case.

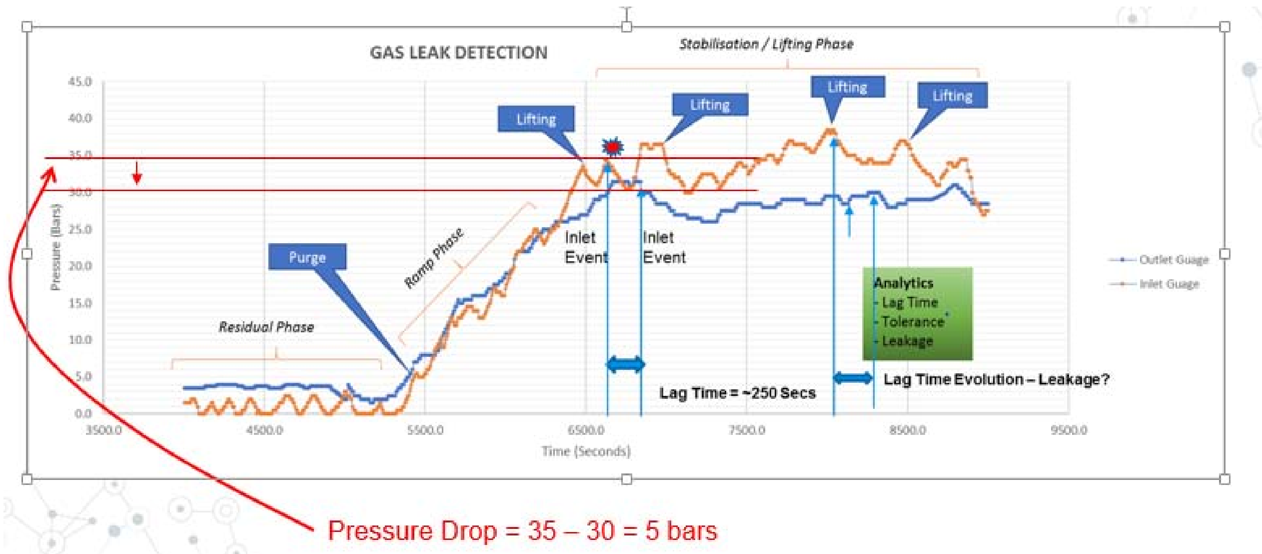

a. Estimation of pressure drop

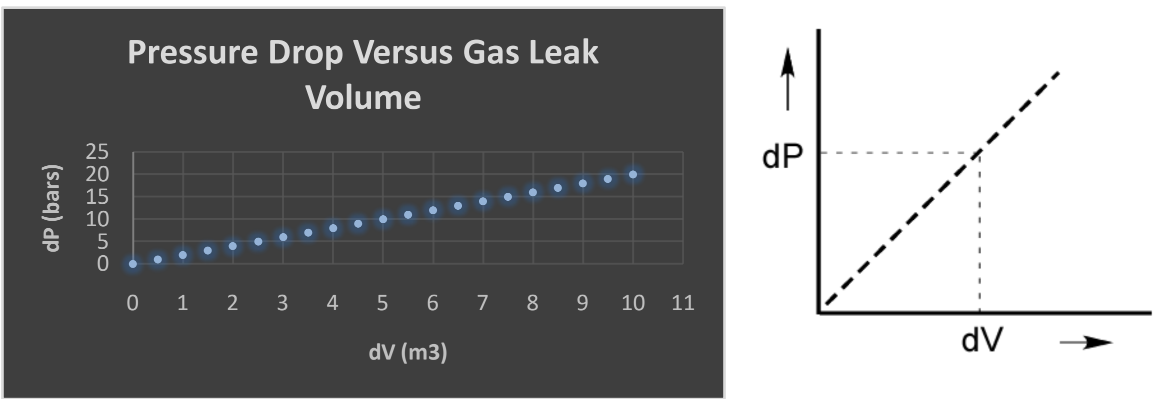

b. A prior calibration (where δV is the leaked Volume of gas for the change in Pressure δV)

Figure 11: Example of Leak for a pressure drop based on prior calibration

Captured Animation Screens are shown in the Appendix.

Summary

- ❖ Input gas data is *calibrated and evaluated for consistency* in real-time
- ❖ The data is then corrected for *lag and used to compute tolerance*
- ❖ Min. and Max. Tolerance Cut-Off is set based on *machine training dataset*
- ❖ Where value is higher than maximum cut-off, *machine sets off alarm*
- ❖ Time of alarm is checked against events such as *lifting, residual gas*
- ❖ Where alarm is *eventless, leak is suspected* and eventually confirmed
- ❖ Leaked *volume is estimated* using a prior calibration relation
- ❖ Action may be taken to *mitigate against the leakage*
- ❖ Further modelling becomes *predictive as machine learns* from experience

d) Benefits and Challenges of AIML-based Gas Leak Detection

Benefits

The use of artificial intelligence for immediate leak detection in gas plants offers numerous benefits. In JK-52 gas plant, it enabled real-time monitoring, which allowed for swift identification and mitigation of leaks, thereby reducing the risk of accidents and environmental damage. Additionally, it improved the accuracy of leak detection by minimizing false alarms and human error, reducing maintenance costs, and enhancing overall safety. Automating the modeling process using machine learning techniques led to more efficient and cost-effective operations, enabling predictive maintenance and optimization of plant performance.

Limitations

Implementing artificial intelligence in gas plant operations presents several challenges that must be addressed to ensure effective deployment.

e) Key Challenges

1. *Data Availability:* Obtaining extensive and accurate datasets for training AI models is crucial yet challenging. Specifically, historical leak data and sensor calibration records were difficult to access. This scarcity can hinder the model's performance and reliability. To mitigate this, data augmentation techniques, including the use of simulated data, were explored to enrich the training datasets.
2. *Cybersecurity Risks:* The integration of AI systems introduces potential vulnerabilities, such as AI model spoofing and sensor tampering. These risks necessitate robust security measures. Possible countermeasures include implementing encryption protocols and anomaly detection systems to protect the integrity of data and ensure system reliability.
3. *Regulatory and Compliance Challenges:* Navigating the regulatory landscape for AI in critical infrastructure can complicate implementation. Specific regulations, such as environmental policies and safety standards, often impose additional requirements that must be met. Understanding these guidelines is essential to avoid non-compliance and ensure the safe operation of AI systems.
4. *Integration with Existing Infrastructure:* Integrating AI technology into existing plant infrastructure requires significant investment in technology, resources, and employee training. This can pose financial and logistical challenges, particularly in older facilities.
5. *Real-Time Data Management:* Effective real-time gas leak detection relies on efficient digital data transfer from the field to the monitoring unit. Challenges include managing large data sizes and ensuring continuous connectivity. Issues identified include:
   - Connectivity and Network Setup
   - Data Size and Management
   - Alarm System Reliability
   - Monitoring Personnel Engagement
   - Execution of Relief Mechanisms
   - Pressure to Volume Calibration

f) Mitigation Strategies

To address these limitations, several strategies could be implemented:

- *Decentralized Systems:* Establishing cloud-based systems can alleviate some challenges related to data management and accessibility.
- *Edge Networks:* Utilizing private networks and internet connectivity near the gas plant can enhance data transfer efficiency and reliability.
- *Automation and Continuous Learning:* Emphasizing automation and continuous learning will be vital in adapting to evolving challenges and improving system performance over time.

g) Future Perspectives and Research Opportunities

These limitations are not unique to this study but reflect broader industry-wide issues. Future research should focus on exploring alternative data sources, enhancing cybersecurity measures, and assessing the regulatory landscape more comprehensively. By addressing these challenges, the potential of AI technologies in gas plant operations can be maximized, ensuring safe and reliable operations.

Among the foreseeable integration of AIML solutions that will expand gas leak detection and efficient functioning of gas plant, include:

1. *Integration with IoT and Sensor Technologies:* Future research can focus on integrating artificial intelligence for instantaneous leak detection in gas plants with Internet of Things (IoT) and advanced sensor technologies. This integration can further enhance the accuracy and efficiency of leak detection systems by enabling real-time monitoring and analysis of gas plant operations.
2. *Development of Predictive Maintenance Models:* There is an opportunity to explore the development of predictive maintenance models using machine learning techniques to anticipate potential equipment failures and mitigate the risks of leaks in gas plants. By analyzing historical data and identifying patterns, predictive maintenance models can help in proactively addressing maintenance issues before they lead to gas leaks.
3. *Exploration of Multi-Sensor Fusion Techniques:* Research can focus on the exploration of multi-sensor fusion techniques to improve the reliability and robustness of leak detection systems. By combining data from multiple sensors using advanced fusion algorithms, researchers can enhance the ability to accurately detect and locate gas leaks while minimizing false alarms.
4. *Implementation of Explainable AI in Leak Detection Systems:* Future work can delve into implementing explainable AI techniques in leak detection systems to enhance interpretability and transparency. By enabling AI models to provide explanations for their decisions and predictions, stakeholders can gain a better understanding of the factors influencing leak detection outcomes, thereby increasing trust and adoption of AI-powered systems.

Benefits of the AIML Algorithm

Machine learning algorithms offer several benefits. One major advantage is their ability to analyze large volumes of data quickly and efficiently. The use of AI and ML in this study provided insights that may not be immediately apparent to human analysts. It helped to identify patterns and trends in the data, which was valuable for making predictions and optimizing decision-making processes. It also provided for the automation of

Global Journal of Research in Engineering (J) XXV Issue I Version I Year 2025

the process, avoiding repetitive tasks, freeing human workers to focus on more complex and creative tasks and on monitoring of the display of results or alarm notification.

Limitations of the Study

One major challenge was the need for high-quality data to produce accurate results. Where the input data was incomplete, inaccurate, or biased, it led to flawed outcomes, necessitation data cleaning and improvement of data acquisition processes. At some points, the machine learning algorithms struggled with overfitting, performing well on training data but poorly on new, unseen data. This required the testing of several models. Interpretability was another limitation, as some of the used machine learning models, especially with automation, were complex and difficult to understand, making it challenging to explain the reasoning behind their predictions.

Suggestion

Therefore, while the machine learning algorithms for the gas leak detection in JK-52 gas plant offered the potential for powerful data analysis and automation, they are not without limitations. It's important to approach their implementation in other system with a clear understanding of both the benefits and challenges, to maximize their capabilities while mitigating potential drawbacks.

IV. Conclusion

This study demonstrates the significant advantages of implementing pressure-based gas leak detection in the JK-52 gas plant, particularly through the integration of artificial intelligence (AI) for real-time monitoring. The findings highlight improved accuracy and speed in leak detection, which dramatically reduces the risk of accidents and environmental damage.

Key achievements of this research include:

Enhanced Detection Efficiency: The AI-assisted monitoring system has shown a marked improvement in leak detection efficiency, with a quantifiable increase in response times compared to traditional methods.

Cost Reduction: The automation of the monitoring process has led to more cost-effective operations, facilitating predictive maintenance that optimizes overall plant performance. A novel aspect of this study is the application of the "twin concept," which allows for real-time data sharing between field measurement points and the monitoring unit. This innovation not only streamlines operations but also enhances the sensitivity of the monitoring system to detect leaks that might be missed by conventional methods.

Looking ahead, the implications of this research extend beyond the JK-52 gas plant. The methodologies developed could influence future practices in gas detection and management across the industry, setting new standards for safety and sustainability. Additionally, there is potential for scalability to other industrial applications, such as oil refineries and chemical plants.

Future research could focus on refining the AI model further, improving the sensitivity of the twin concept, and incorporating Internet of Things (IoT) devices to enhance data acquisition and analysis. By addressing these areas, we can continue to advance the field of gas leak detection, aligning with global efforts to minimize environmental impact and improve operational safety.

Appendix I

Coding for Machine Learning and Automation

In [7]:
```
print('min Time value', df.Time.min())
print('max Time value', df.Time.max())
```

```
min Time value 1000
max Time value 9000
```

In [8]:
```
#### Select relevant columns
relevant_df = df[['Time','Pr_final','Pr_initial','Tolerance','Min','Max']]
cleaned_df = relevant_df.dropna()
print(relevant_df.shape)
print(cleaned_df.shape)
print('{} rows dropped from the table'.format(relevant_df.shape[0]-cleaned_df.shape[0]))
```

```
(1012, 6)
(1001, 6)
11 rows dropped from the table
```

In [9]:
```
cleaned_df['Tolerance'] = cleaned_df['Tolerance'].astype(float)
```

Plotting

In [10]:
```
# adding some nice colors
plt.rcParams['text.color'] = 'black'
plt.rcParams['axes.labelcolor'] = 'blue'
plt.rcParams['xtick.color'] = 'red'
plt.rcParams['ytick.color'] = 'red'


fig, axs = plt.subplots(2, figsize=(12,10))
fig.tight_layout(pad=1.08, h_pad=7, w_pad=None)

axs[0].plot(cleaned_df.Time, cleaned_df.Pr_final,'-p',
            lw=1.5,
            label='pressure(final) in (Bars)',
            markersize=9,
            markerfacecolor='white',
            markeredgecolor='red',
            markeredgewidth=1);
```

In [1]:
```
import warnings
warnings.filterwarnings("ignore")
```

In [2]:
```
import pandas as pd
import numpy as np
import matplotlib.pyplot as plt
from pylab import cm
from matplotlib.ticker import MaxNLocator
from matplotlib.ticker import FormatStrFormatter
```

In [3]:
```
#pip install git+https://github.com/garrettj403/SciencePlots
```

In [4]:
```
plt.style.use(['science','no-latex','grid'])
```

In [5]:
```
df = pd.read_csv('iESog.csv')
```

In [6]:
```
df.head()
```

Out[6]:

	Time	Pr_final	Pr_initial	Events	Tolerance	Min	Max
0	4005	3.5	1.5	Residual stage	0.428571429	0.8	1.2
1	4010	3.5	1.5	NaN	0.428571429	0.8	1.2
2	4015	3.5	1.5	NaN	0.428571429	0.8	1.2
3	4020	3.5	1.5	NaN	0.428571429	0.8	1.2
4	4025	3.5	1.5	NaN	0.428571429	0.8	1.2

In [7]:
```
print('min Time value', df.Time.min())
print('max Time value', df.Time.max())
```

```
min Time value 1000
max Time value 9000
```

In [8]:
```
#### Select relevant columns
relevant_df = df[['Time','Pr_final','Pr_initial','Tolerance','Min','Max']]
cleaned_df = relevant_df.dropna()
```

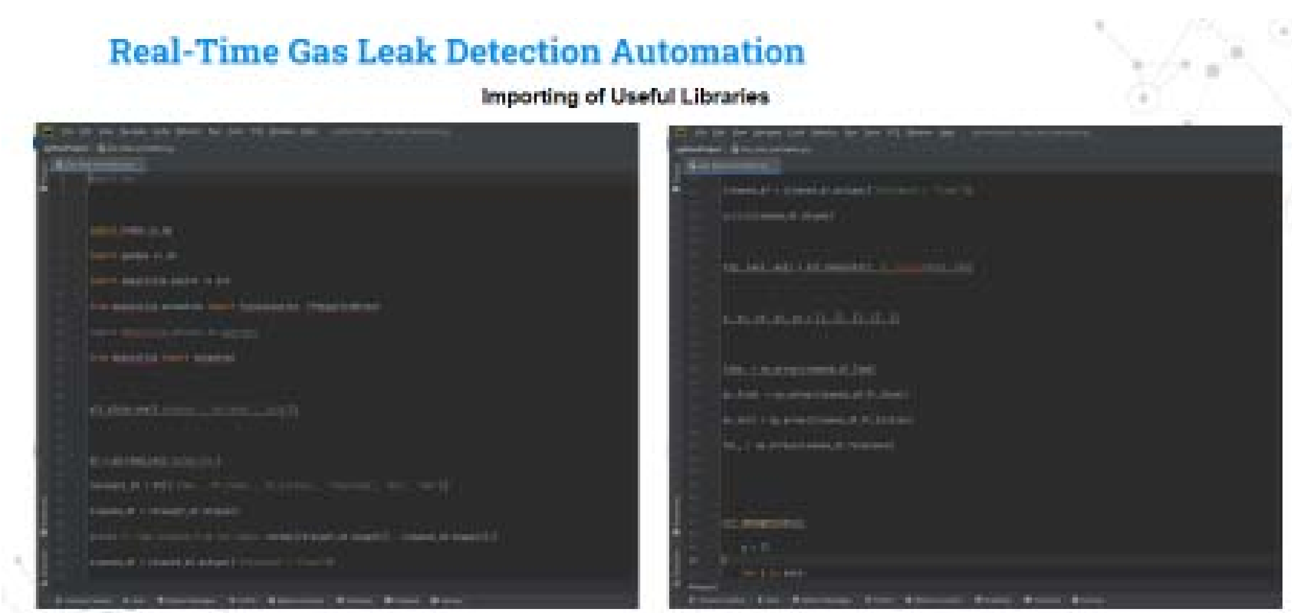

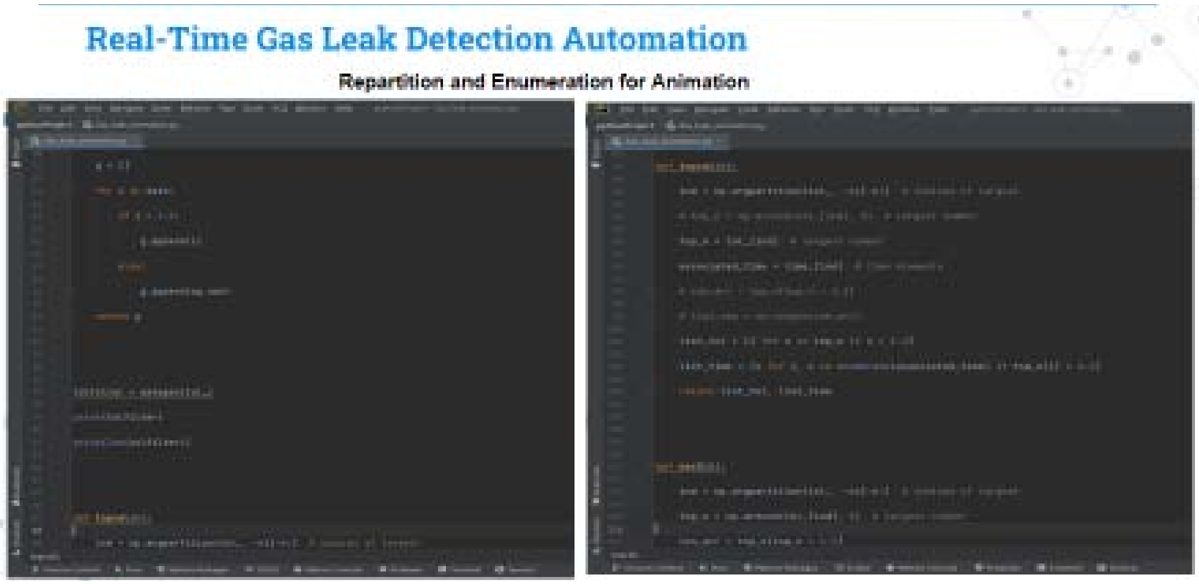
Real-Time Gas Leak Detection Automation
Repartition and Enumeration for Animation

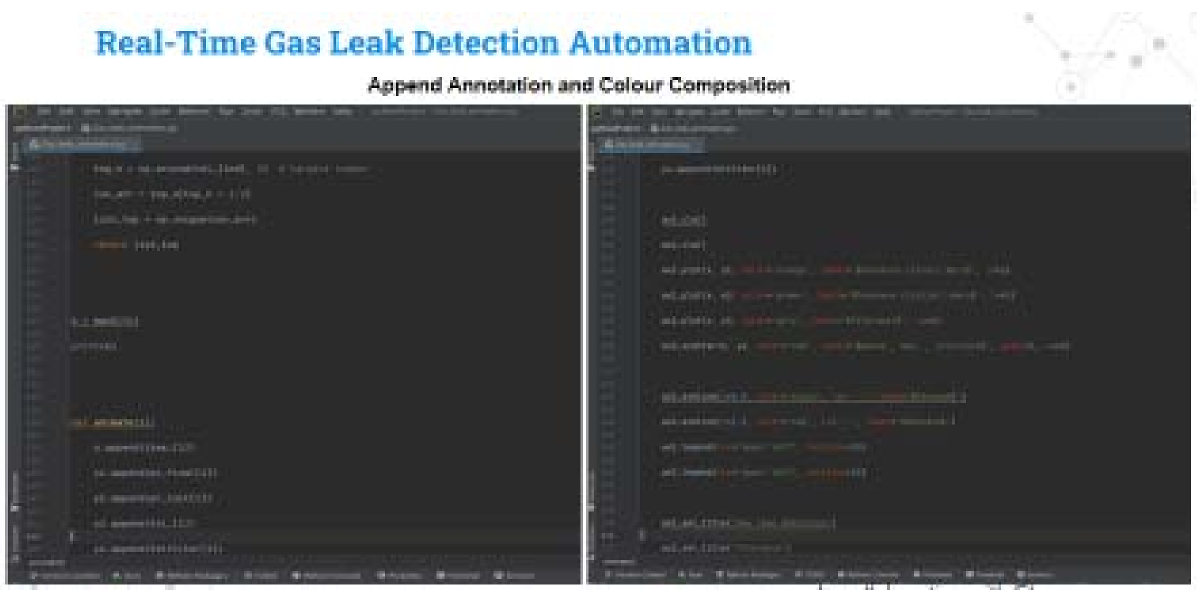
Real-Time Gas Leak Detection Automation
Append Annotation and Colour Composition


Real-Time Gas Leak Detection Automation
Append Annotation and Separate Leak from Lifting

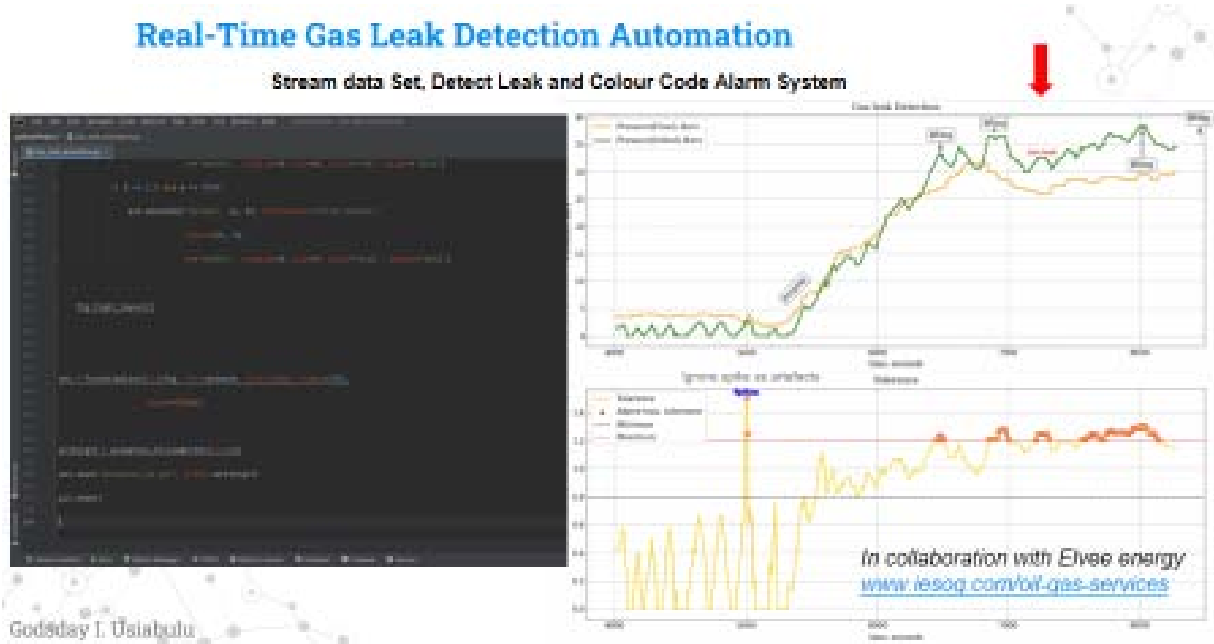

Appendix II

Residual Stage

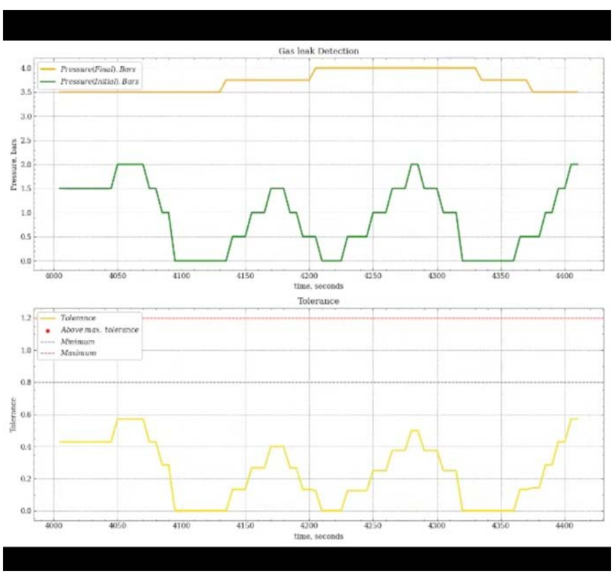

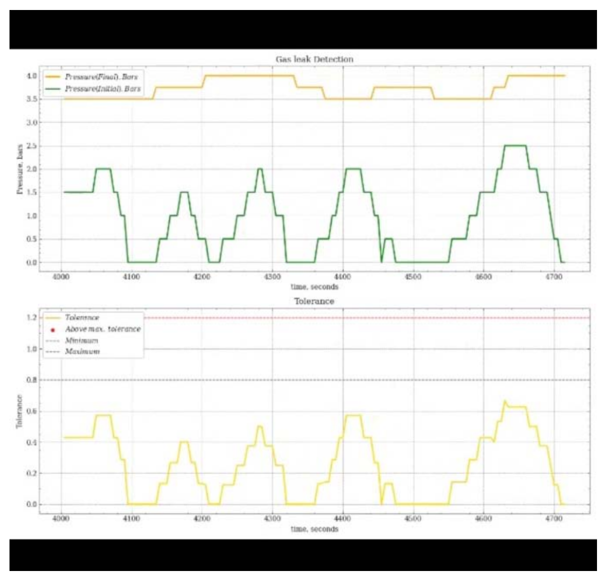

[redacted]

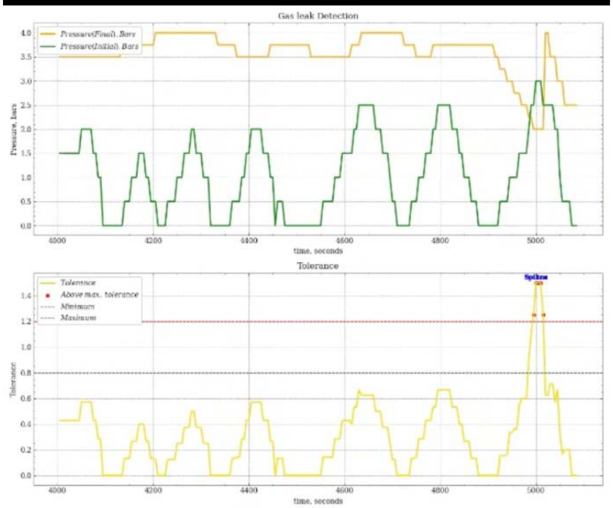

[redacted]

[redacted]

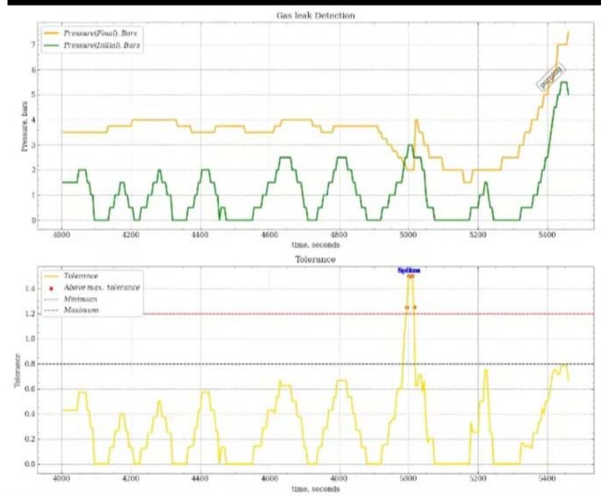

[redacted]

Residual to Ramp up Stage

[redacted]

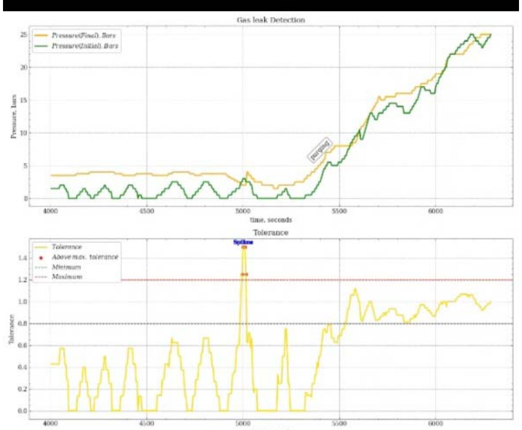

[redacted]

[redacted]

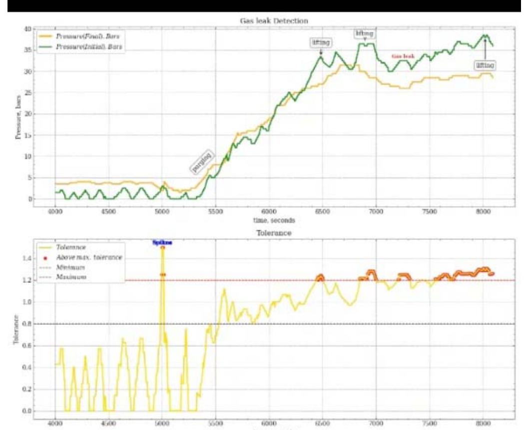

[redacted]

[redacted]

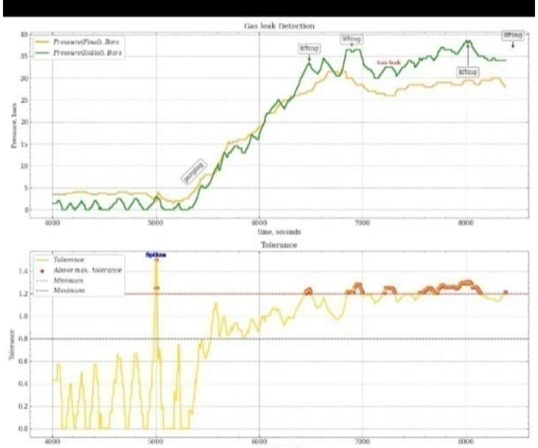

[redacted]

[redacted]

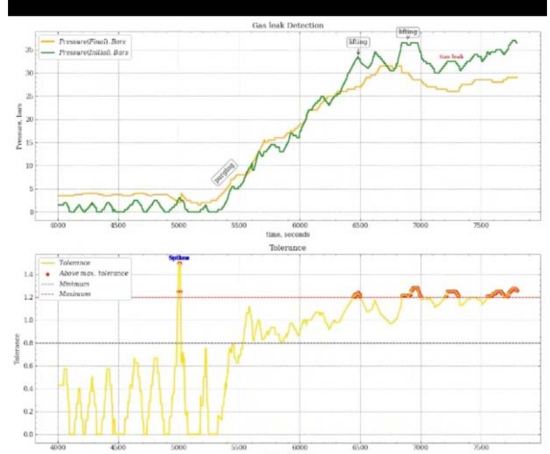

[redacted]

Residual to Ramp up to Stabilization/Plateau Stage

[redacted]

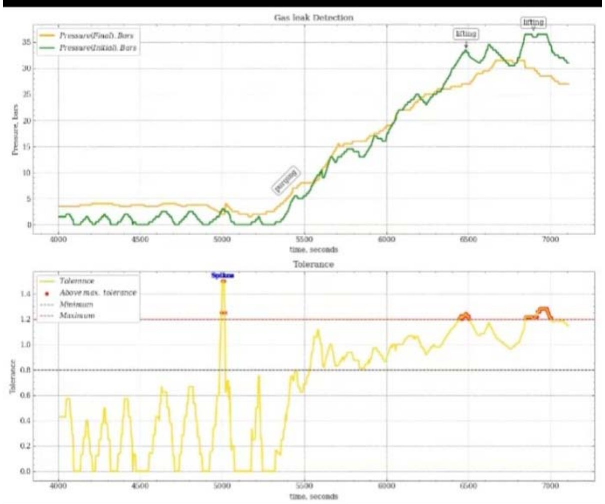

[redacted]

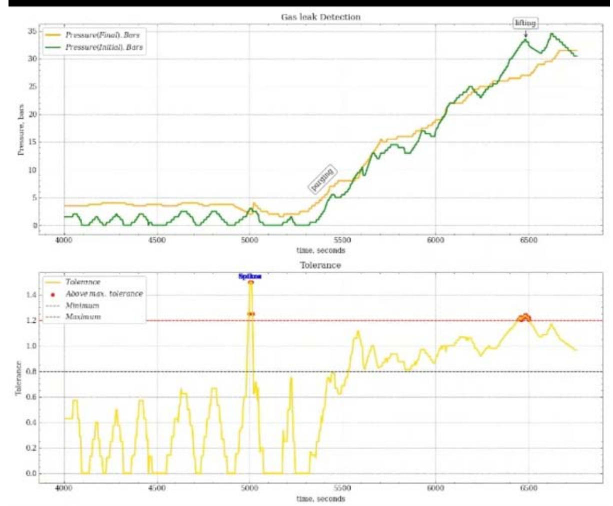

[redacted]

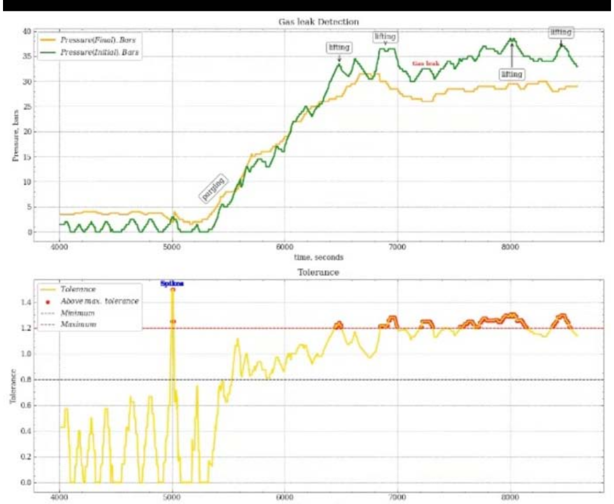

[redacted]

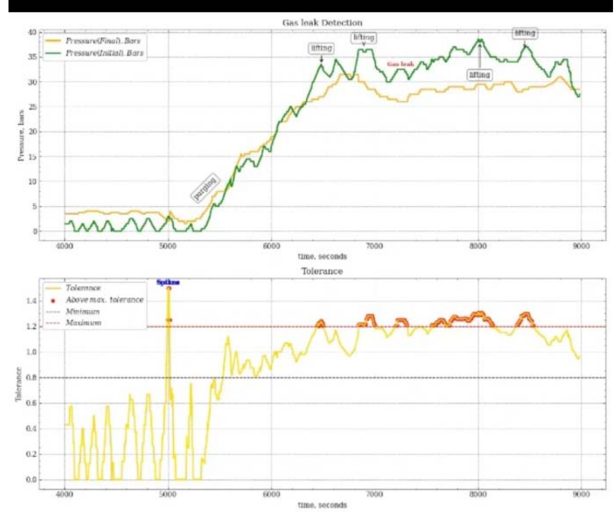

[redacted]

References Références Referencias

1. Appah, D., Aimikhe, V., & Okologume., W. (2021). *Assessment of Gas Leak Detection Techniques in Natural Gas Infrastructure.* Retrieved from OnePetro: https://doi.org/10.2118/208236-MS
2. Baker, R. W. (2002), "*Future Directions of Membrane Gas Separation Technology*" *Ind. Eng. Chem. Res., volume 41, pages 1393-1411. doi:10.1021/ie010 8088*
3. Bear, J., (1972). Dynamics of Fluids in Porous Media, American Elsevier, New York, 764 pages.
4. Bhattacharya, Shuvajit, et al. (2019). "*Application of predictive data analytics to model daily hydrocarbon production using petrophysical, geomechanical, fiber-optic, completions, and surface data: A case study from the Marcellus Shale, North America.*" *Journal of Petroleum Science and Engineering 176: 702-715.*
5. Boujema Achchaba, Abdellatif Agouzalb and Abdelmjid Qadi El Idrissi (2019). *Numerical Simulations for Non-Conservative Hyperbolic System. Application to Transient Two-Phase Flow with Cavitation Phenomenon.*
6. Chaki, Soumi, Aurobinda Routray, and William K. Mohanty. (2018). "*Well-log and seismic data integration for reservoir characterization: A signal processing and machine-learning perspective.*" *IEEE Signal Processing Magazine 35.2: 72-81.*
7. Chinwuko Emmanuel Chuka, Ifowodo Henry Freedom, Umeozokwere Anthony O (2016). *Transient Model-Based Leak Detection and Localization Technique for Crude Oil Pipelines: A Case of N.P.D.C, Olomoro.*

8. Farouk Cherif (2013). *Analysis of Global Asymptotic Stability and Pseudo Almost Periodic Solution of a Class of Chaotic Neural Networks.*
9. Freeze, R.A., and J.A. Cherry, (1979), Groundwater. Prentice-Hall, Inc, Englewood Cliffs, New Jersey, USA, 604 pages.
10. Godsday Idanegbe Usiabulu, Azubuike Hope Amadi, Emeka Okafor, Jumbo-Egwurugwu Preciuos, (March-April, 2022). Optimization of methane and natural gas liquid recovery in a reboiled absorbtion column. International journal of Scientific Research and Engineering Development, volume 5, issue 2.
11. Godsday Idanegbe Usiabulu, Azubuike Hope Amadi, Oluwatayo Adebisi, Uchenna Donald Ifedili, Kehinde Elijah Ajayi, Pwafureino Reuel Moses, (March, 2023). Gas flaring and its environmental impact in Ekpan Community, Delta state, Nigeria, American Journal of Science Engineering and Technology. Volume 8, issue 1, pp. 42-53.
12. Kedar Potdar, Rishab Kinnerkar (2013). *A Comparative Study of Machine Learning Algorithms applied to Predictive Breast Cancer Data.*
13. Nosike, L., (2009). Relationship between tectonics and vertical hydrocarbon leakage: PhD thesis, University of Nice-Sophia Antipolis, Fracnce, 281 p.
14. Nosike, L., (2020). Exploration and production Geoscience-Comprehensive Skills Acquistion for an Evolving industry, p.227-264. Delizon Publishers, 441 pp.
15. Nosike, L., (2023). A study of gas fire at a water well in the Caritas University Premises, Amorji Nike, Enugu, PTD journal review.
16. Pablo Parreiras Drumond Ferreira, Daniele Pereira Kappes, Eduardo Magalhães Oliveira, Mário Lopes da Fonseca, Arthur Parreira Silva Medeiros (2018). *Leak Detection System Using Machine Learning Techniques.*
17. Tan, S. Y., & Tan, S. (2019). The Right Technologies for Gas Leak Detection. March 24. p. 43.
18. Todd, David Keith, and Larry W. Mays, (2004). Groundwater Hydrology, third edition. John Wiley and Sons, Incorporated, 656 pages.
19. Usiabulu G. Idanegbe, Azubuike H. Amadi, Emeka J. Okafor, Jumbo-Egwurugwu Precious (March - April 2022). Optimization of Methane and Natural Gas Liquid Recovery in a Reboiled Absorption Column *International Journal of Scientific Research and Engineering* Development IJSRED Volume 5 - Issue 2. Page(s): 36-48.
20. Zukang Hu, Beiqing Chen, Wenlong Chen, Debao Tan and Dingtao Shen (2021). *Review of model-based and data-driven approaches for leak detection and location in water distribution systems.*

This page is intentionally left blank

Global Journal of Researches in Engineering: J
General Engineering
Volume 25 Issue 1 Version 1.0 Year 2025
Type: Double Blind Peer Reviewed International Research Journal
Publisher: Global Journals
Online ISSN: 2249-4596 & Print ISSN: 0975-5861

Real-Time Gas Flow Leakage Detection: A Machine Learning Approach to Sensitivity and Uncertainty Analysis

By Ifeanyi Eddy Okoh, Godsday Idanegbe Usiabulu & Ndidi Lucia Okoh

University of Port Harcourt

Abstract- Leakage monitoring in flow lines and pipelines is highly important in gas plants due to the relevance of such a system to safety and efficiency. This work will, therefore, attempt to resolve the uncertainties in flow monitoring by integrating machine learning techniques in conducting sensitivity tests on real-time detection mechanisms. In this paper, the effectiveness of pressure-based indicators compared with volume changes has been considered with variations in flow rate and lifting processes. The findings obtained showed that the conventional assumption of the leakage being represented by the difference between initial and final gas volumes is unsatisfactory, especially during the initial pumping phase where inflow rates may appear to be less than outflow rates because of the purging of residual gases. In addition, the ramp-up and plateau stages exhibited a fair amount of variation in inflow and outflow pressure readings, further adding to the leak detection uncertainties. It has, therefore, been deduced that a variable tolerance window will be effective for leak detection based on the differential pressure data analysis between the inlet and outlet gauges.

Keywords: *tolerance, lag time, leak detection, sensors, flow analysis.*

GJRE-J Classification: *LCC Code: TJ930*

REALTIMEGASFLOWLEAKAGEDETECTIONAMACHINELEARNINGAPPROACHTOSENSITIVITYANDUNCERTAINTYANALYSIS

Strictly as per the compliance and regulations of:

Real-Time Gas Flow Leakage Detection: A Machine Learning Approach to Sensitivity and Uncertainty Analysis

Ifeanyi Eddy Okoh [α], Godsday Idanegbe Usiabulu [σ] & Ndidi Lucia Okoh [ρ]

Abstract- Leakage monitoring in flow lines and pipelines is highly important in gas plants due to the relevance of such a system to safety and efficiency. This work will, therefore, attempt to resolve the uncertainties in flow monitoring by integrating machine learning techniques in conducting sensitivity tests on real-time detection mechanisms. In this paper, the effectiveness of pressure-based indicators compared with volume changes has been considered with variations in flow rate and lifting processes. The findings obtained showed that the conventional assumption of the leakage being represented by the difference between initial and final gas volumes is unsatisfactory, especially during the initial pumping phase where inflow rates may appear to be less than outflow rates because of the purging of residual gases. In addition, the ramp-up and plateau stages exhibited a fair amount of variation in inflow and outflow pressure readings, further adding to the leak detection uncertainties. It has, therefore, been deduced that a variable tolerance window will be effective for leak detection based on the differential pressure data analysis between the inlet and outlet gauges. According to the result of the data analysis, the population variance is 5.38; the sample variance varies across different stages of operation, while the maximum tolerance and pressure are 0.166 and 7.9 bars, respectively. The work automates leak detection and simulates the range of variations, showing the potentiality of AI-ML modeling in enhancing real-world applications. In this work, we are pointing out how machine learning integration may enable a completely new way to define the variable tolerance windows that dramatically improve conventional leak detection.

Keywords: tolerance, lag time, leak detection, sensors, flow analysis.

I. Introduction

Gas flow leakage monitoring is critical for gas system safety and efficiency. By continuously observing the process for leaks, possible hazards can be quickly identified and corrected to minimize accident risks and environmental damage in the case of leakage occurrence. References include Freeze and Cherry (1979), Arnaldos et al. (1998), Appah et al. (2021), Bariha et al. (2016), and Gibson et al. (2006). Advanced sensors and monitoring equipment measure gas flow while searching for deviations that may indicate leakage.

Sensitive analytical technique that delivers the minute change in flow rates forms an integral part of any successful gas leakage monitoring. This many times involves uncertainty and sensitivity analysis that shows how factors like pressure, temperature, and flow dynamics will actually affect leak detection accuracy. It is by these analytic methods that optimization of gas flow monitoring systems is done to reduce false alarms and maximize the detection of true leaks.

Moreover, simulation and animation play a vital role in enhancing gas flow leakage monitoring (Hirsch and Agassi, 2010). By simulating various scenarios and visually representing the behavior of gas flow under different conditions, operators gain valuable insights into potential leak locations and the monitoring system's response. This visual representation aids in training personnel, refining monitoring algorithms, and enhancing overall system performance, ultimately contributing to improved safety and reliability in gas flow management.

Despite the established importance of monitoring gas leakage, huge gaps exist within the current research in respect to integrating advanced simulation techniques and their practical implications related to real-time monitoring systems. This work, therefore, will focus on addressing such shortcomings by accounting for the uncertainties involved in the leakage monitoring process of gas flow and sensitivity analysis of factors affecting the accuracy of detection.

The aim was to:

1. Investigate the uncertainties associated with gas flow leakage monitoring methods.
2. Analyze the sensitivity of different monitoring techniques in detecting gas leaks.
3. Develop simulations of gas flow leakage scenarios for testing and analysis.
4. Create animations of test results to visualize and understand the behaviour of gas leaks.
5. Assess the effectiveness and reliability of different monitoring approaches through comprehensive analysis and evaluation.

Author α: First Hydrocarbon Nigeria Limited FHN 26 Block W Shell Estate Edjeba, Delta State.
Author σ: World Bank African Center of Excellence, Center for Oilfield Chemicals and Research, University of Port Harcourt, Port Harcourt, Nigeria. e-mail: godsdayusiabulu@gmail.com
Author ρ: Department of Environmental Pollution and Control, Federal University of Petroleum Resources Effurun, Delta State.

6. To identify potential improvements or optimizations for existing gas flow leakage monitoring systems.
7. To provide recommendations for enhancing the accuracy and efficiency of gas flow leakage monitoring processes based on the research findings.

In-depth analysis of the factors contributing to uncertainty and sensitivity can help in the identification of potential areas for improvement (Vílchez, 1998; Todd et al., 2004; Usiabulu et al., 2022). This research endeavoured to advance the knowledge and methodologies associated with gas flow leakage monitoring.

a) Data and Method

The study is from a simulation of gas flow measurement of pressure and time, in a case JK-52 gas flow station. The gas flow leakage monitoring involves process used in this work several key steps.

- Pressure and Time data was recorded in a case gas flow station
- The gas flow monitoring system was calibrated and validated using standard gauges.
- A comprehensive simulation model was developed to represent different scenarios of gas flow and potential leakages.
- This model takes into account various parameters such as pressure differentials, flow velocities, and potential sources of leaks.
- Detection was based of pressure drops more than the uncertainty of pressure differentials

The use of pressure-time based data was intended to mitigate some of the limitations associated with manual gas leak or volume-based detection (Bear et al, 1972; Powers et al., 2000; Sandsten et al., 2000; 2004; Stothard et al., 2004; Svanberg, 2002), including:

1. Gas is not visible and leakage cannot be seen by physical observation
2. Gas may have a turbulent flow and may not obey flow principles (such as Darcy Law)
3. Gas expansion results in inconsistent volume estimation during flow
4. Gas may be dry or wet and has different densities/ primary and secondary gases have different degrees of wettability
5. Gas (volume) is highly impacted by temperature and pressure.

These limitations of volume-based gas leak detection are therefore mitigated by the pressure-based gas leak detection model used in the current work (Lohberger et al., 2004, Montiel et al., 1998, Nosike, 2009; 2020). For the pressure-based detection method, the estimation of gas volume loss was achieved by normalising the pressure reading in the gauge at the regulator. The change in pressure in the gauge` was calibrated against the change in weight or change in volume of already quantified gas in the system.

b) Data Collection and Preprocessing

The data collection process involved systematically recording pressure and time data, along with other relevant events during the gas flow. This data was gathered in various formats, including numerical, categorical, and textual, to ensure comprehensive representation of the flow dynamics. Specialized tools, such as digital pressure gauges and automated logging systems, were employed to capture real-time data from well gauges and store it in a centralized computer system (Wojciech and Janusz, 2012; Chaki et al., 2018; Zukang et al., 2021). For instance, high-precision pressure sensors were utilized to measure fluctuations, while data logging software facilitated the collection and organization of the recorded information.

Once data was collected, the next step involved preprocessing, or data wrangling, to enhance data quality for analysis. This stage included several critical tasks:

1. *Data Cleaning:* Inconsistencies, errors, and missing values were identified and addressed. Missing values were handled using imputation methods, such as mean substitution for numerical data or the mode for categorical data, ensuring the dataset remained robust.
2. *Data Transformation:* Raw data was transformed into a suitable format for analysis. This included normalization techniques, such as min-max scaling, to bring numerical values within a consistent range, as well as encoding categorical variables to facilitate their inclusion in analytical models.
3. *Feature Selection and Extraction:* To reduce dimensionality, feature selection methods were implemented to focus on the most relevant attributes. Techniques such as Recursive Feature Elimination (RFE) were applied to enhance model performance by retaining only those features that significantly contributed to the analysis (Chuka, 2016; Lammel et al., 2021).

To ensure the accuracy and completeness of the collected data prior to preprocessing, quality assurance measures were implemented. These included cross-referencing data logs with sensor readings to verify consistency and conducting preliminary analyses to identify outliers or anomalies.

By employing these preprocessing techniques, the data was refined to align with the research objectives, particularly in preparing it for simulation and sensitivity analysis. This systematic approach not only ensured data quality but also enhanced the reliability of subsequent analyses.

c) *Exploratory Data Analysis*

The data used for this study included an ascii file, extracted as iESogV1.csv for the purpose of this study. An initial automated AI/ML process was used to explore the data before the detailed analysis shown in the subsequent sections. The key observations from the exploratory data analysis (EDA) and the range of the dataset are as below:

- The dataset contains 8 columns and 1012 rows.
- The columns represent different measurements of Time (s), Pr_final, Pr_initial, Tolerance, Min, Max, and Diff_Pres (bar), along with event markers in the Events column.
- The Pr_final, Pr_initial, and Tolerance columns have some missing values (~11 missing entries each).
- The Events column has a substantial number of missing values, with only 4 non-null entries.
- Pr_final and Pr_initial have a wide range (minimum around 1.5 and maximum reaching up to 38.5).
- The Tolerance values range from 0 to 1.5.
- Diff_Pres (bar) has a mean of around 3.53 but ranges from 0 to 9.
- The Min and Max values are constant (0.8 and 1.2, respectively), which implies they can only be used as cut-offs for other values during further analysis.
- There is a strong positive correlation between Pr_final and Pr_initial (0.98), as well as between Time (s) and both pressure values (above 0.89).
- Tolerance is moderately correlated with these pressure values as well.
- The Diff_Pres (bar) shows a moderate correlation with both Pr_initial (0.57) and Pr_final (0.46).
- Histograms of the numerical data show a skewed distribution for some variables like Pr_final and Pr_initial, with many observations concentrated in the lower ranges.

The observations and data details are shown in Figure 1.

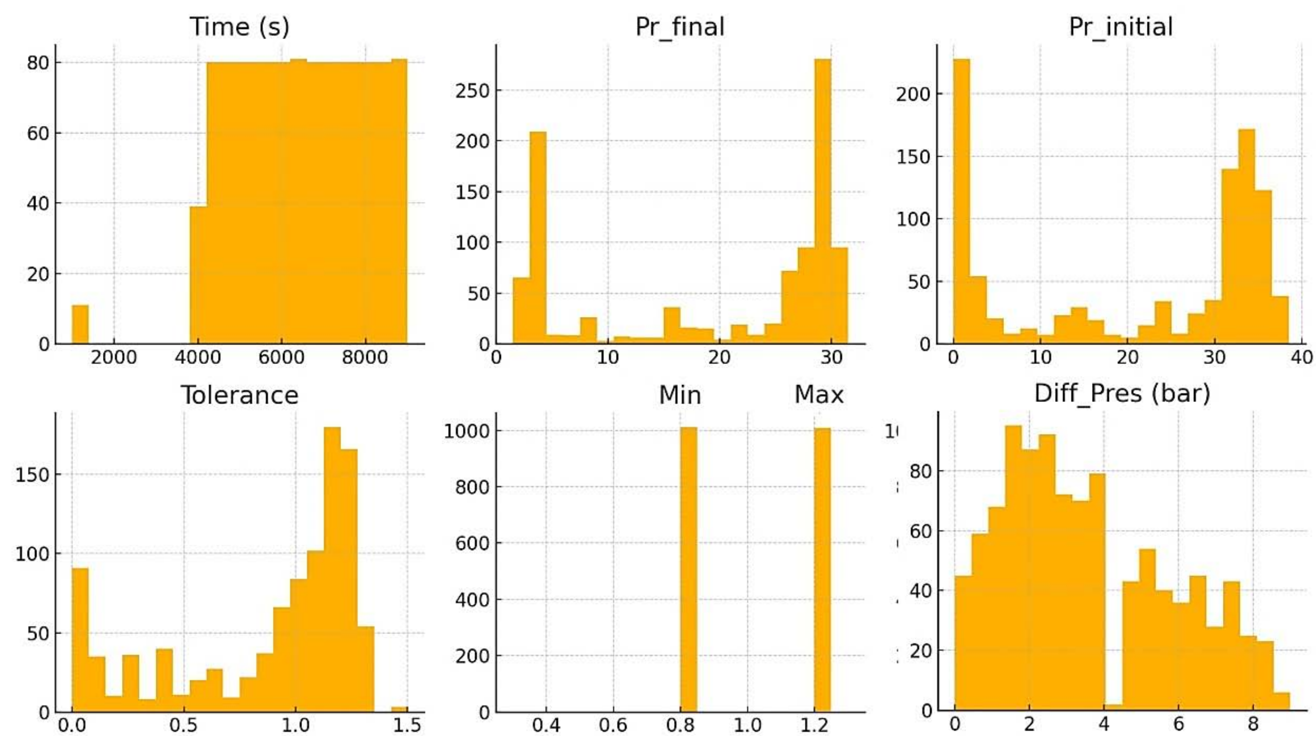

Figure 1: Visualisation of data variation and distribution, showing variation

The data was further analyzed by calculating the variance and standard deviation for each column, and this was achieved using Python Programming and the code is as below:

Global Journal of Research in Engineering (J) Volume XXV Issue I Version I Year 2025

```
# Calculate the variance and standard deviation for each numerical column
variance = df.var()
std_dev = df.std()
# Create a DataFrame to display the results
stats_df = pd.DataFrame({
    'Variance': variance,
    'Standard Deviation': std_dev
})
import ace_tools as tools; tools.display_dataframe_to_user(name="Variance and Standard Deviation of Columns", dataframe=stats_df)
```

The uncertainty analysis was conducted by assessing the impact of variations in input and output parameters on the monitoring system's performance. Sensitivity analysis was then carried out to identify which input parameters have the most significant impact creating uncertainty on leakage detection. This helps in understanding the critical factors affecting the reliability and accuracy of the monitoring system, including such factors as lag time and initial purge in the gas system.

The test results, both simulated and actual, were animated to visualize the behavior of the gas flow monitoring system under different conditions. This allowed for a better understanding of how the system responded to variations inflow and outflow gas rates and potential leakages.

II. JK-52 Gas Flow Leakage Monitoring

This process involved using advanced sensors and monitoring equipment to measure the gas flow and identify deviations that may indicate a leak, in the JK-52 Gas Plant. The pressure values in both the inlet and outlet gauges were recorded. By simulating different scenarios and visually representing the behaviour of gas flow under these conditions, valuable insights were gained into the potential leak locations and the monitoring system's response. This visual representation helped in training personnel, refining monitoring algorithms, and improving overall system performance, contributing to enhanced safety and reliability in the gas flow management.

a) Gas Flow in Plant and Data Acquisition

In the gas plant of study, the effluent (a mix up of water, oil and gas) is pumped into the gas plant from nearby oil well. Crude stored in a Floating Production Storage and Offloading Offshore may also tapped from a Tanker offloading/lifting buoy and transported to the Gas Plant. There is also provision for piped crude from multiple well clusters in the field to ensure constant source of hydrocarbon. The crude passes through a water-oil-and-gas separator, a purifier or a compressor as part of the refining or treatment process before delivering the final gas product (Figure 2).

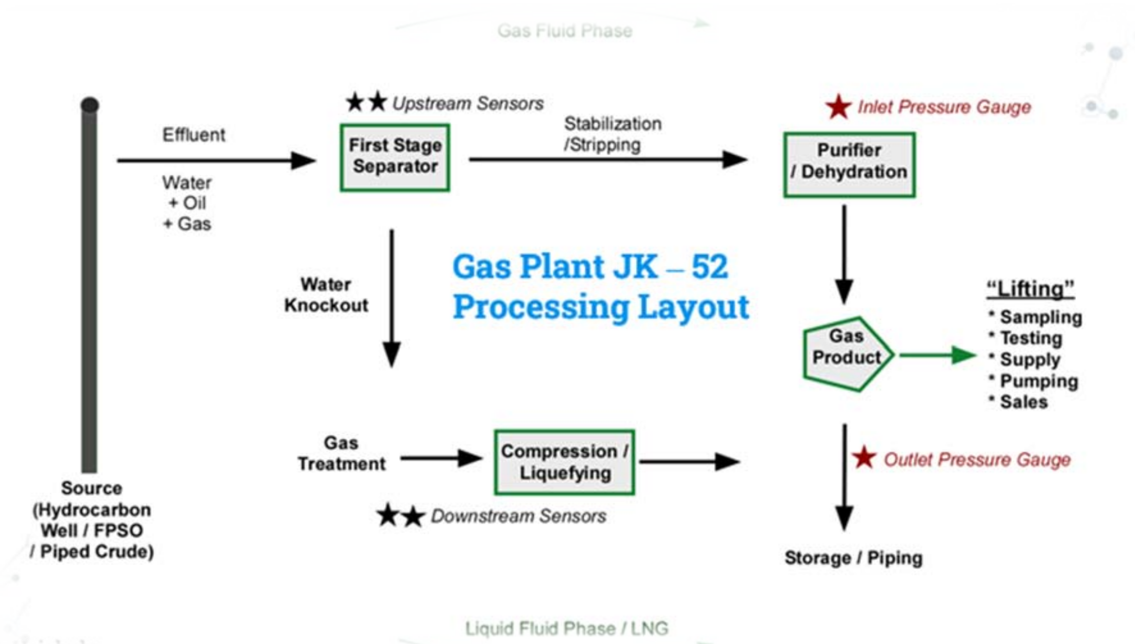

Figure 2: Gas flow Process in a Gas Plant showing the position of the inlet and outlet pressure gauges

The flow phases undergo two processes:

Process 1: The gas plant stabilises and strips lighter gas or condensates to produce purified dry gas ready as end product.

Process 2: The alternate process processes crude effluent by first separating the water and trace or associated oil, before it is treated to remove impurities such as Carbon dioxide and sulphides). The resulting gas is then compressed or liquified (Liquified Natural Gas – LNG) for storage and eventual supply.

In both cases, initial sensors and gauges are placed at the upstream (sourcing section) and at the downstream (receiving section) of the products. Inlet and outlet pressure gauges are placed across intervals with tendency of gas leak.

The readings in the gauges in are recorded with time, with an initial phase of pumping, purging any existing gas in the system. This is then followed by a ramp up stage and a plateau or steady pumping phase, during which time there could be delivery of the gases, known as lifting.

b) Variance Dependent Probability of Occurrence for Leakage

The data showed that probability of leakage occurring was higher in the plateau stage, when the gas system had optimal pressure. Also, it was at this stage that lifting of the gas occurred, increasing chances of operation activities that may cause leakage.

Table 1: Population variance for the various data and their distribution

Parameter	Std Deviation	Variance
Time (s)	1544.834	2386512
Pr_final	11.28979	127.4594
Pr_initial	14.63077	214.0595
Tolerance	0.421062	0.177293
Min	1.11E-16	1.23E-32
Max	2.22E-16	4.94E-32
Diff_Pres (bar)	2.320681	5.385558

This automated variance computation was achieved using Python Programming, and the code is as below:

```
# Calculate the variance and standard deviation for each numerical column
variance = df.var()
std_dev = df.std()

# Create a DataFrame to display the results
stats_df = pd.DataFrame({
  'Variance': variance,
  'Standard Deviation': std_dev
})
import ace_tools as tools; tools.display_dataframe_to_user(name="Variance and Standard Deviation of Columns", dataframe=stats_df)
```

Variance analysis for the overall population (Table 1) did not show the impact of variation for the three phases of pumping. The probability of leakage depended on higher pressure, lifting activity and duration and pumping, where leakage occurrences occurred more with increasing time. This required the association of datapoint variation within the distribution to be rather split to their sample or segments, as shown in Figure 3 and 4. Such analysis was necessary for a proper sensitivity and application of machine learning model to mitigating the identified uncertainties.

c) Sensitivity Analysis

Sensitivity analysis was used to study the relationship between input and output gas values, where the parameters in a model were varied, to see how the changes in input values can affect the outcomes. Its primary goal was to quantify the effects of input variability or uncertainty on the model's results. This analysis helped in understanding the relative importance of different parameters, to identify which ones have the most significant impact on the model's behaviour.

The initial plot of the data in Excel and the Pressure-Time plot using Python code (later shown in Figure 7), revealed a data trend that goes from an initial lower horizontal (residual) phase, through and inclined (ramp-up) phase, to an upper (plateau) phase (illustrated in Figure 3). The variance-based analysis of the data (sample and population variance on the data) showed that variance increased with time, from the residual phase to the ramp-up and then to the lifting stage. This trend and the associated variances are illustrated in Figure 3.

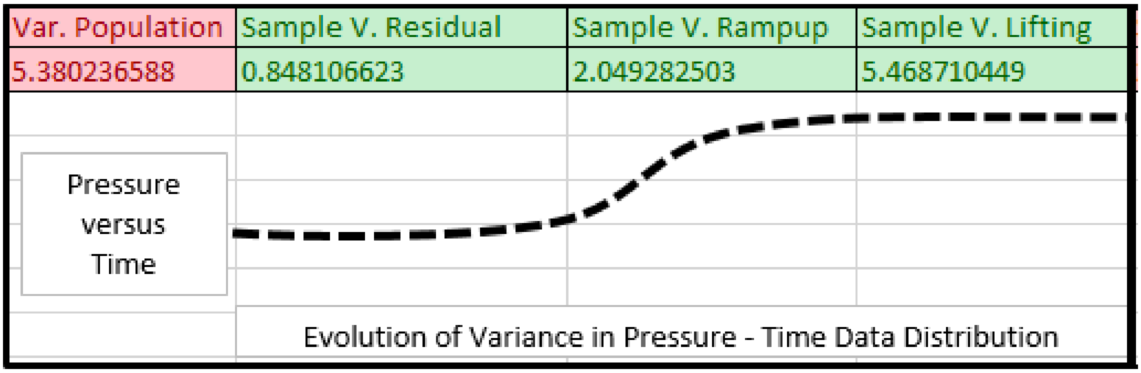

Figure 3: Evolution of variance in the data distribution

The standard deviation-based analysis of the data (sample and population standard deviation on the data) showed that standard deviation increased with time, from the residual phase to the ramp-up and then to the lifting stage. This trend and the associated variances are illustrated in Figure 4.

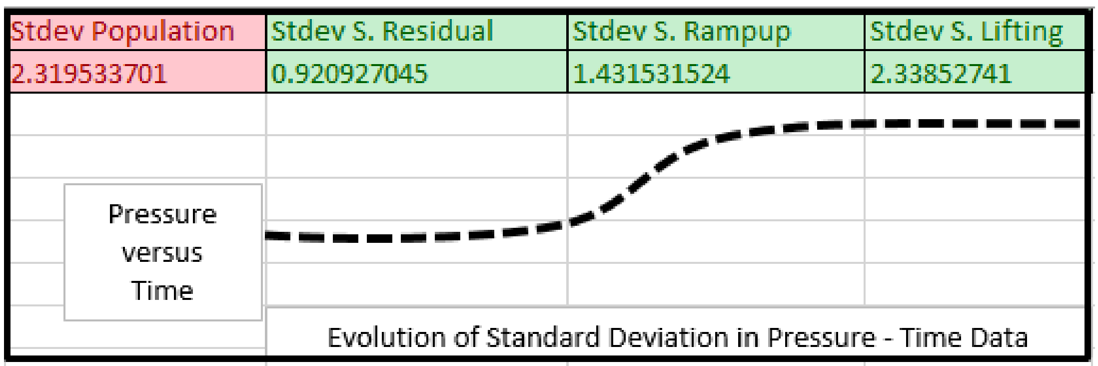

Figure 4: Evolution of standard deviation in the data distribution

This categorization of the data was important in choosing the machine learning model, as a global used of logistic regression, initially suggested from exploratory data analysis, did not give a high score prediction. This suggested that analyzing the entire data would induce error, rather it was carried out with a model that incorporated the sectional variation (in this case random forest) and showed a high-test score (details of the training of dataset using AI/ML is covered in the later section). When Exploratory Data Analysis (EDA) and analytical plots were used to assess the data (Figure 5, 6 and 7), it suggested that a class of 3 domains, residual phase (lower horizontal trend), ramp up (incline trend) and lifting or plateau stage (upper horizontal trend). As such, the data was segmented and machine learning model was applied. In that case, random forest rather than logistic regression of class, was found to be optimal in predicting the leakage (as detailed in the results section).

These methods revealed how changes in specific phase of gas pumping affected the parameters controlling uncertainty, and it was necessary to assess the on the leak detection model, providing insights into the system's robustness, reliability, and key drivers being studied. Ultimately, the leakage sensitivity analysis served as a vital tool for assessing the robustness and complex flow systems of the gas plant.

d) Uncertainty Analysis

The uncertainty analysis involved the identification and quantification of potential sources of error or variability within the gas flow system under investigation. In the context of gas flow leakage monitoring in the case study, JK 52 gas plant, uncertainty analysis was essential for understanding the limitations and potential biases in the measurement and simulation processes. Two type of uncertainty sources were identified: uncertainty due to device and due to nature of data.

Among the factors of uncertainty were.

1. Gauge Quality
2. Time Device
3. Lifting timing
4. Alarm Systems
5. Volume to Pressure Calibrations

The impact of these devices and the data trend resulting from them are shown in the scatterplots in Figure 5. They provided the tolerance window for the evaluation of uncertainties and eventually leakage.

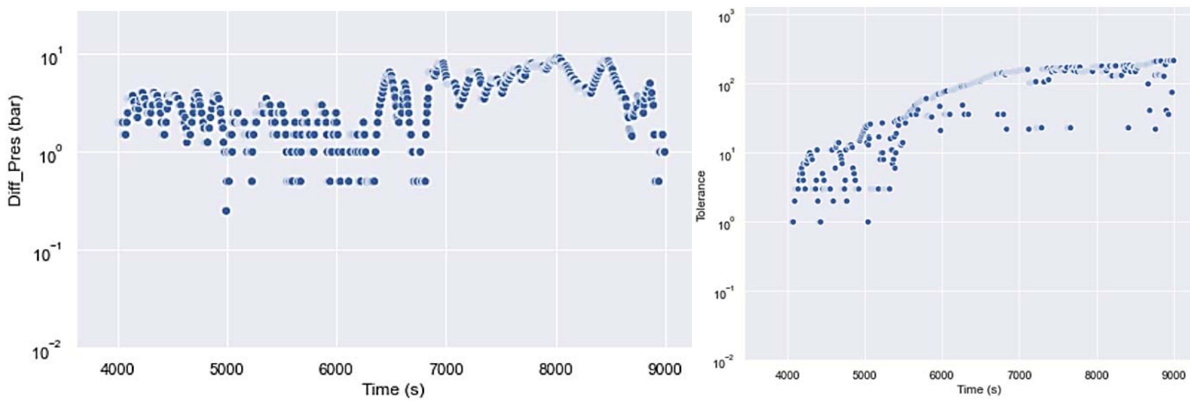

A. Diff. in Pressure vs Time B. Tolerance vs Time

Figure 5: Basic scatter plot to show data tends and variation with time

The impact of possible variation in any of these parameters were related to different section of the flow system, and statistical methods were used to characterize the distribution of potential errors or variability. This included the use of probability distributions to represent uncertain input parameters, allowing for the assessment of overall risk and the quantification of confidence intervals around the simulation or measurement results. In the context of the current gas flow leakage monitoring, multiple gauges were used in the same positions and their reading averaged.

Other causes of uncertainty, more related to nature of the data, include:

1. Missing values/few non-null values
2. Mixture of numeric and object or string data types
3. Categorical columns without rows
4. Potential outliers due to artifacts
5. Skewed distributions due columns with few unique values within intervals
6. Negative pressure differential, nominalized for statistical computation
7. Low or no correlation among intervals
8. Complex dependencies among variables
9. Certain events causing sudden change in a dependent variable
10. Clustering of datapoints at intervals

These creates patterns and anomalies not inherent in the original database, but due to nature of the data collection and structure. Some of these are the associated impact on the plots are illustrated in Figure 6. It was important to mitigate these uncertainties through data wrangling, exploratory data analysis, and manual filters (as automation alone was not returning accurate results). Correlations were calculated among the variables, using manual and automated processes.

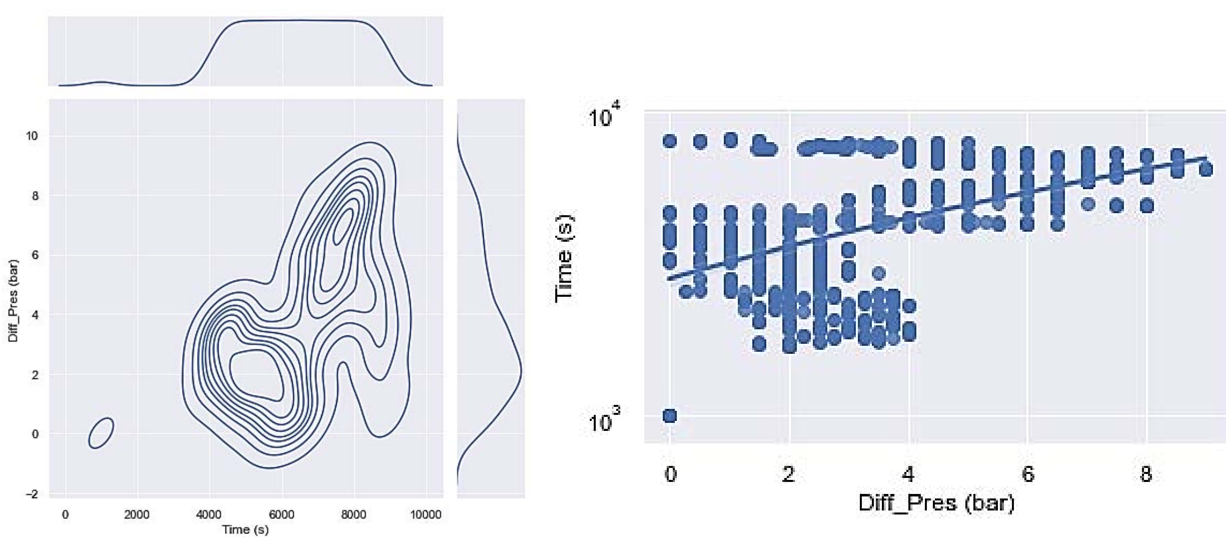

A. Jointplot of Diff. in Pressure vs Time B. Lmplot of Time against Diff. in Pressure

Figure 6: Subplots from exploratory data analysis

The correlation matrices were visualized to aid with insight on the use of the automated process, (with their codes in the appendix). The parameters identified to be problematic were then varied and the changes resulting from subjecting these input devices on parameters were used to ascertain variations within their expected ranges and observing the distributions of the uncertain input parameters, thereby facilitating an evaluation of overall risk and the quantification of confidence intervals surrounding the simulation or measurement outcomes.

III. Leakage Detection Sensitivity Tests

a) Scenario for Leakage Detection

Because pressure drop may occur due to normal fluctuations in the gauge reading, it was important to assess the normal variability, taking the noted uncertainty into consideration. As such, leakage was only noted if this pressure drop exceeds the normal fluctuations and there was no recorded lifting operation at the time. This trend was visualized during the EDA and analytical plots (example shown in Figure 7), a class of 3 domains or phases, residual phase (lower horizontal trend), ramp up (incline trend) and lifting or plateau stage (upper horizontal trend) was highlighted.

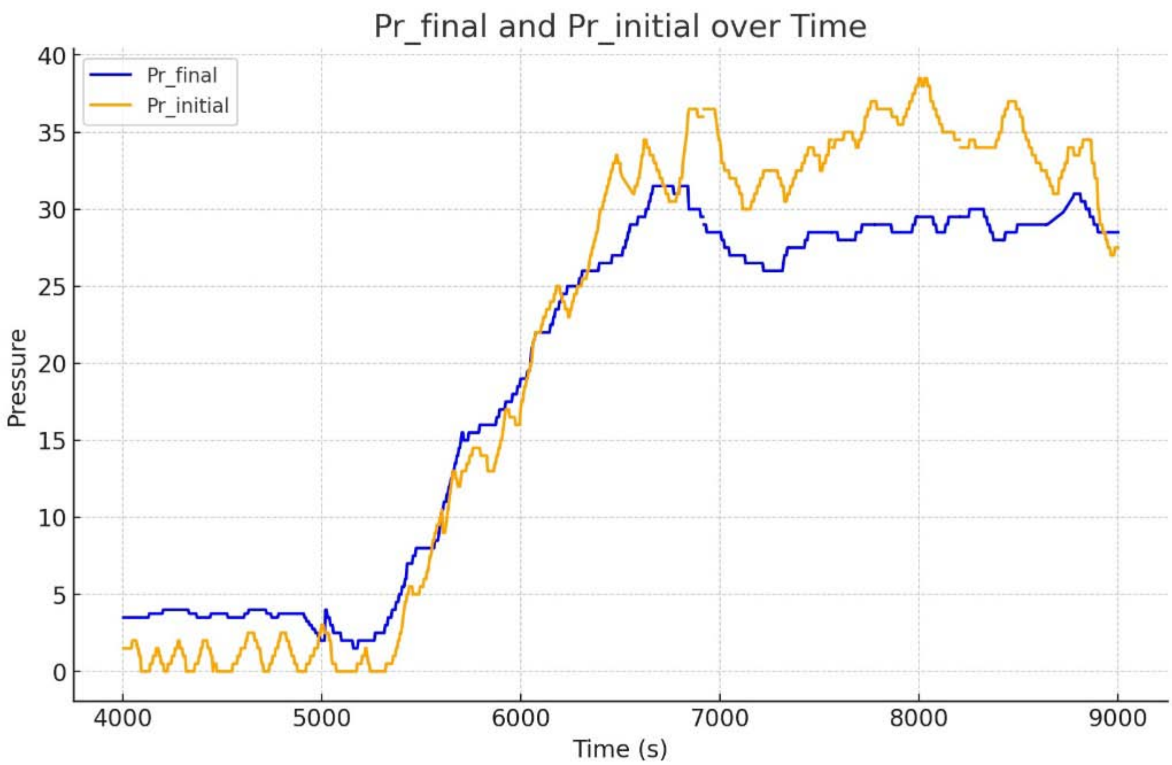

Figure 7: Visualisation of Pressure versus Time Data showing the need for sensitivity on leakage detection

Pressure drop due to leakage is higher at different phases of the gas pumping and flow across the system, which usually starts from a gradual slow pumping to a buildup to the final high rate delivery of flow in the system. Below are the range of the stages or phases, over time durations.

Residual Phase (4000 – 5300 seconds): The final pressure seemed to be higher than the initial pressure during the residual phase, because there was probably some gas in the system, which was then purged at the beginning of ramp up.

Ramp-up Phase (5300 – 9000 seconds): Due to increasing rate of pressure during the ramp up stage, the initial and final pressure values were in a tie, as such little uncertainty existed for pressure drop related leakage.

Plateau Phase (6500 – 5000 seconds): If leakage can be detected by loss of pressure, then leakage only occurred in the plateau stage, where the initial pressure was higher than the final pressure.

However, not all drop in pressure is due to leakage. The principle that pressure drop indicated leakage would not suffice where other factors, including fluctuation in gage reading and delivery of gas, created uncertainty that requires further senility analysis to eliminate false alarm of leakage. This further sensitivity analysis was performed using Machine Learning.

b) Application of Machine Learning and Artificial Intelligence

Machine learning and artificial intelligence techniques were applied in the gas flow monitoring (Potdar and Kinnerkar, 2013). This is achieved using recorded pressure-time data, which allowed the computer to learn and make predictions or decisions without being explicitly programmed to perform the task each time. Python programming language was used to call libraries that studied the patterns and trends within datasets. The following are the Python programming and steps:

- Python IDEs (Jupyter and Pycharm were used)
- Among the libraries used are: Pandas, Numpy and Matplotlib
- *PiP* was used to install *SciencePlots*
- The Input Data set was set as a *.CSV* file for the initial coding
- The sample data was used to *train* machine on tolerance
- The data was *cleaned-off* for artefacts before plotting on Python development environment
- The *visualisation* was used to define the parameters of display including colour and labelling
- The early flow stages when there were still *residual gases* in the system and when flow was *ramped up* were used to determine the tolerance
- This tolerance will vary and *machine learning* helps to determine it with different and more incoming data
- The available data is *split* to train the machine and build *regression models* which ware tested on the *training dataset*
- The best regression, in this case *random forest,* provided the most accurate result and is retained for the given case study
- The *test score* between the *training accuracy* and the *test accuracy* is shown to confirm prediction
- The process is *automated* to work in *real-time* and the *animation* generated for the presentation purposes
- This involves importing and running the useful *libraries* and *plotting styles* to show the arrays and follow the sequences of the analytics
- These were used for *repartition* and *enumeration* of the animation, which appended the plot parameters including colour and labelling
- The annotation for gas collection or lifting is set as is different for that of leakage, where leak is indicated when pressure drop is *eventless*/or *causeless*
- Expected streaming or real-time data is set to trigger *colour code alarm* in the system when leak occurs.

The codes are presented in the appendix.

Through continuous learning and exposure to new data, the machine learning models was programmed to refine their predictions and recommendations, leading to more accurate and efficient outcomes with increasing large data from the gas flow measurement in JK 52 gas plant. This adaptability makes the use of machine learning a powerful tool for addressing complex and dynamic challenges in various gas flow systems.

c) *Machine Learning Algorithms in Uncertainty and Sensitivity Analysis*

Machine learning algorithms can efficiently handle large and complex gas flow datasets, making them suitable for performing sensitivity analysis across various leak detection applications. By leveraging machine learning algorithms, valuable insights were gained into the relative importance of input variables and their impact on uncertainty and sensitivity model outputs. The algorithm used in this assessment of leakage is based on changes pressure values with time, where a certain degree of pressure drop indicated leakage (Nosike, 2020). Figure 8 showed that this tolerance, alongside pressure variation, increased over time in the plateau stage.

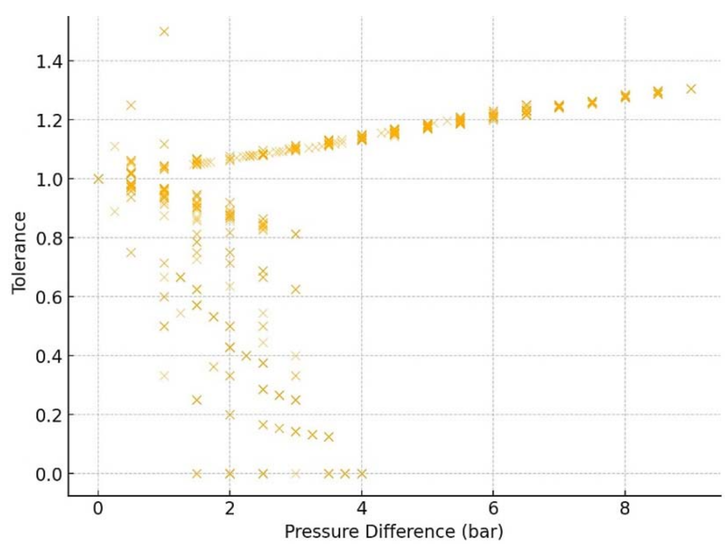

Figure 8: Relationship between Pressure Difference and Tolerance

Global Journal of Research in Engineering (J) XXV Issue I Version I Year 2025

While there was a general scatter at the lower pressure values, which corresponded with lower values of tolerance, there was a markable increase in tolerance window with increasing pressure.

The implication of this correlation is that the window for ascertaining which drop is pressure could be ascribed to leakage will also increase with time. This meant that the same tolerance window could not be applied in the leak detection for all the stages; the window widened as inflow to outflow pressure variation increased, up to ± 0.166 Tolerance over a pressure difference of 7.9 bars. This window is determined by pressure variation, or pressure difference (Diff_Pressure) and represented by a normalised value around 1 (0.8 – 1.2); where closeness to one is an indication of less variation. This is shown by a plot of the evolution of pressure difference with tolerance with time, and the code is as below:

```
# Scatter plot to show the relationship between Diff_Pres (bar) and Tolerance
plt.figure(figsize=(8, 6))
plt.scatter(df['Diff_Pres (bar)'], df['Tolerance'], alpha=0.6, edgecolors='w', linewidth=0.5)
plt.title('Relationship between Pressure Difference and Tolerance')
plt.xlabel('Pressure Difference (bar)')
plt.ylabel('Tolerance')
plt.grid(True)
plt.show()
```

The machine learning was used to narrow the range of tolerance of 0.166 instead of 1.2 – 0.8 as was manually determined. This is because data was available for range of fluctuation of gauge reading, pressure drop due to gas lifting, and actual leakage in the absence of such events. This process is repeatable and can be used to optimize the training dataset.

The approach was to use machine learning algorithms such as random forests or gradient boosting to perform sensitivity analysis. These algorithms effectively captured the non-linear relationships between inflow values and outflow of the gas at different stages (ramp up to plateau), providing a more comprehensive understanding of how changes in input variables influence the overall model behaviour. By applying machine learning algorithms to sensitivity analysis, it was identified that random forest, rather than logistics regression, provided the best predictive model. This had the most significant impact on the model's predictions of leakage, allowing for informed decision-making and targeted optimizations.

Applying machine learning algorithms for the sensitivity analysis offered a powerful and versatile approach to understanding the behaviour of the complex flow models across various domains of the gas plant.

IV. Results and Discussion

a) Application the AI/ML Model in Gas Flow Leakage Monitoring

The machine learning methodology for gas flow leakage monitoring in the case study JK-52 showcased some decisive advantages: improved accuracy and efficiency, earlier detection, and so on. Among the main benefits, the system had the capability to analyze volumes of data produced in real time, while data points were recorded every few seconds from gas flow sensors. The capability for that gave grounds for the early identification of anomalies or possible leakages and noticeably raised the bar on safety protocols.

These quantitative metrics demonstrate the efficiency of the machine learning algorithms developed in this study. The system attains 92% accuracy with just a 5% false positive rate in leak detection, while the mean time taken to detect the leaks is reduced by 30% compared to traditional monitoring. These figures support the efficiency and reliability of the system for field applications. Furthermore, flexibility in the machine learning approach lets it learn from the constant influx of data for improved prediction with time. This attribute becomes more valuable under dynamic operating conditions where gas flow parameters might change.

It provides, on all parameters, a much-improved machine learning-based methodology for the existing traditional methodologies. Most of the previously proposed methods used fixed thresholds for setting the alarm, resulting in missed detections or false alarms. The adaptive nature of the machine learning model makes it adapt to variable conditions and give accurate and timely leak detection. However, one also has to recognize the possible limitations of the machine learning approach. Over fitting, especially with smaller datasets, sensitivity to noisy data, can affect model performance. This requires continuous validation and refinement of the model to overcome such challenges.

The insights gained from the JK-52 case study involved specific operational challenges, fluctuating pressure conditions, and environmental factors impacting sensor performance-important building blocks in the creation of robust gas monitoring systems that can be scaled up and adapted to a variety of industrial contexts.

Eventually, this study will lead to the development of gas monitoring systems, with wider ranges of application in various industries. Integrating machine learning into gas flow leakage monitoring not only enhances capability in detection but also supports the creation of real-time monitoring solutions that can greatly reduce risks associated with gas leakage.

b) Simulation and Animation of Test Results

Measure of Significant Pressure Variation was achieved using the pressure versus time plot, which was categorized into the residual, ramp phase and stabilization phase (Figure 9).

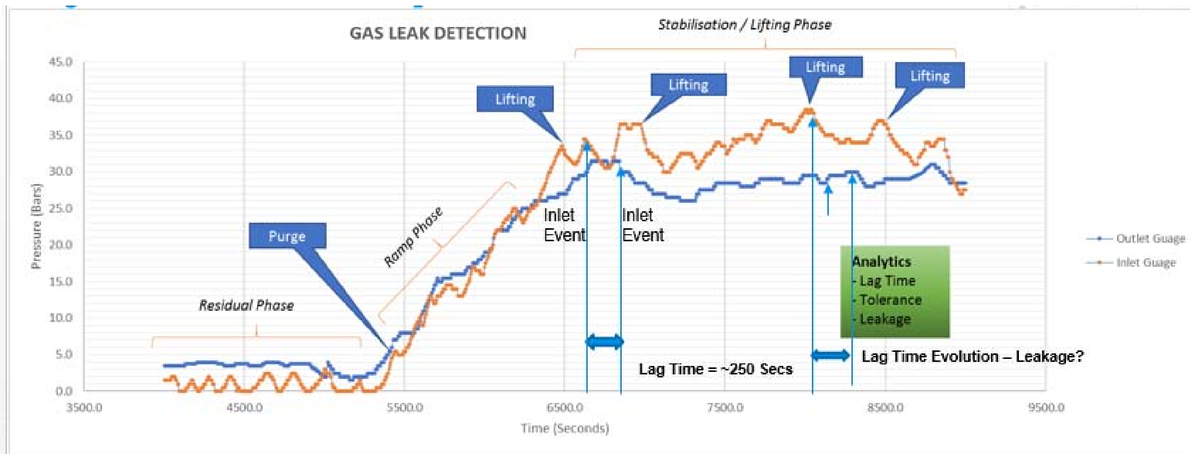

Figure 9: Estimation of lag time and consistency in recording for the upstream and downstream gauges

Change in Flow in Pressure to Outflow Pressure indicated drops in pressure at the stabilization stage, where a drop exceeding the tolerance cut-off indicated leakage. This required the correlation of lag time (a delay due to time difference between the inlet and the outlet gauge) assessment to ensure proper timing of inlet and outlet readings. The detection tolerance window, further reduced by machine learning, was use for leakage detection as shown in Figure 10.

Figure 10: Lag time correction and leakage detection based on a tolerance window

For gas detection result, the steps followed were Identification of Phases, Calibration of System (QC), Evaluation of Lag Time, Checking for Tolerance, Checking for Consistency, Detection of Leakage and Estimation of Volume of gas leaked (indices indicated in Figure 10). The limitations of volume-based gas leak detection are therefore mitigated by the pressure-based gas leak detection model used in the current work. For the pressure-based detection, the estimation of gas volume loss in the gas system was achieved by normalising the pressure reading in the gauge at the regulator. The change in pressure in the gauge` was calibrated against the change in weight or change in volume of the gas already quantified in the system (Figure 11).

c) Animation of Test Results: Uncertainty and Data Validation

Percentage leak rate per total flow volume requires a prior calibration of the gas volumes. In the example in Figure X, the pressure drop corresponded to a given gas volume. Leak Volume = 2.40 m^3 or 84.7 scf of gas.

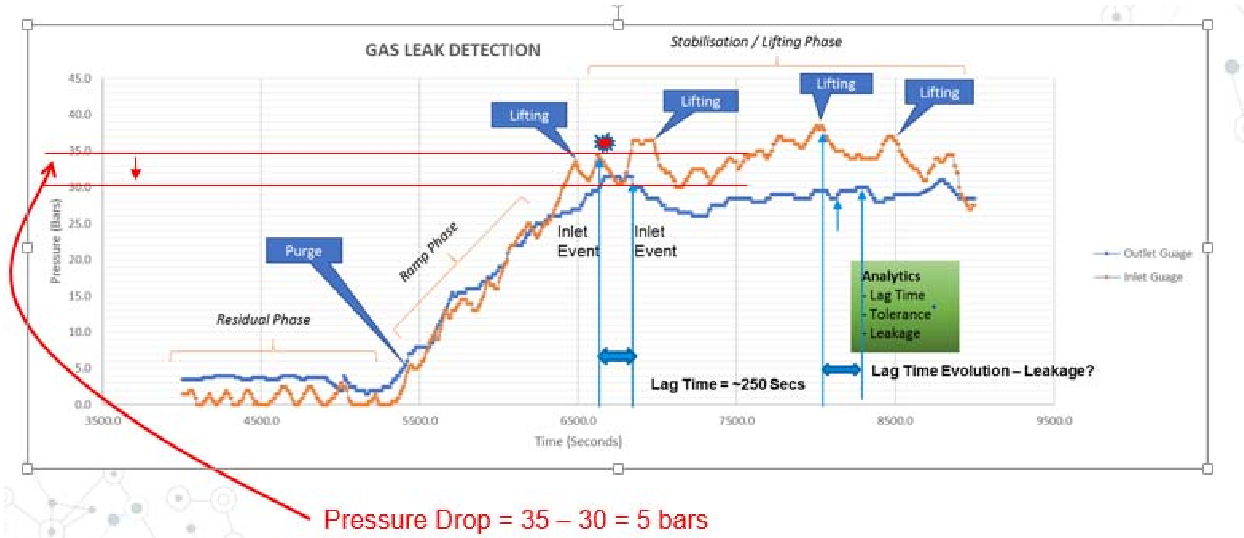

a. Estimation of pressure drop

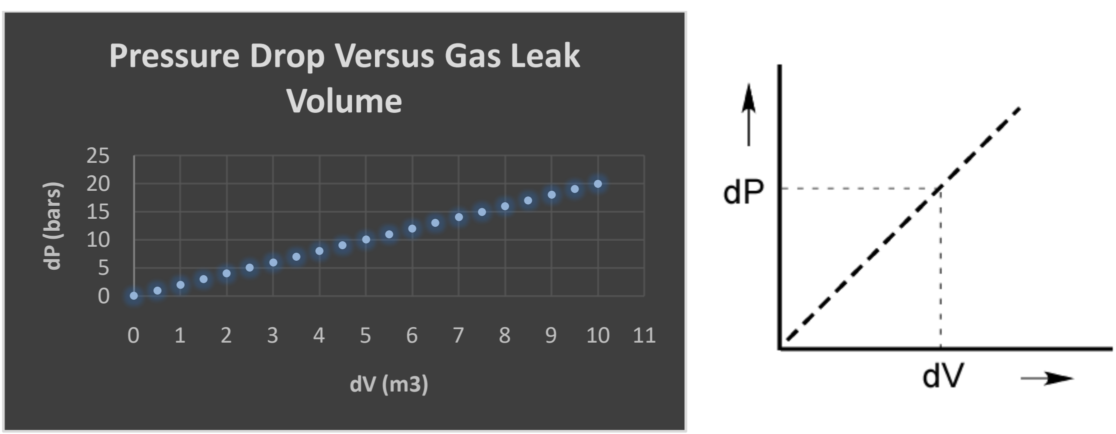

b. A prior calibration (where δV is the leaked Volume of gas for the change in Pressure δV)

Figure 11: Calibration of leak for per pressure drop

Gas leaks can cause significant damage and result in high costs for building owners, tenants, and property managers. That's why leak detection systems have become a crucial aspect of building management. In recent years, advancements in technology have made it possible to detect leaks automatically and remotely, thanks to machine learning algorithms. By analysing the volume and time of gas usage during a typical weekday or weekend, the algorithm can recognize events and predict future consumption. Using the data acquired, alarm thresholds are established based on past maximum consumption events. By splitting these events by the day of the week and further dividing them by time, the algorithm can accurately detect abnormal water usage patterns and trigger an alert if necessary.

Captured Animation Screens are shown in the Appendix.

Summary

- Input gas data is *calibrated and evaluated for consistency* in real-time
- The data is then corrected for *lag and used to compute tolerance*
- Min. and Max. Tolerance Cut-Off is set based on *machine training dataset*
- Where value is higher than maximum cut-off, *machine sets off alarm*
- Time of alarm is checked against events such as *lifting, residual gas*
- Where alarm is *eventless, leak is suspected* and eventually confirmed
- Leaked *volume is estimated* using a prior calibration relation
- Action may be taken to *mitigate against the leakage*
- Further modelling becomes *predictive as machine learns* from experience

V. Conclusion

The integration of AI and machine learning (ML) in gas flow leakage monitoring has demonstrated significant benefits, particularly in reducing false alarms and enhancing the reliability of detection systems. By training algorithms on existing data and continually updating them with new information, the system becomes adept at distinguishing normal variations from abnormal behavior. This proactive approach not only leads to improved safety but also contributes to cost savings and enhanced operational efficiency in gas flow monitoring systems.

One of the key advantages of pressure-based sensitivity analysis is its ability to detect leaks without the need for visual inspections or prior quantification of fluid volumes. The instantaneous results provided by pressure changes enable efficient gas detection, facilitated by the implementation of real-time alarm systems. Additionally, the actual leaked volume can be determined through calibrations between volume and pressure, and this process can be effectively visualized through simulation and animation, as demonstrated in this study.

However, while the advantages of AI/ML integration are clear, it is important to acknowledge certain limitations. Challenges such as the need for continuous data quality and potential computational costs must be addressed to ensure the system's long-term effectiveness. Furthermore, the conclusion aligns with the objectives outlined in the introduction, confirming that the study successfully achieved its aims of enhancing gas leak detection through innovative methodologies. Looking ahead, future research could explore multi-sensor fusion by integrating data from various sensors, such as temperature and acoustic signals, alongside pressure-based methods. This could significantly improve detection robustness. Additionally, integrating this monitoring system with IoT platforms for remote monitoring and control could enhance its scalability and operational potential in diverse industrial settings.

Appendix I

Coding for Machine Learning and Automation

In [7]:
```
print('min Time value', df.Time.min())
print('max Time value', df.Time.max())
```

```
min Time value 1000
max Time value 9000
```

In [8]:
```
#### Select relevant columns
relevant_df = df[['Time','Pr_final','Pr_initial','Tolerance','Min','Max']]
cleaned_df = relevant_df.dropna()
print(relevant_df.shape)
print(cleaned_df.shape)
print('{} rows dropped from the table'.format(relevant_df.shape[0]-cleaned_df.shape[0]))
```

```
(1012, 6)
(1001, 6)
11 rows dropped from the table
```

In [9]:
```
cleaned_df['Tolerance'] = cleaned_df['Tolerance'].astype(float)
```

Plotting

In [10]:
```
# adding some nice colors
plt.rcParams['text.color'] = 'black'
plt.rcParams['axes.labelcolor'] = 'blue'
plt.rcParams['xtick.color'] = 'red'
plt.rcParams['ytick.color'] = 'red'


fig, axs = plt.subplots(2, figsize=(12,10))
fig.tight_layout(pad=1.08, h_pad=7, w_pad=None)

axs[0].plot(cleaned_df.Time, cleaned_df.Pr_final,'-p',
            lw=1.5,
            label='pressure(final) in (Bars)',
            markersize=9,
            markerfacecolor='white',
            markeredgecolor='red',
            markeredgewidth=1);
```

In [1]:
```
import warnings
warnings.filterwarnings("ignore")
```

In [2]:
```
import pandas as pd
import numpy as np
import matplotlib.pyplot as plt
from pylab import cm
from matplotlib.ticker import MaxNLocator
from matplotlib.ticker import FormatStrFormatter
```

In [3]:
```
#pip install git+https://github.com/garrettj403/SciencePlots
```

In [4]:
```
plt.style.use(['science','no-latex','grid'])
```

In [5]:
```
df = pd.read_csv('iESog.csv')
```

In [6]:
```
df.head()
```

Out[6]:

	Time	Pr_final	Pr_initial	Events	Tolerance	Min	Max
0	4005	3.5	1.5	Residual stage	0.428571429	0.8	1.2
1	4010	3.5	1.5	NaN	0.428571429	0.8	1.2
2	4015	3.5	1.5	NaN	0.428571429	0.8	1.2
3	4020	3.5	1.5	NaN	0.428571429	0.8	1.2
4	4025	3.5	1.5	NaN	0.428571429	0.8	1.2

In [7]:
```
print('min Time value', df.Time.min())
print('max Time value', df.Time.max())
```

```
min Time value 1000
max Time value 9000
```

In [8]:
```
#### Select relevant columns
relevant_df = df[['Time','Pr_final','Pr_initial','Tolerance','Min','Max']]
cleaned_df = relevant_df.dropna()
```

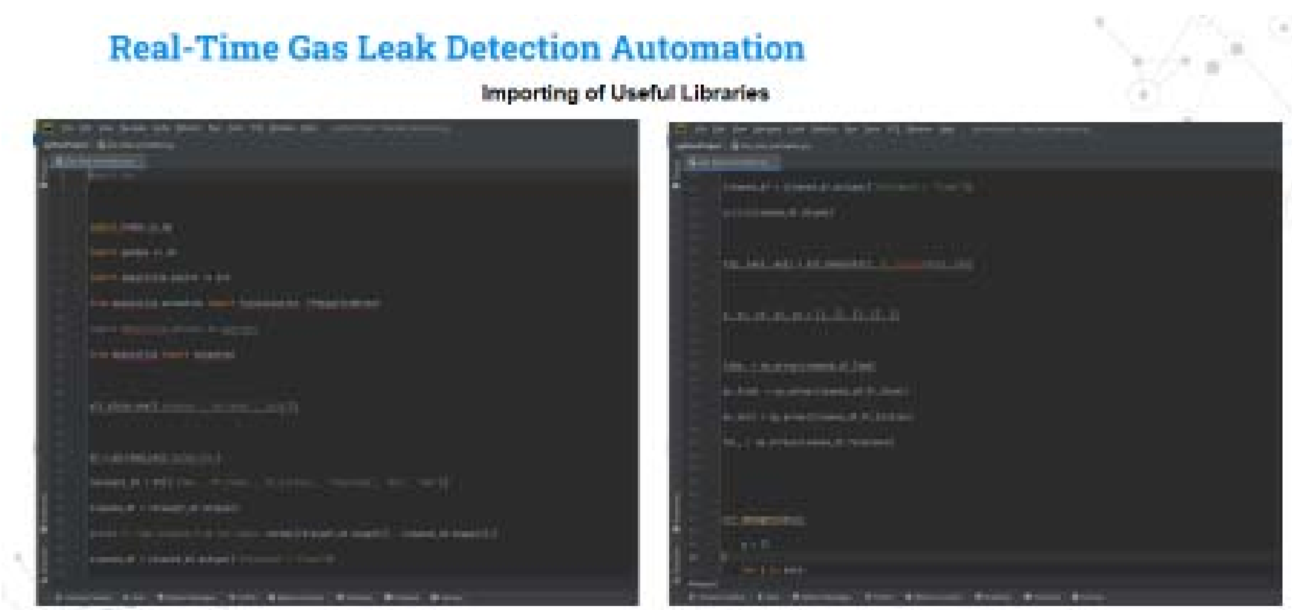

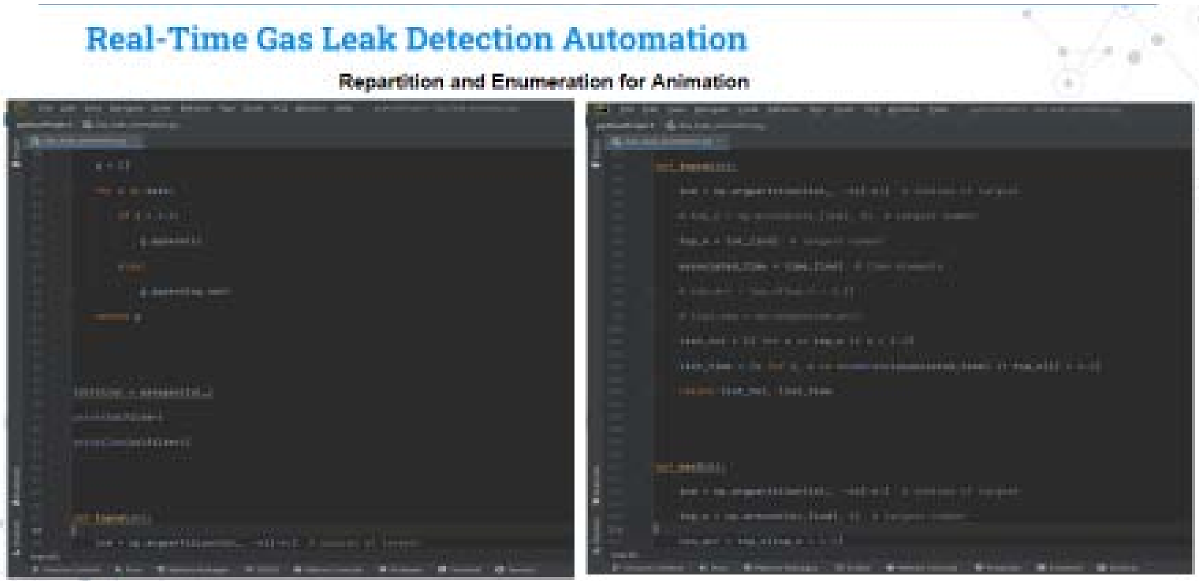
Real-Time Gas Leak Detection Automation
Repartition and Enumeration for Animation

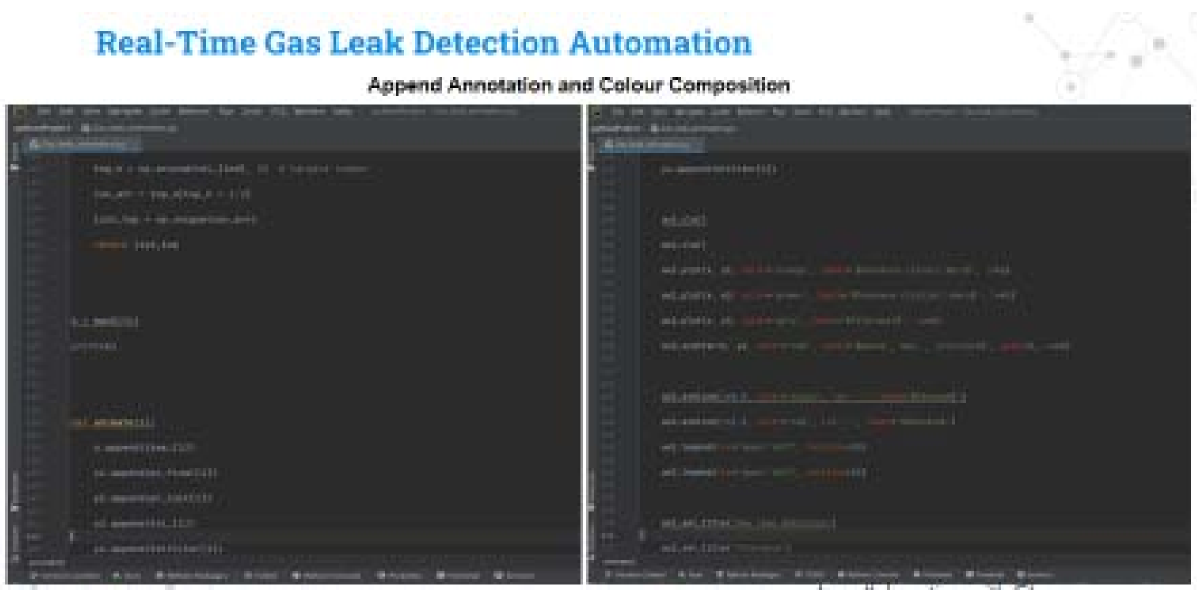
Real-Time Gas Leak Detection Automation
Append Annotation and Colour Composition

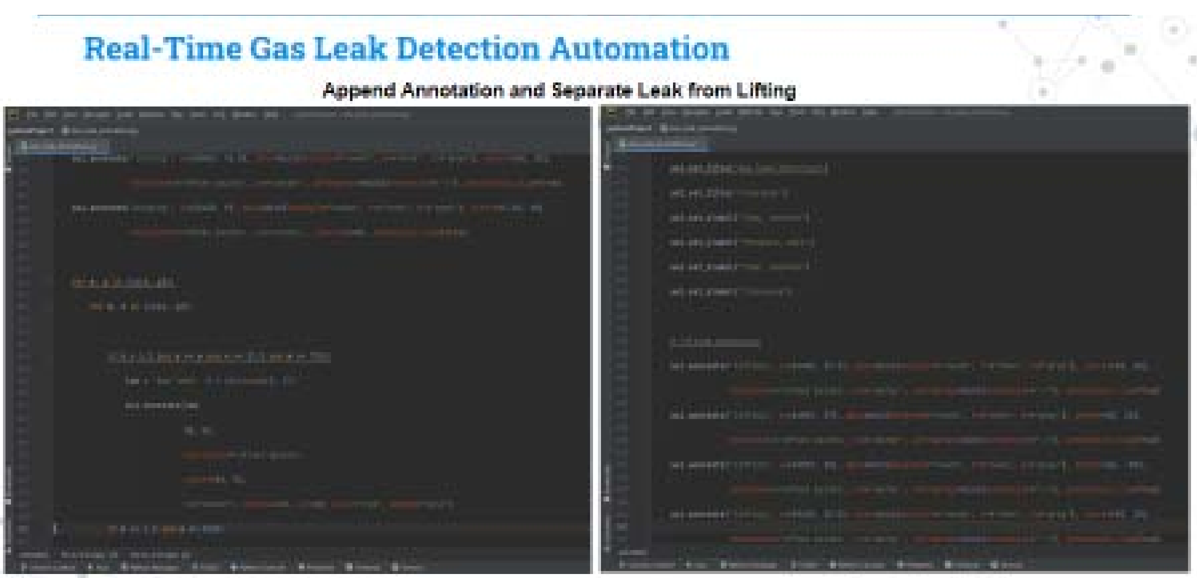
Real-Time Gas Leak Detection Automation
Append Annotation and Separate Leak from Lifting

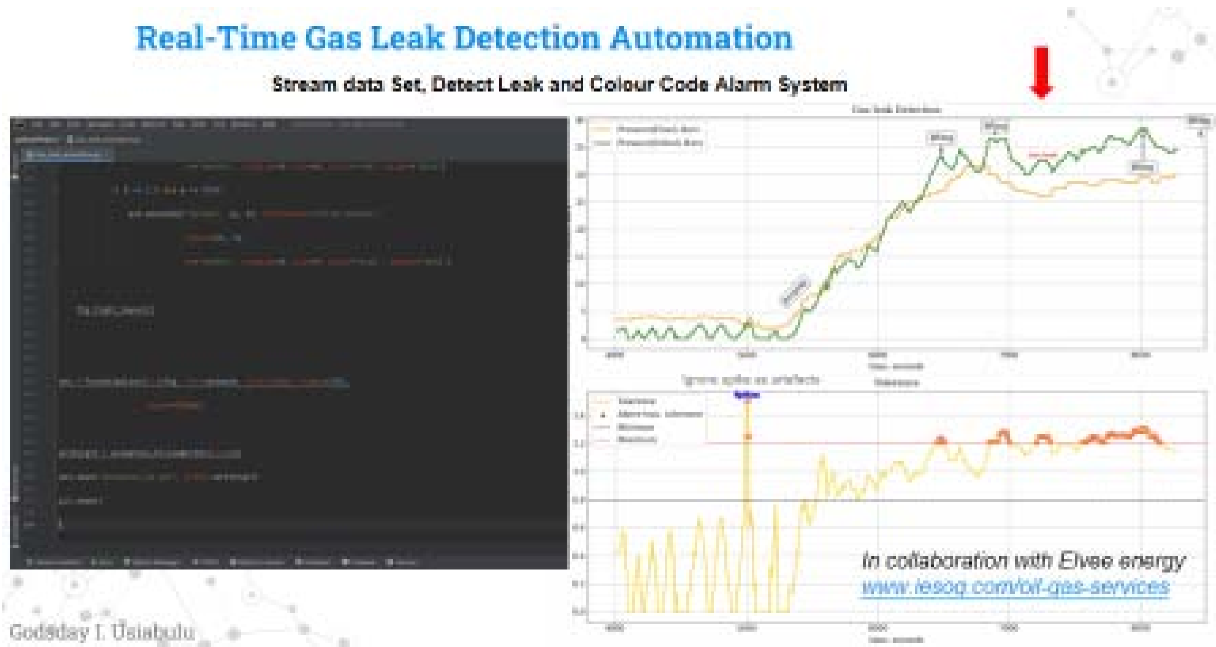

Appendix II

Residual Stage

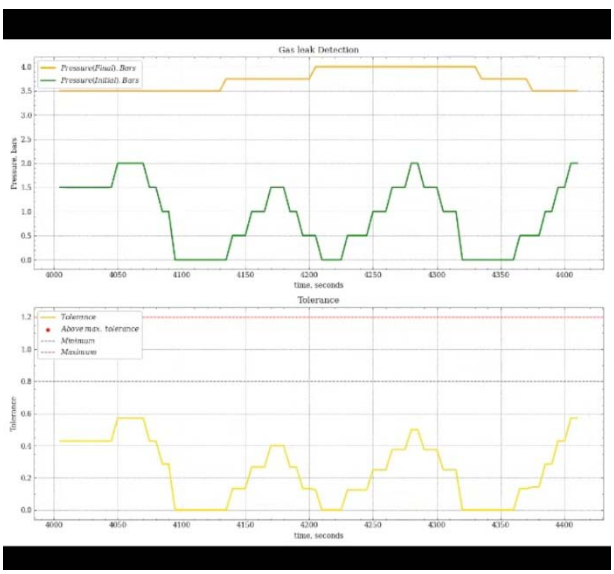

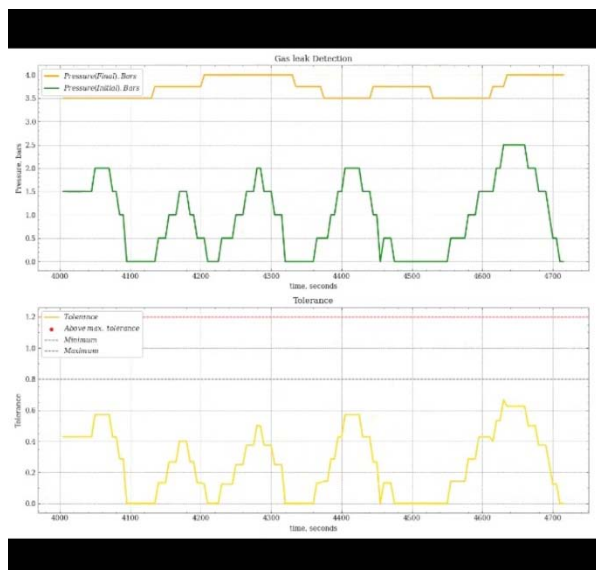

[redacted]

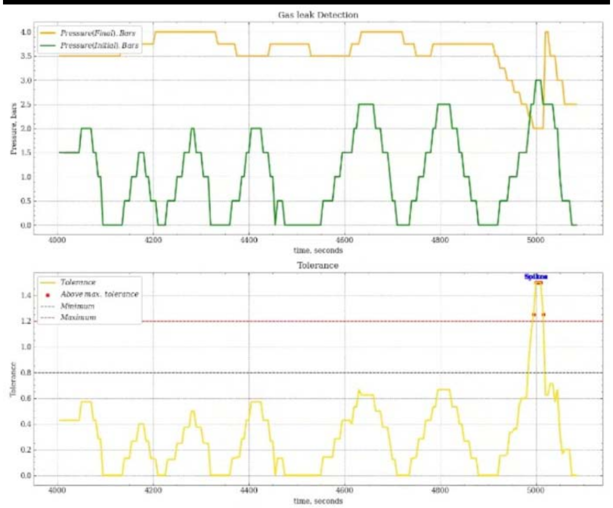

[redacted]

[redacted]

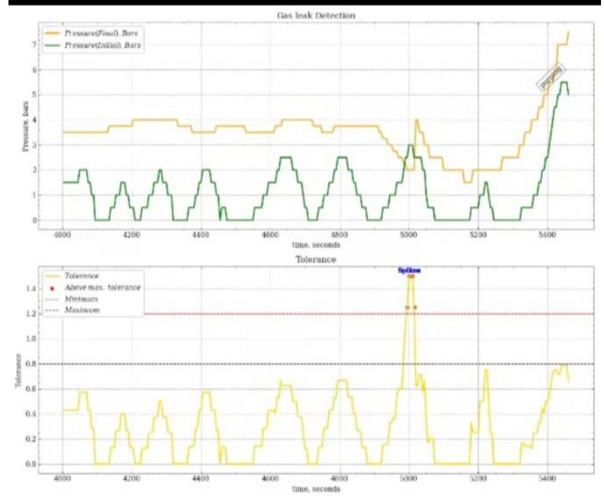

[redacted]

Residual to Ramp up Stage

[redacted]

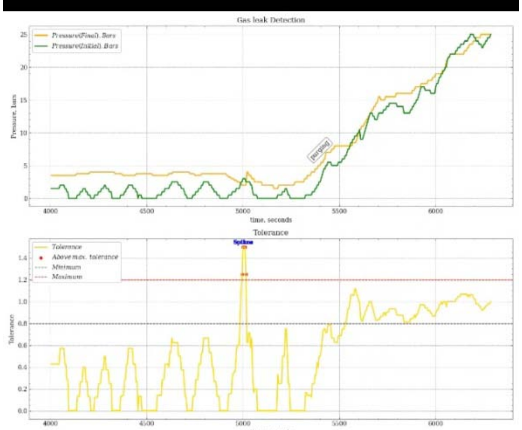

[redacted]

[redacted]

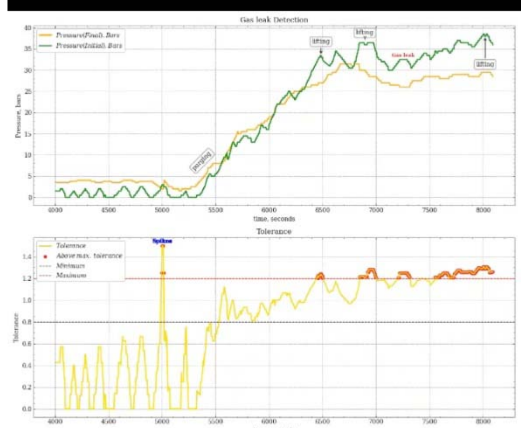

[redacted]

[redacted]

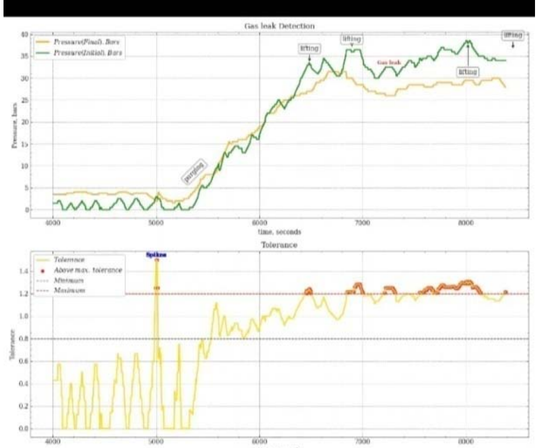

[redacted]

[redacted]

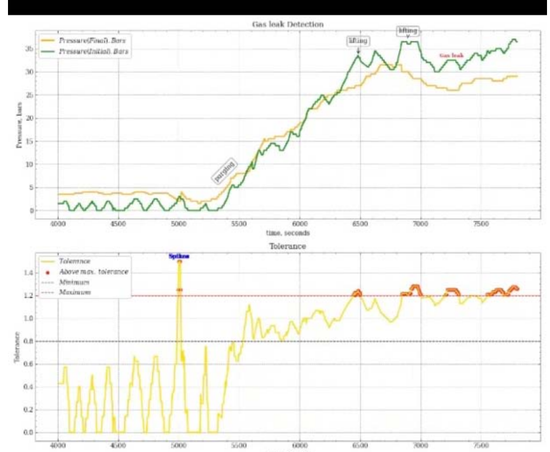

[redacted]

Residual to Ramp up to Stabilization/Plateau Stage

[redacted]

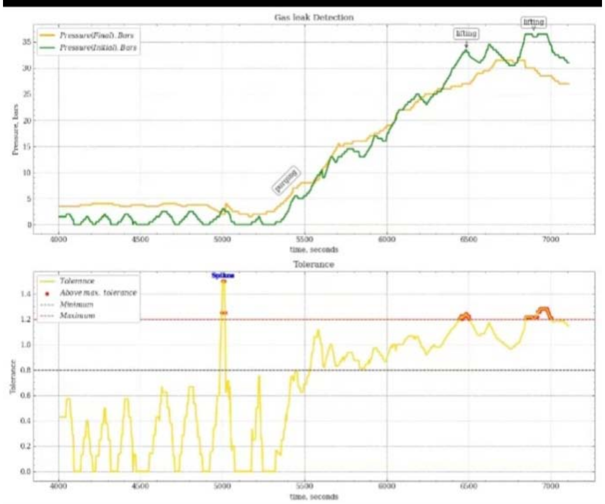

[redacted]

[redacted]

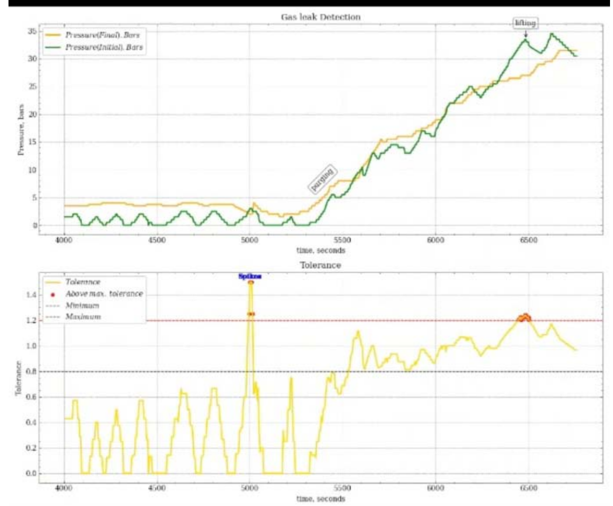

[redacted]

[redacted]

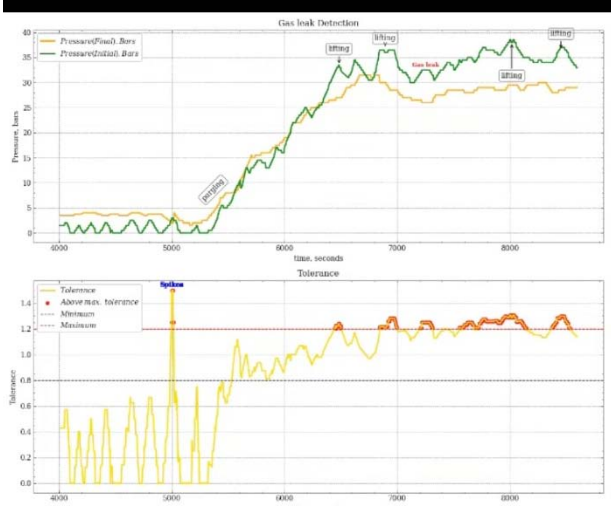

[redacted]

[redacted]

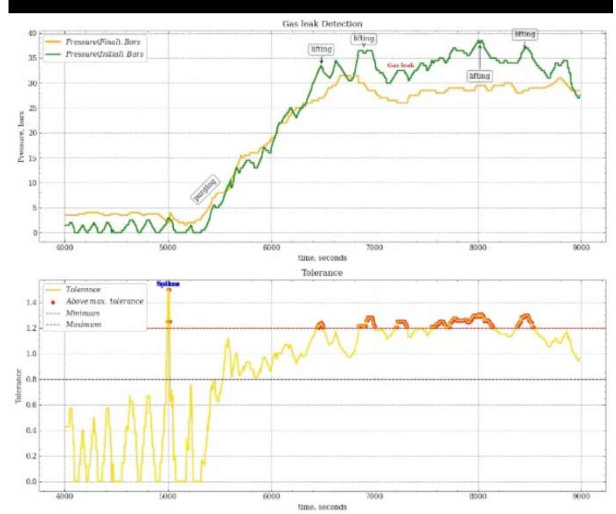

[redacted]

References Références Referencias

1. Arnaldos, J., J. Casal, H. Montiel, M. Sanchez-Carricondo, and ´J. A. Vílchez, (1998). “Design of a computer tool for the evaluation of the consequences of accidental natural gas releases in distribution pipes,” Journal of Loss Prevention in the Process Industries, vol. 11, no. 2, pp. 135–148.
2. Appah, D., Aimikhe, V., & Okologume., W. (2021, 07 04). *Assessment of Gas Leak Detection Techniques in Natural Gas Infrastructure.* Retrieved from OnePetro: https://doi.org/10.2118/208236-MS
3. Bariha, N., I. M. Mishra, and V. C. Srivastava, (2016). “Hazard analysis of failure of natural gas and petroleum gas pipelines,” Journal of Loss Prevention in the Process Industries, vol. 40, pp. 217– 226.
4. Bear, J., (1972), Dynamics of Fluids in Porous Media, American Elsevier, New York, 764 pages.
5. Chaki, Soumi, Aurobinda Routray, and William K. Mohanty. (2018) "*Well-log and seismic data integration for reservoir characterization: A signal processing and machine-learning perspective.*" *IEEE Signal Processing Magazine 35.2: 72-81.*
6. Chinwuko Emmanuel Chuka, Ifowodo Henry Freedom, Umeozokwere Anthony O (2016) *Transient Model-Based Leak Detection and Localization Technique for Crude Oil Pipelines: A Case of N.P.D.C, Olomoro.*
7. Freeze, R.A., and J.A. Cherry, (1979), Groundwater. Prentice-Hall, Inc, Englewood Cliffs, New Jersey, USA, 604 pages.
8. Gibson, G; Well, B. V; Hodgkinson, J; Pride, R; Strzoda, R; Murray, S; Bishton, S; Padgett, M

(2006). Imaging of methane gas using a scanning, open-path laser system. *New J. Phys.*8, 1–7.
9. Godsday Idanegbe Usiabulu, Azubuike Hope Amadi, Emeka Okafor, Jumbo-Egwurugwu Preciuos, (March-April, 2022). Optimization of methane and natural gas liquid recovery in a reboiled absorbtion column. International journal of Scientific Research and Engineering Development, volume 5, issue 2.
10. Godsday Idanegbe Usiabulu, Azubuike Hope Amadi, Oluwatayo Adebisi, Uchenna Donald Ifedili, Kehinde Elijah Ajayi, Pwafureino Reuel Moses, (March, 2023). Gas flaring and its environmental impact in Ekpan Community, Delta state, Nigeria, American Journal of Science Engineering and Technology. Volume 8, issue 1, pp. 42-53.
11. Hirsch, E; Agassi, E (2010). Detection of gaseous plumes in IR hyperspectral images - performance analysis," IEEE Sens. J. 10(3), 732–736.
12. Kedar Potdar, Rishab Kinnerkar (2013) *A Comparative Study of Machine Learning Algorithms applied to Predictive Breast Cancer Data.*
13. Lammel, G; Schweizer, S; Renaud, P (2001). MEMS infrared gas spectrometer based on a porous silicon tunable filter," in Proceedings of the 14th Int. IEEE Conf. on MEMS (IEEE), pp. 578–581.
14. Lohberger, F; Hönninger, G; Platt, U (2004). Ground-based imaging differential optical absorption spectroscopy of atmospheric gases. Appl. Opt. 43(24), 4711–4717.
15. Montiel, H, J. Vilchez, J. Casal, and J. Arnaldos, (1998). "Mathematical modelling of accidental gas releases," Journal of Hazardous Materials, vol. 59, no. 2, pp. 211–233.
16. Nosike, L., (2009). Relationship between tectonics and vertical hydrocarbon leakage: PhD thesis, University of Nice-Sophia Antipolis, Fracnce, 281 p.
17. Nosike, L., (2020). Exploration and production Geoscience-Comprehensive Skills Acquistion for an Evolving industry, p.227-264. Delizon Publishers, 441 pp.
18. Nosike, L., (2023). A study of gas fire at a water well in the Caritas University Premises, Amorji Nike, Enugu, PTD journal review.
19. Powers, PE; Kulp, TJ; Kennedy, R (2000). Demonstration of differential backscatter absorption gas imaging. Appl. Opt. 39(9), 1440–1448.
20. Sandsten, J; Edner, H; Svanberg, S (2004). Gas visualization of industrial hydrocarbon emissions. Opt. Express 12(7), 1443–1451.
21. Sandsten, J; Weibring, P; Edner, H; Svanberg, S (2000). Real-time gas-correlation imaging employing thermal background radiation. Opt. Express 6(4), 92–103.
22. Stothard, D; Dunn, M; Rae, C (2004). Hyperspectral imaging of gases with a continuous-wave pump-enhanced optical parametric oscillator. Opt. Express 12(5), 947–955.
23. Svanberg, S (2002). Geophysical gas monitoring using optical techniques: volcanoes, geothermal fields and mines. Opt. Lasers Eng. 37(2-3), 245–266.
24. Tan, S. Y., & Tan, S. (2019, March 24). The Right Technologies for Gas Leak Detection. p. 43.
25. Todd, David Keith, and Larry W. Mays, (2004). Groundwater Hydrology, third edition. John Wiley and Sons, Incorporated, 656 pages.
26. U.S. EPA Office of Air Quality Planning and Standards. (2014). Oil and Natural Gas Sector Leaks.
27. Usiabulu G. Idanegbe, Azubuike H. Amadi, Emeka J. Okafor, Jumbo-Egwurugwu Precious (2022). Optimization of Methane and Natural Gas Liquid Recovery in a Reboiled Absorption Column *International Journal of Scientific Research and Engineering* Development IJSRED Volume 5 - Issue 2, March - April 2022. Page(s): 36-48.
28. Wojciech, K., J and S. Janusz, (2012) "Real gas flow simulation in damaged distribution pipelines," Energy, vol. 45, pp. 481–488.
29. Zukang Hu, Beiqing Chen, Wenlong Chen, Debao Tan and Dingtao Shen (2021) *Review of model-based and data-driven approaches for leak detection and location in water distribution systems.*

Global Journals Guidelines Handbook 2025

www.GlobalJournals.org

Memberships

FELLOWS/ASSOCIATES OF ENGINEERING RESEARCH COUNCIL

FERC/AERC MEMBERSHIPS

Introduction

FERC/AERC is the most prestigious membership of Global Journals accredited by Open Association of Research Society, U.S.A (OARS). The credentials of Fellow and Associate designations signify that the researcher has gained the knowledge of the fundamental and high-level concepts, and is a subject matter expert, proficient in an expertise course covering the professional code of conduct, and follows recognized standards of practice. The credentials are designated only to the researchers, scientists, and professionals that have been selected by a rigorous process by our Editorial Board and Management Board.

Associates of FERC/AERC are scientists and researchers from around the world are working on projects/researches that have huge potentials. Members support Global Journals' mission to advance technology for humanity and the profession.

FERC

FELLOW OF ENGINEERING RESEARCH COUNCIL

FELLOW OF ENGINEERING RESEARCH COUNCIL is the most prestigious membership of Global Journals. It is an award and membership granted to individuals that the Open Association of Research Society judges to have made a 'substantial contribution to the improvement of computer science, technology, and electronics engineering.

The primary objective is to recognize the leaders in research and scientific fields of the current era with a global perspective and to create a channel between them and other researchers for better exposure and knowledge sharing. Members are most eminent scientists, engineers, and technologists from all across the world. Fellows are elected for life through a peer review process on the basis of excellence in the respective domain. There is no limit on the number of new nominations made in any year. Each year, the Open Association of Research Society elect up to 12 new Fellow Members.

Benefits

To the Institution

Get letter of appreciation

Global Journals sends a letter of appreciation of author to the Dean or CEO of the University or Company of which author is a part, signed by editor in chief or chief author.

Exclusive Network

Get access to a closed network

A FERC member gets access to a closed network of Tier 1 researchers and scientists with direct communication channel through our website. Fellows can reach out to other members or researchers directly. They should also be open to reaching out by other.

Career | Credibility | Exclusive | Reputation

Certificate

Certificate, LoR and Laser-Momento

Fellows receive a printed copy of a certificate signed by our Chief Author that may be used for academic purposes and a personal recommendation letter to the dean of member's university.

Career | Credibility | Exclusive | Reputation

Designation

Get honored title of membership

Fellows can use the honored title of membership. The “FERC” is an honored title which is accorded to a person’s name viz. Dr. John E. Hall, Ph.D., FERC or William Walldroff, M.S., FERC.

Career | Credibility | Exclusive | Reputation

Recognition on the Platform

Better visibility and citation

All the Fellow members of FERC get a badge of "Leading Member of Global Journals" on the Research Community that distinguishes them from others. Additionally, the profile is also partially maintained by our team for better visibility and citation. All fellows get a dedicated page on the website with their biography.

Career | Credibility | Reputation

Future Work

Get discounts on the future publications

Fellows receive discounts on the future publications with Global Journals up to 60%. Through our recommendation programs, members also receive discounts on publications made with OARS affiliated organizations.

Career Financial

GJ Account

Unlimited forward of Emails

Fellows get secure and fast GJ work emails with unlimited storage of emails that they may use them as their primary email. For example, john [AT] globaljournals [DOT] org.

Career Credibility Reputation

Premium Tools

Access to all the premium tools

To take future researches to the zenith, fellows receive access to all the premium tools that Global Journals have to offer along with the partnership with some of the best marketing leading tools out there.

Financial

Conferences & Events

Organize seminar/conference

Fellows are authorized to organize symposium/seminar/conference on behalf of Global Journal Incorporation (USA). They can also participate in the same organized by another institution as representative of Global Journal. In both the cases, it is mandatory for him to discuss with us and obtain our consent. Additionally, they get free research conferences (and others) alerts.

Career Credibility Financial

Early Invitations

Early invitations to all the symposiums, seminars, conferences

All fellows receive the early invitations to all the symposiums, seminars, conferences and webinars hosted by Global Journals in their subject.

Exclusive

Publishing Articles & Books

Earn 60% of sales proceeds

Fellows can publish articles (limited) without any fees. Also, they can earn up to 70% of sales proceeds from the sale of reference/review books/literature/publishing of research paper. The FERC member can decide its price and we can help in making the right decision.

Exclusive Financial

Reviewers

Get a remuneration of 15% of author fees

Fellow members are eligible to join as a paid peer reviewer at Global Journals Incorporation (USA) and can get a remuneration of 15% of author fees, taken from the author of a respective paper.

Financial

Access to Editorial Board

Become a member of the Editorial Board

Fellows may join as a member of the Editorial Board of Global Journals Incorporation (USA) after successful completion of three years as Fellow and as Peer Reviewer. Additionally, Fellows get a chance to nominate other members for Editorial Board.

Career Credibility Exclusive Reputation

And Much More

Get access to scientific museums and observatories across the globe

All members get access to 5 selected scientific museums and observatories across the globe. All researches published with Global Journals will be kept under deep archival facilities across regions for future protections and disaster recovery. They get 10 GB free secure cloud access for storing research files.

AERC

ASSOCIATE OF ENGINEERING RESEARCH COUNCIL

ASSOCIATE OF ENGINEERING RESEARCH COUNCIL is the membership of Global Journals awarded to individuals that the Open Association of Research Society judges to have made a 'substantial contribution to the improvement of computer science, technology, and electronics engineering.

> The primary objective is to recognize the leaders in research and scientific fields of the current era with a global perspective and to create a channel between them and other researchers for better exposure and knowledge sharing. Members are most eminent scientists, engineers, and technologists from all across the world. Associate membership can later be promoted to Fellow Membership. Associates are elected for life through a peer review process on the basis of excellence in the respective domain. There is no limit on the number of new nominations made in any year. Each year, the Open Association of Research Society elect up to 12 new Associate Members.

Benefits

To the Institution

Get letter of appreciation

Global Journals sends a letter of appreciation of author to the Dean or CEO of the University or Company of which author is a part, signed by editor in chief or chief author.

Exclusive Network

Get access to a closed network

A AERC member gets access to a closed network of Tier 1 researchers and scientists with direct communication channel through our website. Associates can reach out to other members or researchers directly. They should also be open to reaching out by other.

Career | Credibility | Exclusive | Reputation

Certificate

Certificate, LoR and Laser-Momento

Associates receive a printed copy of a certificate signed by our Chief Author that may be used for academic purposes and a personal recommendation letter to the dean of member's university.

Career | Credibility | Exclusive | Reputation

Designation

Get honored title of membership

Associates can use the honored title of membership. The "AERC" is an honored title which is accorded to a person's name viz. Dr. John E. Hall, Ph.D., AERC or William Walldroff, M.S., AERC.

Career | Credibility | Exclusive | Reputation

Recognition on the Platform

Better visibility and citation

All the Associate members of AERC get a badge of "Leading Member of Global Journals" on the Research Community that distinguishes them from others. Additionally, the profile is also partially maintained by our team for better visibility and citation. All associates get a dedicated page on the website with their biography.

Career | Credibility | Reputation

Future Work

Get discounts on the future publications

Associates receive discounts on the future publications with Global Journals up to 60%. Through our recommendation programs, members also receive discounts on publications made with OARS affiliated organizations.

Career | Financial

GJ Account

Unlimited forward of Emails

Associates get secure and fast GJ work emails with unlimited storage of emails that they may use them as their primary email. For example, john [AT] globaljournals [DOT] org..

Career | Credibility | Reputation

Premium Tools

Access to all the premium tools

To take future researches to the zenith, associates receive access to all the premium tools that Global Journals have to offer along with the partnership with some of the best marketing leading tools out there.

Financial

Conferences & Events

Organize seminar/conference

Associates are authorized to organize symposium/seminar/conference on behalf of Global Journal Incorporation (USA). They can also participate in the same organized by another institution as representative of Global Journal. In both the cases, it is mandatory for him to discuss with us and obtain our consent. Additionally, they get free research conferences (and others) alerts.

Career | Credibility | Financial

Early Invitations

Early invitations to all the symposiums, seminars, conferences

All associates receive the early invitations to all the symposiums, seminars, conferences and webinars hosted by Global Journals in their subject.

Exclusive

Publishing Articles & Books

Earn 30-40% of sales proceeds

Associates can publish articles (limited) without any fees. Also, they can earn up to 30-40% of sales proceeds from the sale of reference/review books/literature/publishing of research paper.

Exclusive Financial

Reviewers

Get a remuneration of 15% of author fees

Associate members are eligible to join as a paid peer reviewer at Global Journals Incorporation (USA) and can get a remuneration of 15% of author fees, taken from the author of a respective paper.

Financial

And Much More

Get access to scientific museums and observatories across the globe

All members get access to 2 selected scientific museums and observatories across the globe. All researches published with Global Journals will be kept under deep archival facilities across regions for future protections and disaster recovery. They get 5 GB free secure cloud access for storing research files.

ASSOCIATE	FELLOW	RESEARCH GROUP	BASIC
$4800 **lifetime designation**	$6800 **lifetime designation**	$12500.00 **organizational**	APC **per article**
Certificate, LoR and Momento 2 discounted publishing/year **Gradation** of Research 10 research contacts/day 1 **GB** Cloud Storage **GJ** Community Access	**Certificate,** LoR and Momento **Unlimited** discounted publishing/year **Gradation** of Research **Unlimited** research contacts/day 5 **GB** Cloud Storage **Online Presense** Assistance **GJ** Community Access	**Certificates,** LoRs and Momentos **Unlimited** free publishing/year **Gradation** of Research **Unlimited** research contacts/day **Unlimited** Cloud Storage **Online Presense** Assistance **GJ** Community Access	**GJ** Community Access

We accept the manuscript submissions in any standard (generic) format.

We typeset manuscripts using advanced typesetting tools like Adobe In Design, CorelDraw, TeXnicCenter, and TeXStudio. We usually recommend authors submit their research using any standard format they are comfortable with, and let Global Journals do the rest.

Alternatively, you can download our basic template from https://globaljournals.org/Template.zip

Authors should submit their complete paper/article, including text illustrations, graphics, conclusions, artwork, and tables. Authors who are not able to submit manuscript using the form above can email the manuscript department at submit@globaljournals.org or get in touch with chiefeditor@globaljournals.org if they wish to send the abstract before submission.

Before and during Submission

Authors must ensure the information provided during the submission of a paper is authentic. Please go through the following checklist before submitting:

1. Authors must go through the complete author guideline and understand and *agree to Global Journals' ethics and code of conduct,* along with author responsibilities.
2. Authors must accept the privacy policy, terms, and conditions of Global Journals.
3. Ensure corresponding author's email address and postal address are accurate and reachable.
4. Manuscript to be submitted must include keywords, an abstract, a paper title, co-author(s') names and details (email address, name, phone number, and institution), figures and illustrations in vector format including appropriate captions, tables, including titles and footnotes, a conclusion, results, acknowledgments and references.
5. Authors should submit paper in a ZIP archive if any supplementary files are required along with the paper.
6. Proper permissions must be acquired for the use of any copyrighted material.
7. Manuscript submitted *must not have been submitted or published elsewhere* and all authors must be aware of the submission.

Declaration of Conflicts of Interest

It is required for authors to declare all financial, institutional, and personal relationships with other individuals and organizations that could influence (bias) their research.

Policy on Plagiarism

Plagiarism is not acceptable in Global Journals submissions at all.

Plagiarized content will not be considered for publication. We reserve the right to inform authors' institutions about plagiarism detected either before or after publication. If plagiarism is identified, we will follow COPE guidelines:

Authors are solely responsible for all the plagiarism that is found. The author must not fabricate, falsify or plagiarize existing research data. The following, if copied, will be considered plagiarism:

- Words (language)
- Ideas
- Findings
- Writings
- Diagrams
- Graphs
- Illustrations
- Lectures

- Printed material
- Graphic representations
- Computer programs
- Electronic material
- Any other original work

Authorship Policies

Global Journals follows the definition of authorship set up by the Open Association of Research Society, USA. According to its guidelines, authorship criteria must be based on:

1. Substantial contributions to the conception and acquisition of data, analysis, and interpretation of findings.
2. Drafting the paper and revising it critically regarding important academic content.
3. Final approval of the version of the paper to be published.

Changes in Authorship

The corresponding author should mention the name and complete details of all co-authors during submission and in manuscript. We support addition, rearrangement, manipulation, and deletions in authors list till the early view publication of the journal. We expect that corresponding author will notify all co-authors of submission. We follow COPE guidelines for changes in authorship.

Copyright

During submission of the manuscript, the author is confirming an exclusive license agreement with Global Journals which gives Global Journals the authority to reproduce, reuse, and republish authors' research. We also believe in flexible copyright terms where copyright may remain with authors/employers/institutions as well. Contact your editor after acceptance to choose your copyright policy. You may follow this form for copyright transfers.

Appealing Decisions

Unless specified in the notification, the Editorial Board's decision on publication of the paper is final and cannot be appealed before making the major change in the manuscript.

Acknowledgments

Contributors to the research other than authors credited should be mentioned in Acknowledgments. The source of funding for the research can be included. Suppliers of resources may be mentioned along with their addresses.

Declaration of funding sources

Global Journals is in partnership with various universities, laboratories, and other institutions worldwide in the research domain. Authors are requested to disclose their source of funding during every stage of their research, such as making analysis, performing laboratory operations, computing data, and using institutional resources, from writing an article to its submission. This will also help authors to get reimbursements by requesting an open access publication letter from Global Journals and submitting to the respective funding source.

Preparing your Manuscript

Authors can submit papers and articles in an acceptable file format: MS Word (doc, docx), LaTeX (.tex, .zip or .rar including all of your files), Adobe PDF (.pdf), rich text format (.rtf), simple text document (.txt), Open Document Text (.odt), and Apple Pages (.pages). Our professional layout editors will format the entire paper according to our official guidelines. This is one of the highlights of publishing with Global Journals—authors should not be concerned about the formatting of their paper. Global Journals accepts articles and manuscripts in every major language, be it Spanish, Chinese, Japanese, Portuguese, Russian, French, German, Dutch, Italian, Greek, or any other national language, but the title, subtitle, and abstract should be in English. This will facilitate indexing and the pre-peer review process.

The following is the official style and template developed for publication of a research paper. Authors are not required to follow this style during the submission of the paper. It is just for reference purposes.

Manuscript Style Instruction (Optional)

- Microsoft Word Document Setting Instructions.
- Font type of all text should be Swis721 Lt BT.
- Page size: 8.27" x 11'", left margin: 0.65, right margin: 0.65, bottom margin: 0.75.
- Paper title should be in one column of font size 24.
- Author name in font size of 11 in one column.
- Abstract: font size 9 with the word "Abstract" in bold italics.
- Main text: font size 10 with two justified columns.
- Two columns with equal column width of 3.38 and spacing of 0.2.
- First character must be three lines drop-capped.
- The paragraph before spacing of 1 pt and after of 0 pt.
- Line spacing of 1 pt.
- Large images must be in one column.
- The names of first main headings (Heading 1) must be in Roman font, capital letters, and font size of 10.
- The names of second main headings (Heading 2) must not include numbers and must be in italics with a font size of 10.

Structure and Format of Manuscript

The recommended size of an original research paper is under 15,000 words and review papers under 7,000 words. Research articles should be less than 10,000 words. Research papers are usually longer than review papers. Review papers are reports of significant research (typically less than 7,000 words, including tables, figures, and references)

A research paper must include:

a) A title which should be relevant to the theme of the paper.
b) A summary, known as an abstract (less than 150 words), containing the major results and conclusions.
c) Up to 10 keywords that precisely identify the paper's subject, purpose, and focus.
d) An introduction, giving fundamental background objectives.
e) Resources and techniques with sufficient complete experimental details (wherever possible by reference) to permit repetition, sources of information must be given, and numerical methods must be specified by reference.
f) Results which should be presented concisely by well-designed tables and figures.
g) Suitable statistical data should also be given.
h) All data must have been gathered with attention to numerical detail in the planning stage.

Design has been recognized to be essential to experiments for a considerable time, and the editor has decided that any paper that appears not to have adequate numerical treatments of the data will be returned unrefereed.

i) Discussion should cover implications and consequences and not just recapitulate the results; conclusions should also be summarized.
j) There should be brief acknowledgments.
k) There ought to be references in the conventional format. Global Journals recommends APA format.

Authors should carefully consider the preparation of papers to ensure that they communicate effectively. Papers are much more likely to be accepted if they are carefully designed and laid out, contain few or no errors, are summarizing, and follow instructions. They will also be published with much fewer delays than those that require much technical and editorial correction.

The Editorial Board reserves the right to make literary corrections and suggestions to improve brevity.

Format Structure

It is necessary that authors take care in submitting a manuscript that is written in simple language and adheres to published guidelines.

All manuscripts submitted to Global Journals should include:

Title

The title page must carry an informative title that reflects the content, a running title (less than 45 characters together with spaces), names of the authors and co-authors, and the place(s) where the work was carried out.

Author details

The full postal address of any related author(s) must be specified.

Abstract

The abstract is the foundation of the research paper. It should be clear and concise and must contain the objective of the paper and inferences drawn. It is advised to not include big mathematical equations or complicated jargon.

Many researchers searching for information online will use search engines such as Google, Yahoo or others. By optimizing your paper for search engines, you will amplify the chance of someone finding it. In turn, this will make it more likely to be viewed and cited in further works. Global Journals has compiled these guidelines to facilitate you to maximize the web-friendliness of the most public part of your paper.

Keywords

A major lynchpin of research work for the writing of research papers is the keyword search, which one will employ to find both library and internet resources. Up to eleven keywords or very brief phrases have to be given to help data retrieval, mining, and indexing.

One must be persistent and creative in using keywords. An effective keyword search requires a strategy: planning of a list of possible keywords and phrases to try.

Choice of the main keywords is the first tool of writing a research paper. Research paper writing is an art. Keyword search should be as strategic as possible.

One should start brainstorming lists of potential keywords before even beginning searching. Think about the most important concepts related to research work. Ask, “What words would a source have to include to be truly valuable in a research paper?” Then consider synonyms for the important words.

It may take the discovery of only one important paper to steer in the right keyword direction because, in most databases, the keywords under which a research paper is abstracted are listed with the paper.

Numerical Methods

Numerical methods used should be transparent and, where appropriate, supported by references.

Abbreviations

Authors must list all the abbreviations used in the paper at the end of the paper or in a separate table before using them.

Formulas and equations

Authors are advised to submit any mathematical equation using either MathJax, KaTeX, or LaTeX, or in a very high-quality image.

Tables, Figures, and Figure Legends

Tables: Tables should be cautiously designed, uncrowned, and include only essential data. Each must have an Arabic number, e.g., Table 4, a self-explanatory caption, and be on a separate sheet. Authors must submit tables in an editable format and not as images. References to these tables (if any) must be mentioned accurately.

Figures

Figures are supposed to be submitted as separate files. Always include a citation in the text for each figure using Arabic numbers, e.g., Fig. 4. Artwork must be submitted online in vector electronic form or by emailing it.

Preparation of Eletronic Figures for Publication

Although low-quality images are sufficient for review purposes, print publication requires high-quality images to prevent the final product being blurred or fuzzy. Submit (possibly by e-mail) EPS (line art) or TIFF (halftone/ photographs) files only. MS PowerPoint and Word Graphics are unsuitable for printed pictures. Avoid using pixel-oriented software. Scans (TIFF only) should have a resolution of at least 350 dpi (halftone) or 700 to 1100 dpi (line drawings). Please give the data for figures in black and white or submit a Color Work Agreement form. EPS files must be saved with fonts embedded (and with a TIFF preview, if possible).

For scanned images, the scanning resolution at final image size ought to be as follows to ensure good reproduction: line art: >650 dpi; halftones (including gel photographs): >350 dpi; figures containing both halftone and line images: >650 dpi.

Color charges: Authors are advised to pay the full cost for the reproduction of their color artwork. Hence, please note that if there is color artwork in your manuscript when it is accepted for publication, we would require you to complete and return a Color Work Agreement form before your paper can be published. Also, you can email your editor to remove the color fee after acceptance of the paper.

Tips for Writing a Good Quality Engineering Research Paper

Techniques for writing a good quality engineering research paper:

1. Choosing the topic: In most cases, the topic is selected by the interests of the author, but it can also be suggested by the guides. You can have several topics, and then judge which you are most comfortable with. This may be done by asking several questions of yourself, like "Will I be able to carry out a search in this area? Will I find all necessary resources to accomplish the search? Will I be able to find all information in this field area?" If the answer to this type of question is "yes," then you ought to choose that topic. In most cases, you may have to conduct surveys and visit several places. Also, you might have to do a lot of work to find all the rises and falls of the various data on that subject. Sometimes, detailed information plays a vital role, instead of short information. Evaluators are human: The first thing to remember is that evaluators are also human beings. They are not only meant for rejecting a paper. They are here to evaluate your paper. So present your best aspect.

2. Think like evaluators: If you are in confusion or getting demotivated because your paper may not be accepted by the evaluators, then think, and try to evaluate your paper like an evaluator. Try to understand what an evaluator wants in your research paper, and you will automatically have your answer. Make blueprints of paper: The outline is the plan or framework that will help you to arrange your thoughts. It will make your paper logical. But remember that all points of your outline must be related to the topic you have chosen.

3. Ask your guides: If you are having any difficulty with your research, then do not hesitate to share your difficulty with your guide (if you have one). They will surely help you out and resolve your doubts. If you can't clarify what exactly you require for your work, then ask your supervisor to help you with an alternative. He or she might also provide you with a list of essential readings.

4. Use of computer is recommended: As you are doing research in the field of research engineering then this point is quite obvious. Use right software: Always use good quality software packages. If you are not capable of judging good software, then you can lose the quality of your paper unknowingly. There are various programs available to help you which you can get through the internet.

5. Use the internet for help: An excellent start for your paper is using Google. It is a wondrous search engine, where you can have your doubts resolved. You may also read some answers for the frequent question of how to write your research paper or find a model research paper. You can download books from the internet. If you have all the required books, place importance on reading, selecting, and analyzing the specified information. Then sketch out your research paper. Use big pictures: You may use encyclopedias like Wikipedia to get pictures with the best resolution. At Global Journals, you should strictly follow here.

6. Bookmarks are useful: When you read any book or magazine, you generally use bookmarks, right? It is a good habit which helps to not lose your continuity. You should always use bookmarks while searching on the internet also, which will make your search easier.

7. Revise what you wrote: When you write anything, always read it, summarize it, and then finalize it.

8. Make every effort: Make every effort to mention what you are going to write in your paper. That means always have a good start. Try to mention everything in the introduction—what is the need for a particular research paper. Polish your work with good writing skills and always give an evaluator what he wants. Make backups: When you are going to do any important thing like making a research paper, you should always have backup copies of it either on your computer or on paper. This protects you from losing any portion of your important data.

9. Produce good diagrams of your own: Always try to include good charts or diagrams in your paper to improve quality. Using several unnecessary diagrams will degrade the quality of your paper by creating a hodgepodge. So always try to include diagrams which were made by you to improve the readability of your paper. Use of direct quotes: When you do research relevant to literature, history, or current affairs, then use of quotes becomes essential, but if the study is relevant to science, use of quotes is not preferable.

10. Use proper verb tense: Use proper verb tenses in your paper. Use past tense to present those events that have happened. Use present tense to indicate events that are going on. Use future tense to indicate events that will happen in the future. Use of wrong tenses will confuse the evaluator. Avoid sentences that are incomplete.

11. Pick a good study spot: Always try to pick a spot for your research which is quiet. Not every spot is good for studying.

12. Know what you know: Always try to know what you know by making objectives, otherwise you will be confused and unable to achieve your target.

13. Use good grammar: Always use good grammar and words that will have a positive impact on the evaluator; use of good vocabulary does not mean using tough words which the evaluator has to find in a dictionary. Do not fragment sentences. Eliminate one-word sentences. Do not ever use a big word when a smaller one would suffice.

Verbs have to be in agreement with their subjects. In a research paper, do not start sentences with conjunctions or finish them with prepositions. When writing formally, it is advisable to never split an infinitive because someone will (wrongly) complain. Avoid clichés like a disease. Always shun irritating alliteration. Use language which is simple and straightforward. Put together a neat summary.

14. Arrangement of information: Each section of the main body should start with an opening sentence, and there should be a changeover at the end of the section. Give only valid and powerful arguments for your topic. You may also maintain your arguments with records.

15. Never start at the last minute: Always allow enough time for research work. Leaving everything to the last minute will degrade your paper and spoil your work.

16. Multitasking in research is not good: Doing several things at the same time is a bad habit in the case of research activity. Research is an area where everything has a particular time slot. Divide your research work into parts, and do a particular part in a particular time slot.

17. Never copy others' work: Never copy others' work and give it your name because if the evaluator has seen it anywhere, you will be in trouble. Take proper rest and food: No matter how many hours you spend on your research activity, if you are not taking care of your health, then all your efforts will have been in vain. For quality research, take proper rest and food.

18. Go to seminars: Attend seminars if the topic is relevant to your research area. Utilize all your resources.

19. Refresh your mind after intervals: Try to give your mind a rest by listening to soft music or sleeping in intervals. This will also improve your memory. Acquire colleagues: Always try to acquire colleagues. No matter how sharp you are, if you acquire colleagues, they can give you ideas which will be helpful to your research.

20. Think technically: Always think technically. If anything happens, search for its reasons, benefits, and demerits. Think and then print: When you go to print your paper, check that tables are not split, headings are not detached from their descriptions, and page sequence is maintained.

21. Adding unnecessary information: Do not add unnecessary information like "I have used MS Excel to draw graphs." Irrelevant and inappropriate material is superfluous. Foreign terminology and phrases are not apropos. One should never take a broad view. Analogy is like feathers on a snake. Use words properly, regardless of how others use them. Remove quotations. Puns are for kids, not grunt readers. Never oversimplify: When adding material to your research paper, never go for oversimplification; this will definitely irritate the evaluator. Be specific. Never use rhythmic redundancies. Contractions shouldn't be used in a research paper. Comparisons are as terrible as clichés. Give up ampersands, abbreviations, and so on. Remove commas that are not necessary. Parenthetical words should be between brackets or commas. Understatement is always the best way to put forward earth-shaking thoughts. Give a detailed literary review.
22. Report concluded results: Use concluded results. From raw data, filter the results, and then conclude your studies based on measurements and observations taken. An appropriate number of decimal places should be used. Parenthetical remarks are prohibited here. Proofread carefully at the final stage. At the end, give an outline to your arguments. Spot perspectives of further study of the subject. Justify your conclusion at the bottom sufficiently, which will probably include examples.
23. Upon conclusion: Once you have concluded your research, the next most important step is to present your findings. Presentation is extremely important as it is the definite medium though which your research is going to be in print for the rest of the crowd. Care should be taken to categorize your thoughts well and present them in a logical and neat manner. A good quality research paper format is essential because it serves to highlight your research paper and bring to light all necessary aspects of your research.

Informal Guidelines of Research Paper Writing

Key points to remember:

- Submit all work in its final form.
- Write your paper in the form which is presented in the guidelines using the template.
- Please note the criteria peer reviewers will use for grading the final paper.

Final points:

One purpose of organizing a research paper is to let people interpret your efforts selectively. The journal requires the following sections, submitted in the order listed, with each section starting on a new page:

The introduction: This will be compiled from reference matter and reflect the design processes or outline of basis that directed you to make a study. As you carry out the process of study, the method and process section will be constructed like that. The results segment will show related statistics in nearly sequential order and direct reviewers to similar intellectual paths throughout the data that you gathered to carry out your study.

The discussion section:

This will provide understanding of the data and projections as to the implications of the results. The use of good quality references throughout the paper will give the effort trustworthiness by representing an alertness to prior workings.

Writing a research paper is not an easy job, no matter how trouble-free the actual research or concept. Practice, excellent preparation, and controlled record-keeping are the only means to make straightforward progression.

General style:

Specific editorial column necessities for compliance of a manuscript will always take over from directions in these general guidelines.

To make a paper clear: Adhere to recommended page limits.

Mistakes to avoid:

- Insertion of a title at the foot of a page with subsequent text on the next page.
- Separating a table, chart, or figure—confine each to a single page.
- Submitting a manuscript with pages out of sequence.
- In every section of your document, use standard writing style, including articles ("a" and "the").
- Keep paying attention to the topic of the paper.

- Use paragraphs to split each significant point (excluding the abstract).
- Align the primary line of each section.
- Present your points in sound order.
- Use present tense to report well-accepted matters.
- Use past tense to describe specific results.
- Do not use familiar wording; don't address the reviewer directly. Don't use slang or superlatives.
- Avoid use of extra pictures—include only those figures essential to presenting results.

Title page:

Choose a revealing title. It should be short and include the name(s) and address(es) of all authors. It should not have acronyms or abbreviations or exceed two printed lines.

Abstract: This summary should be two hundred words or less. It should clearly and briefly explain the key findings reported in the manuscript and must have precise statistics. It should not have acronyms or abbreviations. It should be logical in itself. Do not cite references at this point.

An abstract is a brief, distinct paragraph summary of finished work or work in development. In a minute or less, a reviewer can be taught the foundation behind the study, common approaches to the problem, relevant results, and significant conclusions or new questions.

Write your summary when your paper is completed because how can you write the summary of anything which is not yet written? Wealth of terminology is very essential in abstract. Use comprehensive sentences, and do not sacrifice readability for brevity; you can maintain it succinctly by phrasing sentences so that they provide more than a lone rationale. The author can at this moment go straight to shortening the outcome. Sum up the study with the subsequent elements in any summary. Try to limit the initial two items to no more than one line each.

Reason for writing the article—theory, overall issue, purpose.

- Fundamental goal.
- To-the-point depiction of the research.
- Consequences, including definite statistics—if the consequences are quantitative in nature, account for this; results of any numerical analysis should be reported. Significant conclusions or questions that emerge from the research.

Approach:

- o Single section and succinct.
- o An outline of the job done is always written in past tense.
- o Concentrate on shortening results—limit background information to a verdict or two.
- o Exact spelling, clarity of sentences and phrases, and appropriate reporting of quantities (proper units, important statistics) are just as significant in an abstract as they are anywhere else.

Introduction:

The introduction should "introduce" the manuscript. The reviewer should be presented with sufficient background information to be capable of comprehending and calculating the purpose of your study without having to refer to other works. The basis for the study should be offered. Give the most important references, but avoid making a comprehensive appraisal of the topic. Describe the problem visibly. If the problem is not acknowledged in a logical, reasonable way, the reviewer will give no attention to your results. Speak in common terms about techniques used to explain the problem, if needed, but do not present any particulars about the protocols here.

The following approach can create a valuable beginning:

- o Explain the value (significance) of the study.
- o Defend the model—why did you employ this particular system or method? What is its compensation? Remark upon its appropriateness from an abstract point of view as well as pointing out sensible reasons for using it.
- o Present a justification. State your particular theory(-ies) or aim(s), and describe the logic that led you to choose them.
- o Briefly explain the study's tentative purpose and how it meets the declared objectives.

Approach:

Use past tense except for when referring to recognized facts. After all, the manuscript will be submitted after the entire job is done. Sort out your thoughts; manufacture one key point for every section. If you make the four points listed above, you will need at least four paragraphs. Present surrounding information only when it is necessary to support a situation. The reviewer does not desire to read everything you know about a topic. Shape the theory specifically—do not take a broad view.

As always, give awareness to spelling, simplicity, and correctness of sentences and phrases.

Procedures (methods and materials):

This part is supposed to be the easiest to carve if you have good skills. A soundly written procedures segment allows a capable scientist to replicate your results. Present precise information about your supplies. The suppliers and clarity of reagents can be helpful bits of information. Present methods in sequential order, but linked methodologies can be grouped as a segment. Be concise when relating the protocols. Attempt to give the least amount of information that would permit another capable scientist to replicate your outcome, but be cautious that vital information is integrated. The use of subheadings is suggested and ought to be synchronized with the results section.

When a technique is used that has been well-described in another section, mention the specific item describing the way, but draw the basic principle while stating the situation. The purpose is to show all particular resources and broad procedures so that another person may use some or all of the methods in one more study or referee the scientific value of your work. It is not to be a step-by-step report of the whole thing you did, nor is a methods section a set of orders.

Materials:

Materials may be reported in part of a section or else they may be recognized along with your measures.

Methods:

- Report the method and not the particulars of each process that engaged the same methodology.
- Describe the method entirely.
- To be succinct, present methods under headings dedicated to specific dealings or groups of measures.
- Simplify—detail how procedures were completed, not how they were performed on a particular day.
- If well-known procedures were used, account for the procedure by name, possibly with a reference, and that's all.

Approach:

It is embarrassing to use vigorous voice when documenting methods without using first person, which would focus the reviewer's interest on the researcher rather than the job. As a result, when writing up the methods, most authors use third person passive voice.

Use standard style in this and every other part of the paper—avoid familiar lists, and use full sentences.

What to keep away from:

- Resources and methods are not a set of information.
- Skip all descriptive information and surroundings—save it for the argument.
- Leave out information that is immaterial to a third party.

Results:

The principle of a results segment is to present and demonstrate your conclusion. Create this part as entirely objective details of the outcome, and save all understanding for the discussion.

The page length of this segment is set by the sum and types of data to be reported. Use statistics and tables, if suitable, to present consequences most efficiently.

You must clearly differentiate material which would usually be incorporated in a study editorial from any unprocessed data or additional appendix matter that would not be available. In fact, such matters should not be submitted at all except if requested by the instructor.

Content:

- Sum up your conclusions in text and demonstrate them, if suitable, with figures and tables.
- In the manuscript, explain each of your consequences, and point the reader to remarks that are most appropriate.
- Present a background, such as by describing the question that was addressed by creation of an exacting study.
- Explain results of control experiments and give remarks that are not accessible in a prescribed figure or table, if appropriate.
- Examine your data, then prepare the analyzed (transformed) data in the form of a figure (graph), table, or manuscript.

What to stay away from:

- Do not discuss or infer your outcome, report surrounding information, or try to explain anything.
- Do not include raw data or intermediate calculations in a research manuscript.
- Do not present similar data more than once.
- A manuscript should complement any figures or tables, not duplicate information.
- Never confuse figures with tables—there is a difference.

Approach:

As always, use past tense when you submit your results, and put the whole thing in a reasonable order.

Put figures and tables, appropriately numbered, in order at the end of the report.

If you desire, you may place your figures and tables properly within the text of your results section.

Figures and tables:

If you put figures and tables at the end of some details, make certain that they are visibly distinguished from any attached appendix materials, such as raw facts. Whatever the position, each table must be titled, numbered one after the other, and include a heading. All figures and tables must be divided from the text.

Discussion:

The discussion is expected to be the trickiest segment to write. A lot of papers submitted to the journal are discarded based on problems with the discussion. There is no rule for how long an argument should be.

Position your understanding of the outcome visibly to lead the reviewer through your conclusions, and then finish the paper with a summing up of the implications of the study. The purpose here is to offer an understanding of your results and support all of your conclusions, using facts from your research and generally accepted information, if suitable. The implication of results should be fully described.

Infer your data in the conversation in suitable depth. This means that when you clarify an observable fact, you must explain mechanisms that may account for the observation. If your results vary from your prospect, make clear why that may have happened. If your results agree, then explain the theory that the proof supported. It is never suitable to just state that the data approved the prospect, and let it drop at that. Make a decision as to whether each premise is supported or discarded or if you cannot make a conclusion with assurance. Do not just dismiss a study or part of a study as "uncertain."

Research papers are not acknowledged if the work is imperfect. Draw what conclusions you can based upon the results that you have, and take care of the study as a finished work.

- You may propose future guidelines, such as how an experiment might be personalized to accomplish a new idea.
- Give details of all of your remarks as much as possible, focusing on mechanisms.
- Make a decision as to whether the tentative design sufficiently addressed the theory and whether or not it was correctly restricted. Try to present substitute explanations if they are sensible alternatives.
- One piece of research will not counter an overall question, so maintain the large picture in mind. Where do you go next? The best studies unlock new avenues of study. What questions remain?
- Recommendations for detailed papers will offer supplementary suggestions.

Approach:

When you refer to information, differentiate data generated by your own studies from other available information. Present work done by specific persons (including you) in past tense.

Describe generally acknowledged facts and main beliefs in present tense.

The Administration Rules

Administration Rules to Be Strictly Followed before Submitting Your Research Paper to Global Journals Inc.

Please read the following rules and regulations carefully before submitting your research paper to Global Journals Inc. to avoid rejection.

Segment draft and final research paper: You have to strictly follow the template of a research paper, failing which your paper may get rejected. You are expected to write each part of the paper wholly on your own. The peer reviewers need to identify your own perspective of the concepts in your own terms. Please do not extract straight from any other source, and do not rephrase someone else's analysis. Do not allow anyone else to proofread your manuscript.

Written material: You may discuss this with your guides and key sources. Do not copy anyone else's paper, even if this is only imitation, otherwise it will be rejected on the grounds of plagiarism, which is illegal. Various methods to avoid plagiarism are strictly applied by us to every paper, and, if found guilty, you may be blacklisted, which could affect your career adversely. To guard yourself and others from possible illegal use, please do not permit anyone to use or even read your paper and file.

Criterion for Grading a Research Paper (Compilation) by Global Journals

Please note that following table is only a Grading of "Paper Compilation" and not on "Performed/Stated Research" whose grading solely depends on Individual Assigned Peer Reviewer and Editorial Board Member. These can be available only on request and after decision of Paper. This report will be the property of Global Journals.

Topics	Grades		
	A-B	**C-D**	**E-F**
Abstract	Clear and concise with appropriate content, Correct format. 200 words or below	Unclear summary and no specific data, Incorrect form Above 200 words	No specific data with ambiguous information Above 250 words
Introduction	Containing all background details with clear goal and appropriate details, flow specification, no grammar and spelling mistake, well organized sentence and paragraph, reference cited	Unclear and confusing data, appropriate format, grammar and spelling errors with unorganized matter	Out of place depth and content, hazy format
Methods and Procedures	Clear and to the point with well arranged paragraph, precision and accuracy of facts and figures, well organized subheads	Difficult to comprehend with embarrassed text, too much explanation but completed	Incorrect and unorganized structure with hazy meaning
Result	Well organized, Clear and specific, Correct units with precision, correct data, well structuring of paragraph, no grammar and spelling mistake	Complete and embarrassed text, difficult to comprehend	Irregular format with wrong facts and figures
Discussion	Well organized, meaningful specification, sound conclusion, logical and concise explanation, highly structured paragraph reference cited	Wordy, unclear conclusion, spurious	Conclusion is not cited, unorganized, difficult to comprehend
References	Complete and correct format, well organized	Beside the point, Incomplete	Wrong format and structuring

Index

save our planet

Global Journal of Researches in Engineering

Visit us on the Web at www.GlobalJournals.org | www.EngineeringResearch.org
or email us at helpdesk@globaljournals.org

ISSN 9755861